FACULDADE DE CIÊNCIAS E TECNOLOGIA
UNIVERSIDADE NOVA DE LISBOA

Department of Physics

Functional Studies on Magnetic Resonance

2009 / 2010

João Pedro Ribeiro Miranda

Siemens S.A.

Lisboa

FACULDADE DE CIÊNCIAS E TECNOLOGIA
UNIVERSIDADE NOVA DE LISBOA

Department of Physics

Functional Studies on Magnetic Resonance

21560 João Pedro Ribeiro Miranda

Siemens S.A.

Dissertation submitted in *Faculdade de Ciências e Tecnologia* of *Universidade Nova de Lisboa* for the degree of Master in Biomedical Engineering

Outubro de 2010

Supervisor in FCT/UNL: Prof.ª Dr.ª Carla Pereira

Supervisor in Siemens S.A.: Eng.º Filipe Janela

I dedicate this thesis to my parents:

João and Anabela Miranda

Acknowledgements

Throughout the last five years that culminate in this thesis, several people have crossed my way and have marked my personal and professional evolution. I take this opportunity to acknowledge their influence.

I would like to start by thanking SIEMENS and Eng. Filipe Janela for the opportunity of developing my work in this environment. It has truly been a great challenge and has made me develop a large amount of skills.

I also acknowledge my other supervisor Prof.ª Carla Quintão. More than the scientific advice given, which were crucial, the support and experience shared throughout all the stages of my thesis were of great importance for me to reach this goal. I am deeply thankful.

I am also thankful to Dr. Pedro Vilela and Prof.ª Patrícia Figueiredo for suggesting this study and for all the orientation provided.

At SIEMENS I would also like to thank Dr.ª Celina Lourenço for all help and constant care provided along this internship. Your reviews have also been of great importance to my work.

I also acknowledge Eng. Inês Sousa for all the scientific advice and for introducing me to this area of studies. Your teachings, especially on the early stages of my work, were of high importance.

I also wish to thank Eng. Marco Pimentel, for the help and orientation provided in a crucial stage of my study.

An acknowlegdement word goes to my MSc. colleagues here at SIEMENS, especially to Catarina Barros and Patrícia Silva, who made this experience more bearable.

An additional word to acknowledge Eng. João Amaro, for constant care an experience shared and to Eng. Carlos Caldeira for the fine conversations.

At FCT I would like to thank my friends Carlos, André, Nuno, Francisco, Cláudio, Joana and Ana Sofia. These last years have been filled with moments I will never forget. Thank you!

A special acknowledgement goes to Dr.ª Helena Veríssimo for the help provided in a crucial part of my internship. Vielen Dank!

I thank my family, for all the support, especially my grandmothers Maria José and Helena who always have a supportive word.

I thank my "little" sister Ana, for always being by my side. In many ways, you are already an example to me.

I gratefully acknowledge all the support given by my girlfriend Ana. Everything you have done throughout this thesis has made this work possible. Simple words written here would never make justice to what you mean to me. Throughout all these pages I may find a little piece of you. Thank you!

Last, but definetly not least, I would like to thank my parents, João and Anabela, to whom I dedicate this thesis. The last few months have been truly challenging but with your assistance and advice I have managed to never loose my path. I take this opportunity to also thank you for all the love, care and comprehension you have had throughout every stage of my life. I will never be able to express how much you mean to me.

Abstract

Title: Functional Studies on Magnetic Resonance

Background: Magnetic Resonance Imaging (MRI) is an imaging technique used primarily to produce high quality structural and functional images of the human body. Functional MRI techniques, among which are included the Arterial Spin Labeling (ASL) and the Blood Oxygenation Level-Dependent (BOLD), are used to measure brain activity. Several studies have shown that ASL holds several advantages when compared with BOLD, namely the fact of being more reproducible and perfusion quantitative.

Purpose: The main aim of this work is to obtain perfusion quantification of the human brain within several of its territories and to compare the results obtained using two different ASL protocols. Secondarily this study aimed to validate an ASL protocol to be used in clinical exams – Protocol #2 by comparing the values obtained for all the regions considered with the ones present in literature.

Methods: The methodology used in this study was applied to fifteen adult volunteers. Two ASL protocols were used in a single functional imaging session. Subjects were asked to perform a motor finger tapping task with their right hand while being scanned. Images were acquired on a 3 Tesla equipment – Magnetom Verio MRI System from *SIEMENS* in Hospital da Luz. For the definition of the regions to study the Talairach anatomical atlas was used and the brain was segmented considering five different segmentation levels.

Results: Perfusion quantification studies have demonstrated that ASL allows a correct calculation of Cerebral Blood Flow (CBF), especially when compared to other studies which used other invasive perfusion measuring techniques. The perfusion values obtained for several regions considered are in agreement with the ones available in literature.

Conclusions: ASL protocols are now becoming commercially available and have been demonstrating coherent results with other techniques already established. The current study presents one of the first detailed perfusion studies using this technique to evaluate several structures of the brain. The adequacy of Protocol 2 for functional studies was also proved considering the stimulus used.

Keywords (Theme): Functional Magnetic Resonance Imaging (fMRI), Cerebral Blood Flow (CBF)

Keywords (Technology): Arterial Spin Labeling (ASL)

Resumo

Título: Estudos Funcionais em Ressonância Magnética

Introdução: A imagem por Ressonância Magnética é uma técnica utilizada para se obterem principalmente imagens estruturais e funcionais de alta qualidade do corpo humano. As técnicas de Ressonância Magnética Funcional, entre as quais se incluem o Arterial Spin Labeling e o Blood Oxygenation Level Dependent são utilizadas para medir e estudar a actividade cerebral. Vários estudos têm demonstrado que o ASL tem várias vantagens quando comparado com o BOLD principalmente pelo facto de ser mais reprodutível e de permitir a quantificação da perfusão cerebral.

Objectivo: O principal objectivo deste trabalho é a quantificação da perfusão em determinados territórios cerebrais e comparar os resultados obtidos através de dois diferentes protocolos de ASL. Este estudo teve também o objectivo de validar um protocolo para ser usado em exames clínicos – Protocolo 2, comparando os valores obtidos para todas as regiões consideradas com os existentes na literatura.

Métodos: A metodologia utilizada neste estudo foi aplicada a quinze voluntários adultos. Dois protocolos ASL foram usados numa sessão única de imagem funcional. Os indivíduos executaram uma tarefa motora com a mão direita enquanto estavam a ser examinados. As imagens foram adquiridas num equipamento de 3 Tesla - Magnetom Verio MRI System - da SIEMENS no Hospital da Luz. Para a definição das regiões a estudar o atlas anatómico de Talairach foi utilizado e o cérebro foi segmentado em diversas regiões considerando-se cinco níveis de segmentação diferentes.

Resultados: Estudos de quantificação de perfusão têm demonstrado que o ASL permite um cálculo correcto do Fluxo Sanguíneo Cerebral, especialmente quando comparado com outros estudos que utilizaram outras técnicas invasivas de quantificação de perfusão. Os valores de perfusão obtidos para diversas regiões consideradas estão de acordo com os disponíveis na literatura.

Conclusões: Protocolos de ASL estão agora a tornar-se disponíveis comercialmente e têm demonstrado resultados coerentes com outras técnicas já estabelecidas. Este trabalho representa um dos primeiros estudos de perfusão cerebral detalhada utilizando a técnica ASL para avaliar diversas estruturas do cérebro. A adequação do Protocolo 2 para estudos funcionais também foi provada, considerando o estímulo utilizado.

Palavras Chave (Tema): Ressonância Magnética Funcional, Fluxo Sanguíneo Cerebral

Palavras Chave (Tecnologias): Arterial Spin Labeling (ASL)

Contents

Acknowledgements ..... **vii**

Abstract ..... **ix**

Resumo ..... **xi**

Contents ..... **xiii**

List of Figures ..... **xv**

List of Tabels ..... **xix**

Acronyms ..... **xxi**

1 Introduction **1**

1.1 Background **1**

1.2 Project Presentation **2**

1.3 Contributions of the work **3**

1.4 Structure of the thesis **3**

1.5 Company Presentation **4**

2 Neuroanatomy and Functional Neuroimaging **7**

2.1 Brain Structure **7**

2.1.1 Cerebrum 8

2.2 Functional Organization of the Brain **9**

2.3 Talairach Atlas **10**

2.4 Cerebrovascular Anatomy **11**

2.4.1 Cerebral Arteries 11

2.4.2 Cerebral Vascular Territories 13

2.5 Cerebral Perfusion **15**

2.5.1 Perfusion 15

2.5.2 Perfusion Measuring Techniques 16

3 Magnetic Resonance Imaging **17**

3.1 Physics Principles of MRI **17**

3.2 MR pulse sequences **19**

3.3 Blood-Oxygenation Level Dependent fMRI ... 22

3.4 Perfusion fMRI – Arterial Spin Labeling ... 24

3.4.1 Arterial Spin Labeling Techniques – PASL and CASL ... 25

3.4.2 Perfusion Quantification ... 27

3.4.3 ASL Pulse Sequences ... 30

4 Methods ... 33

4.1 Subjects ... 33

4.2 Image Acquisition ... 34

4.3 ASL Image Processing ... 35

4.3.1 Perfusion Quantification Method ... 35

4.3.2 CBF Quantification in Activation and Rest Conditions ... 35

4.4 Perfusion Maps Registration and Brain Territories Segmentation ... 36

5 Results ... 39

5.1 CBF Quantification – Comparison between Protocols ... 39

5.2 CBF Quantification – Brain Regions ... 41

5.2.1 First level of segmentation - Hemisphere ... 41

5.2.2 Second level of segmentation - Lobe ... 44

5.2.3 Third level of segmentation – Gyrus ... 47

5.2.4 Fourth level segmentation – Tissue Type ... 52

5.2.5 Fifth level segmentation – Cell Type ... 54

6 Conclusions ... 59

6.1 Summary of the thesis and objectives achieved ... 59

6.2 Other work undertaken ... 60

6.3 Limitations & Future work ... 61

6.4 Final findings ... 61

References ... 63

Appendix A – Auxiliar Information for Perfusion Quantification ... 71

Appendix B – Mean perfusion values for third and fifth level of segmentation ... 85

Appendix C – Implementation of Functional Paradigms ... 93

List of Figures

Figure 2.1 – Representation of brain anatomic structure – main divisions (adapted from (10)) *8*

Figure 2.2 – Illustration of brain's anatomic structure – representation of the four lobes (10)..... *8*

Figure 2.3 – Illustration of the location of the five primary sensory areas and the primary motor cortex (13) *10*

Figure 2.4 – Illustration of the five segmentation levels that were taken into account in the current study (14) *11*

Figure 2.5 – Illustration of the arterial circulation of the brain (adapted from (10)) ... *12*

Figure 2.6 – Representation of vascular territories of the cerebral arteries (courtesy of Dr. Savoiardo) *14*

Figure 3.1 – The magnetization M precesses around the z axis with the angle α, and it is divided into the longitudinal component, M_z and the transverse component M_{xy}. A RF coil is placed in the y axis direction to collect the MR signal. (38) *19*

Figure 3.2 – Graphic of EPI k-space coverage order during one TR (40)...... *20*

Figure 3.3 – GRE-EPI pulse sequence scheme – After the application of the 90° excitation pulse it may be seen the FID signal that is acquired (adapted from (40)) ... *21*

Figure 3.4 – SE-EPI pulse sequence scheme – Unlike GRE-EPI in SE-EPI we may see two pulses applied that produce a series of waveforms (adapted from (40))...... *21*

Figure 3.5 – Different contrasts a) T_1 weighted b) Proton-density weighted c)T_2 weighted..... *22*

Figure 3.6 – Hemodynamic changes in neuronal activity. a) Rest b) Activation – Red circles represent oxyhemoglobin and its increase is well seen. The blue circles represent deoxyhemoglobin and its relative decrease is also patent in the scheme (adapted from (43)). *23*

Figure 3.7 – Hemodynamic response function (HRF) - a) response to brief stimulus b) response to long stimulus. (adapted from (44))..... *24*

Figure 3.8 – The EPISTAR PASL sequence, which labels everything at once and uses two 180° + 180° = 0° pulses for the control images. As it may ben seen in the top sequence,

an inversion pulse (green) is applied and the signal generated by the inverted spins (blue) is acquired at t=TI. On the bottom sequence the inversion pulse is not applied (orange) and the spins (red) are not inverted, generating a control image. (adapted from (47)) *25*

Figure 3.9 – The FAIR PASL sequence compared with EPISTAR sequence. EPISTAR sequence is described in Figure 3.8. For the FAIR sequence it is possible to view the position of the applied inversion label (adapted from (49)). *26*

Figure 3.10 – CASL sequence scheme. In CASL there is a continuous inversion pulsed applied in the Inversion Plane. After a period of time δt in which the blood arrives to the acquisition plane the signal is acquired. The signal will weaken as the labeled water in the blood moves through the tissue (54)...... *27*

Figure 3.11 - Theoretical curves of pulsed ASL signal versus time calculated from Equation 3.9. (55) *30*

Figure 3.12 – Pulse sequence for Q2TIPS. On the right are shown the locations of the in-plane pre-saturation slab, the imaging slice(s), periodic saturation slice and inversion slab used in the PICORE labeling scheme. Double in-plane 90º presaturation pulses are followed by a hyperbolic secant inversion tagging pulse. The gradient lobe in gray is alternately applied for tag and control states. The first inversion time TI_1 allows the inverted arterial spins to flow to the imaging slab. Periodic saturation pulses applied from TI_1 to TI_{1S} (TI_{1S} is the stop time) consist of a train of 90º excitation pulses each followed by a crusher gradient that eliminates the signal from the large feeding arteries (58). Single or multislice EPI acquisition is applied at TI_2. (57)..... *31*

Figure 5.1 – Perfusion map from a male subject. The nine axial slices are displayed from bottom to top. The ninth slice is not displayed as it does not present information. *40*

Figure 5.2 – Plot comparing mean perfusion values (ml/100g/min) for both protocols. *41*

Figure 5.3 – Left Cerebrum in a) Talairach Standard Space b) ASL space – perfusion map *42*

Figure 5.4 - Plot comparing mean perfusion values (ml/100g/min) for both protocols and for the two states in first segmentation level. *43*

Figure 5.5 – Left Temporal Lobe in a) Talairach Standard Space b) ASL space – perfusion map *44*

Figure 5.6 - Plots comparing mean perfusion values (ml/100g/min) for both protocols in second segmentation level for a) Protocol 1 b) Protocol 2 ..... *45*

Figure 5.7 - Left Precentral Gyrus in a) Talairach Standard Space b) ASL space – perfusion map *47*

Figure 5.8 – Plot comparing mean perfusion values (ml/100g/min) for Protocol 1 in third segmentation level. *48*

Figure 5.9- Plot comparing mean perfusion values (ml/100g/min) for Protocol 2 in third segmentation level. *49*

Figure 5.10 – White Matter in a) Talairach Standard Space b) ASL space – perfusion map *52*

Figure 5.11 - Plot comparing mean perfusion values (ml/100g/min) for both protocols in second segmentation level for Protocol 1 and Protocol 2..... *53*

Figure 5.12 – Corpus Callosum in a) Talairach Standard Space b) ASL space – perfusion map *54*

Figure 5.13 - Plot comparing mean perfusion values (ml/100g/min) for Protocol 1 in fifth segmentation level. *55*

Figure 5.14 - Plot comparing mean perfusion values (ml/100g/min) for Protocol 2 in fifth segmentation level. *56*

List of Tabels

Table 4.1 – Acquisition parameters – EPI readout *34*

Table 4.2 – Acquisition parameters – PICORE Q2TIPS *34*

Table 5.1 – Mean CBF values (ml/100g/min) in GM for each subject for both protocols *40*

Table 5.2 – Mean perfusion values (ml/100g/min) in first level segmentation regions of the brain *43*

Table 5.3 – Mean CBF values (ml/100g/min) in second level segmented brain regions *46*

Table 5.4 – CBF mean values obtained in current study copmpared with the ones from literature: *51*

Table 5.5 - Mean perfusion values (ml/100g/min) in fourth level segmentation regions of the brain *53*

Table B.1 – Mean perfusion values (ml/100g/min) in third level segmentation regions of the brain *85*

Table B.2 - Mean perfusion values (ml/100g/min) in third level segmentation regions of the brain *89*

Acronyms

ASL	Arterial Spin Labeling
ATP	Adenosine Triphosphate
BOLD	Blood Oxygenation Level-Dependent
CASL	Continuous Arterial Spin Labeling
CBV	Cerebral Blood Volume
CCA	Common Carotid Artery
CVR	Cerebrovascular Reactivity
DSC	Dynamic Susceptibility Contrast
DU	Doppler Ultrasound
EPI	Echo-planar Imaging
EPISTAR	Echo Planar Imaging and Signal Targeting with Alternating Radiofrequency
FOV	Field of View
GLM	General Linear Model
GRE	Gradient-echo Sequence
HRF	Hemodynamic Response Function
MPRAGE	Magnetization Prepared Rapid Acquisition Gradient Echo
MR	Magnetic Resonance
MRI	Magnetic Resonance Imaging
MTT	Mean Transit Time
NMR	Nuclear Magnetic Resonance
PASL	Pulsed Arterial Spin Labeling
PCT	Perfusion Computed Tomography
PET	Positron Emission Technique
PICORE	Proximal Inversion with a Control for Off-Resonance Effects
Q2TIPS	QUIPSS II with Thin-Slice TI_1 Periodic Saturation

QUIPSS	Quantitative Imaging of Perfusion using a Single Subtraction
rCBF	Regional Cerebral Blood Flow
RF	Radio Frequency
SE	Spin-echo Sequence
SPECT	Single Photon Emission Computed Tomography
T_1	Longitudinal Relaxation Time
T_2	Transverse Relaxation Time
TE	Echo Time
TI	Inversion Time
TR	Repetition Time
XeCT	Xenon-enhanced Computed Tomography

B_0	External Magnetic Field
ν	Precession Frequency
γ	Gyromagnetic Ratio

1 Introduction

1.1 Background

Magnetic Resonance Imaging (MRI) is a technique used in clinical diagnosis to obtain structural and functional images of the brain that does not require ionizing radiation. Within the last years, MRI has become more sophisticated and rigorous, especially concerning its spacial resolution and contrast. (1)

Functional MRI (fMRI) can be used to obtain the neuronal responses to stimulus. The most commonly used techniques are Blood Oxygenation Level-Dependent (BOLD) contrast and, more recently, Arterial Spin Labeling (ASL). (2)

Functional MRI allows evaluating regional changes in brain activity in response to sensory processes, motor activity and complex cognitive functions such as problem solving and memory. When a patient is asked to perform a task or is stimulated by any means, the increased neuronal activity triggers an influx of oxygenated blood to support the metabolic demands of the activated brain regions. In result, the blood flow, volume and oxygenation are increased in the activated brain regions which thereby have different magnetic properties. These changes can be detected non-invasively by MRI, allowing researchers to track brain function. Functional MRI techniques have

introduced major improvements in brain function assessment and mapping as compared to other invasive perfusion measuring techniques available (3) (4) (5).

Both BOLD and ASL are non invasive techniques that can be used to detect the neuronal response to a stimulus and thereby evaluate brain function. Some studies have demonstrated that ASL holds several advantages when compared with BOLD, namely the fact of being more reproducible and allowing perfusion quantification (6). However, ASL has also some drawbacks mainly related to its low Signal to Noise Ratio (SNR), but high field MRI scanners are now benefiting this technique by improving this parameter (7).

ASL has recently been available for clinical purposes and is not yet recognised as the gold standard for brain functional studies. However, using high field scanners, its capacity to quantify perfusion non-invasively is turning ASL in an important technique to take into account in clinical exams.

1.2 Project Presentation

The main aim of this work is to obtain perfusion quantification of the human brain within several of its territories and to compare the results obtained using two different ASL protocols.

As an innovative technique it is also important to compare the values calculated with others obtained by other techniques. However, it was rather difficult to find in literature values for all the regions considered in the current work.

These regions were calculated regarding five different segmentation levels of the brain, dividing the brain within its hemispheres, lobes, gyri, tissue and cell types The detail applied in this study was important to obtain perfusion quantification in areas where it has not been measured yet, specially in the fifth level – Cell Types.

The current work is integrated in a more general study that is being conducted by the R&D group of Siemens Portugal which is validating and developing new acquisition parameters for ASL.

All the work undertaken in this project opens the doors for a more detailed study on Cerebral Blood Flow (CBF) within brain's vascular territories.

In order to obtain functional data, fifteen subjects were scanned while performing a motor finger tapping test with their right hand.

Image analysis was performed in FMRIB's Software Library (FSL).

Data analysis was performed with FSL and self written Linux Shell Scripts that are attached to this document.

1.3 Contributions of the work

The major contribution of the current work is a systematic study of perfusion quantification using ASL in pre-established cerebral regions of healthy volunteers in rest and during a functional motor task.

In order to perform a correct perfusion evaluation of the brain it is important to study it in detail. This work provides a study in great detail of the human brain, dividing the brain within its hemispheres, lobes, gyri, tissue and cell types. It may be used in the future not only for comparative purposes but also to promote an even more detailed evaluation of the brain's perfusion.

Moreover, the validation of the ASL technique for both rest perfusion quantification and fMRI is of high importance for the introduction of this technique in clinical routine. This kind of study has also an impact for *SIEMENS*. Being the first company to have ASL commercially available it is of high interest for them to see their solutions being well received in clinical routines.

The great difficulty to find similar studies for value comparison illustrates the innovation that is evident in this project.

1.4 Structure of the thesis

For a better understanding of the current work and for a correct interpretation of the results, this thesis initiates by giving a theoretical introduction to Functional Neuroimaging in Chapter 2. The second chapter presents the description of the brain's structure and its functional organization, a summary of cerebrovascular anatomy and a brief introduction to the concept of Cerebral Blood Flow and measurement of perfusion.

The third chapter presents a general approach to Magnetic Resonance Imaging and its physics, as well as a more detailed description about techniques used in Functional Magnetic Resonance Imaging.

The description of the methodology of data analysis is provided in the fourth chapter and the results obtained are presented in Chapter 5 as well as its discussion.

The main conclusions drawn from this project and other undertaken work are exposed in Chapter 6.

1.5 Company Presentation

With 500 production centres in 50 countries and representation in 190 countries, Siemens is spread all over the world. In Portugal, Siemens S.A. encloses two factories, software research & development centres (Lisbon and Oporto) and has a significant representation all over the country through its partners and company headquarters. Since 2008, the company is organized in three major sectors: Industry, Energy and Healthcare.

The **Industry Sector** and its solutions address Industry customers regarding production, transportation and building systems. This Sector is organized in five divisions: Industry Automation and Drive Technologies, Building Technologies, Industry Solutions, Mobility and OSRAM.

The **Energy Sector** offers products and solutions for generation, transmission and distribution of electrical energy. This Sector is organized in six divisions: Fossil Power Generation, Renewable Energy, Oil & Gas, Energy Service, Power Transmission and Power Distribution.

The **Healthcare Sector** stands for innovative products and complete solutions, as well as service and consulting in healthcare industry. This Sector is organized in three divisions: Imaging & Information Technologies, Workflow & Solutions and Diagnostics.

The Imaging & IT Division provides imaging systems for early diagnosis and intervention, as well as for a more effective prevention, namely Magnetic Resonance Imaging Systems (MR), Computer Tomography Systems (CT), Radiography and Angiography Systems, Positron Emission Tomography Systems (PET/CT), Single-Photon Emission Tomography Systems (SPECT and SPECT/CT), Ultrasound Units, among others. These systems are networked with high-performance healthcare IT to optimize processes (such as hospital data systems like **Soarian®**, image processing systems like **Syngo®**, and knowledge-based technologies for diagnoses support).

The Workflow & Solutions Division provides complete solutions for fields such as cardiology, oncology and neurology. This Division offers solutions for, e.g. women's health (mammography), urology, surgery and audiology. It also provides turnkey solutions (including national health IT systems, complete solutions for healthcare providers), and consulting. In addition, Workflow & Solutions is responsible for the Sector's service business and for managing customer relations.

The Diagnostics Division covers business with in-vitro diagnostics, including immune diagnostics and molecular analysis. The Division's solutions range from point-of-care applications to automation of large laboratories.

Thus, Siemens Healthcare Sector is the first fully integrated diagnosis company, providing a complete technological portfolio for the entire supply chain in healthcare **Siemens IT Solutions and Services**, leader in Information Technologies services, works as a transverse business unit.

In Portugal, Siemens SA Healthcare Sector is a market leader in the healthcare area, known for its competence and innovation skills in diagnostic and therapy systems, as well as information technologies and systems' integration. In recent years, Siemens SA Healthcare Sector has promoted the contact and cooperation with key partners in the areas of science and biomedical technology, namely Universities and Research Institutes, establishing a knowledge network and strategic partnerships and thus promoting innovation, research and development in healthcare.

Today, the Healthcare Sector's R&D Group in Portugal is comprised by over 15 elements, working in strategic areas, such as Information Systems, Computational Imaging, Automatic Medical Imaging Analysis, Modelling and Decision Support Tools and Strategic Technology Evaluation. This collaborating work has already been demonstrated by one approved patent application, two filed invention disclosures and over ten scientific publications.

Recent Milestones in Portugal

- Breast Pathology Service in Hospital de São João in Oporto, Hospital da Luz in Lisbon and Clínica Dr. João Carlos Costa in Viana do Castelo – first total patient focus units, including all necessary technologies for the complete clinical process;
- Hospital da Luz in Lisbon – first hospital in Portugal with SOARIAN ® clinical information system, becoming one of the most modern health care installations in Europe;
- Clínica Quadrantes, in Lisbon – in-vitro diagnostics and information technology systems, which together with a PET/CT system, complemented the existing Siemens in-vivo diagnostic systems at the clinic;
- Universidade de Coimbra – 3 Tesla Magnetic Resonance Imaging System exclusively for neuroscience research. This unit is part of the Brain Imaging

Network Grid, a scientific cooperation network which integrates the Universities of Coimbra, Aveiro, Porto and Minho.

R&D Highlights:

- Patent number DE 10 2007 053 393, System zur automatisierten Erstellung medizinischer Reports;
- F. Soares, P. Andruszkiewicz, M. Freire, P. Cruz e M. Pereira, Self-Similarity Analysis Applied to 2D Breast Cancer Imaging, HPC-Bio 07 - First International Workshop on High Performance Computing Applied to Medical Data and Bioinformatics, Riviera, France (2007);
- J. Martins, C. Granja, A. Mendes e P. Cruz, Gestão do fluxo de trabalho em diagnóstico por imagem: escalonamento baseado em simulação, Informática de Saúde – Boas práticas e novas perspectivas, edições Universidade Fernando Pessoa, Porto (2007);
- F. Soares, M. Freire, M. Pereira, F. Janela, J. Seabra, Towards the Detection of Microcalcifications on Mammograms Through Multifractal Detrended Fluctuation Analysis, 2009 IEEE Pacific Rim Conference on Communications, Computers and Signal Processing, Victoria, B.C., Canada (2009).

2 Neuroanatomy and Functional Neuroimaging

The human brain has always been one of the organs that most aroused the curiosity of researchers throughout the years. The attempts to study its function and even its blood flow proved to be mainly fruitless and scientists have always been eager to discover and study methods that make the evaluation of brain's function possible. The current work is one more approach to develop scientific knowledge of the brain. Some general considerations on this organ are described in the following chapters.

2.1 Brain Structure

The human brain is the center where all the great motor, sensory and cognitive functions are elaborated. Its average weight is 1370 grams representing only about 2% of the human weight although receiving 25% of all the blood volume that leaves the heart (8).

The brain is composed of three main parts: the forebrain, midbrain, and hindbrain. The forebrain consists of the cerebrum, thalamus, and hypothalamus (part of the limbic

system). The midbrain consists of the tectum and tegmentum. The hindbrain is made of the cerebellum, pons and medulla. The midbrain, pons, and medulla together are referred to as the brainstem (9). An illustration of this divison may be seen in *Figure 2.1*.

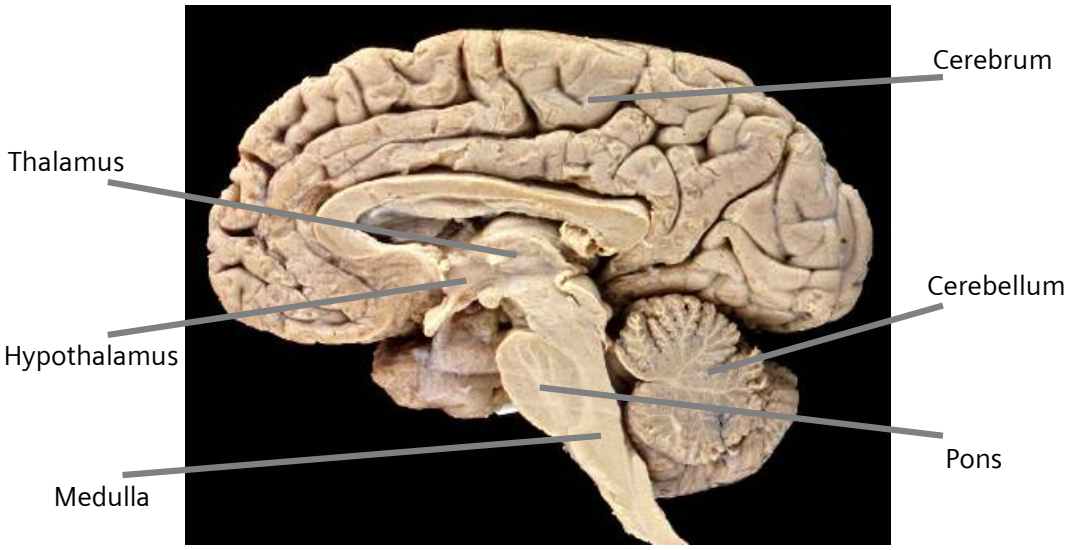

Figure 2.1 – Representation of brain anatomic structure – main divisions (adapted from (10))

2.1.1 Cerebrum

The cerebrum is nearly symmetrical, composed by two hemispheres, separated by the longitudinal fissure, each one divided into four lobes (*Figure 2.2*). The frontal and parietal lobes are separated by the central sulcus, and the temporal lobe is separated by the lateral fissure. The corpus callosum joins left and right hemispheres (8).

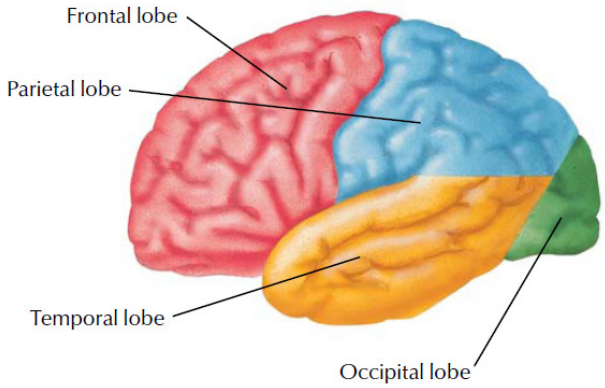

Figure 2.2 – Illustration of brain's anatomic structure – representation of the four lobes (10)

It is composed of an outer layer of gray matter, internally supported by deep brain white matter, and it is responsible for the so called "higher functions", such as thinking and cognition (8).

Gray matter consists of cell bodies of neurons, while white matter consists of axons that connect neurons. The axons are often surrounded by a fatty insulating cover called myelin, which gives the white matter its distinctive colouration. The function of this fatty sheath is to insulate nerve endings, enable smooth movements of brain signals and to accelerate the transmission of the nerve signals (8). Finally there are also the glial cells. These are not just homeostatic, providing a stable environment to neurons, but they also communicate with each other and with neurons in a manner that is cooperative, yielding many of the changes in nervous system function that leads to adaptative behaviour of the whole organism. (11)

2.2 Functional Organization of the Brain

The functional organization of much of the brain is poorly understood. However many of the regions involved in sensory and motor function have already been identified.

There are three main blocks involved in the organization of the behavior. The first one is composed of the brain stem and the old cortex and it is responsible for wakefulness and the response to stimuli. The second block, composed by the posterior area of the cerebrum, plays a key role in the analysis, coding and storage of information. The third block, the anterior area of the cerebrum, is involved in the formation of intentions and programs. (12)

A more detailed distribution of the location of the five primary sensory areas and the primary motor cortex is illustrated in *Figure 2.3*:

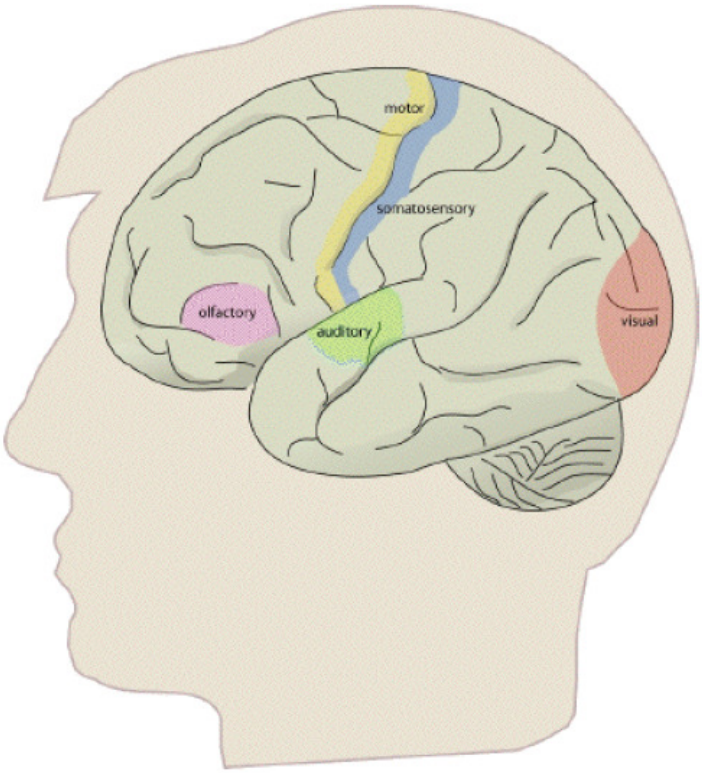

Figure 2.3 – Illustration of the location of the five primary sensory areas and the primary motor cortex (13)

2.3 Talairach Atlas

The Talairach atlas is based on anatomical landmarks of the brain of a 60 years old female.

The Talairach atlas is highly detailed, has well labeled brain sections for all three dimensions and features-a coordinate system that allows studying the brain in alignment with the space described in the atlas.

However, this atlas presents some major drawbacks, mainly the fact of being derived from only one subject and the fact that it ignores left-right hemispheric differences, only one hemisphere was studied and all the information gathered was extrapolated to the other one.

This atlas was used in the current work in order to divide the brain in five different levels of segmentation, as it may be seen in *Figure 2.4*:

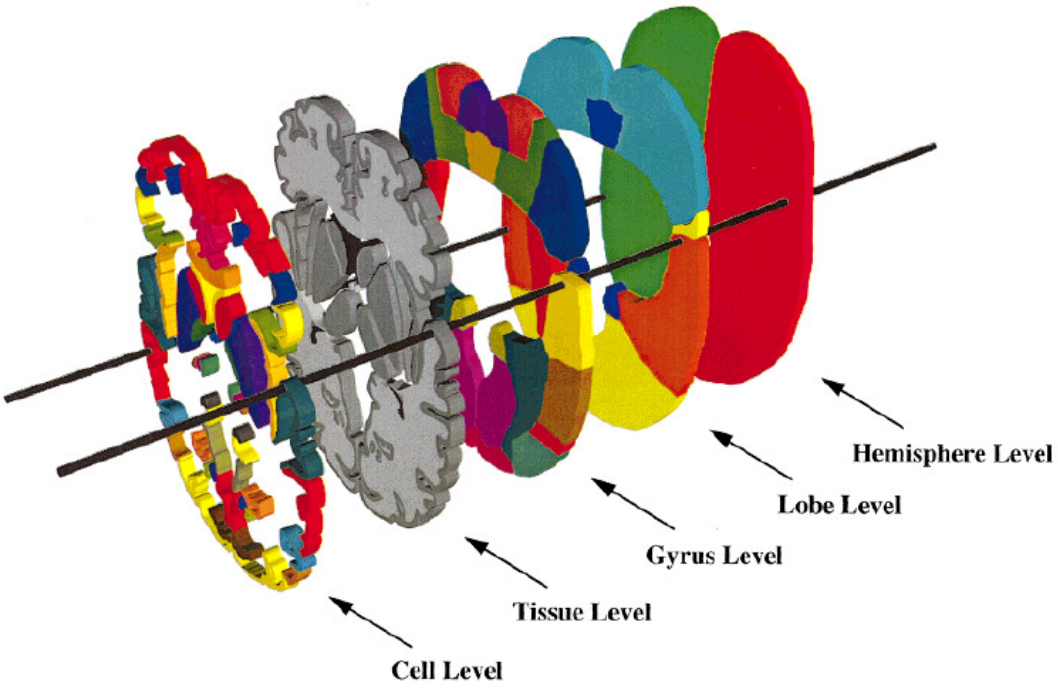

Figure 2.4 – Illustration of the five segmentation levels that were taken into account in the current study (14)

The anatomical region labels, available in *www.talairach.org/labels.txt* and whose information was used in this work, were electronically derived from axial sectional images in the 1988 Talairach Atlas. (15)

2.4 Cerebrovascular Anatomy

As previously stated, the human brain requires about 25% of the entire blood volume. The brain receives its blood supply from the heart by way of the aortic arch that gives rise to the brachiocephalic artery, left common carotid artery (CCA) and the left subclavian artery. (16)

2.4.1 Cerebral Arteries

After the path described above, the blood supply is carried into the brain by the two internal carotid arteries and the two vertebral arteries that anastomose at the base of the brain to form the Circle of Willis (17).

Carotid arteries and their branches supply the anterior portion of the brain while the vertebrobasilar system supplies the posterior portion of the brain - *Figure 2.5*.

2.4.1.1 Carotid Arterial System

The left Common Carotid Artery (CCA) arises from the aortic arch while the right one arises from the bifurcation of the Brachiocephalic trunk.

The external carotid artery starts at the bifurcation of the CCA. Its branches supply the jaw, face, neck and meninges.

The internal carotid artery starts at the carotid sinus at bifurcation of CCA at the level of the upper border of the thyroid cartilage at the level of the fourth cervical vertebra. It passes up the neck without any branches to the base of the skull where it enters the carotid canal of the petrous bone. It then runs through the cavernous sinus, pierces the dura mater and then ascends to bifurcate into anterior cerebral artery and the larger middle cerebral artery. (18)

Some branches of the internal carotid artery are the ophthalmic artery, the posterior communicating artery and the anterior choroidal artery.

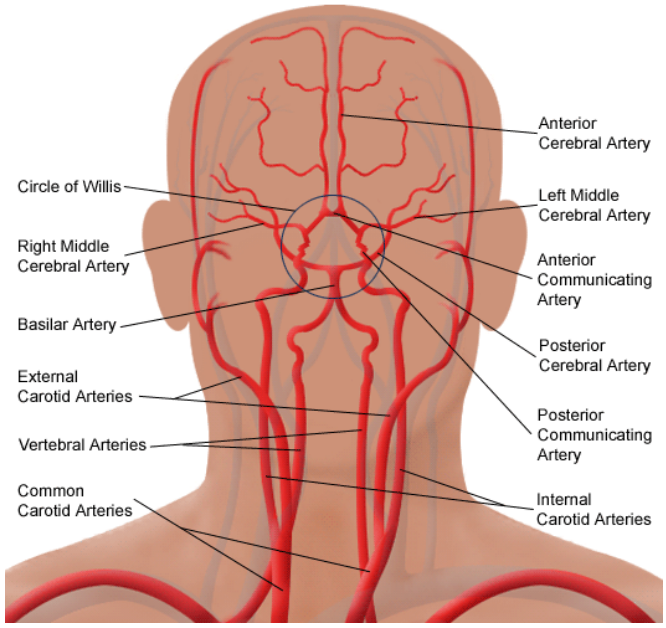

Figure 2.5 – Illustration of the arterial circulation of the brain (adapted from (10))

To conclude this system, there are also two other main arteries that need reference: the Anterior Cerebral Artery (ACA) and the Middle Cerebral Artery (MCA).

The first one passes anteromedially via the horizontal plane to enter the interhemispheric fissure and anastomoses with the contralateral anterior cerebral artery via the anterior communicating artery forming the anterior portion of the circle of Willis (*Figure 2.5*). It supplies the anterior and the medial parts of the cerebral hemispheres.

The second one is the largest branch of the internal carotid artery and appears to be almost its direct continuation. It passes through the lateral sulcus where it then branches and projects to many parts of the lateral cerebral cortex. It also supplies blood to the anterior temporal lobes and the insular cortices.

2.4.2 Cerebral Vascular Territories

The brain can naturally be divided into vascular territories which are regions based on the feeding artery of each region (19). Therefore, and taking into account what was said previously, it is possible to divide the brain into some main regions.

The Posterior Inferior Cerebellar Artery (PICA) territory is on the inferior occipital surface of the cerebellum and is in equilibrium with the territory of the Anterior Inferior Cerebellar Artery (AICA), which is on the lateral side. (Figure 2.7) (19) (18) (20)

The Superior Cerebellar Artery (SCA) territory is in the superior and tentorial surface of the cerebellum. (Figure 2.7) (18) (20)

The branches from the vertebral and basilar arteries supply the medulla oblongata and the pons. (Figure 2.7) (20) (17)

The territory of the Anterior Choroidal Artery (AChaA) is part of the hippocampus, the posterior limb of the internal capsule and extends upwards to the area lateral to the posterior part of the cella media. (Figure 2.7) (18)

The lateral Lenticulo-Striate Arteries (LSAs) are deep penetrating arteries of the MCA. Their territory includes most of the basal ganglia. The medial LSAs arise from the ACA. (18) Heubner's artery is the largest of the medial LSAs and supplies the anteromedial part of the head of the caudate and anteroinferior internal capsule. (*Figure 2.6*) (18)

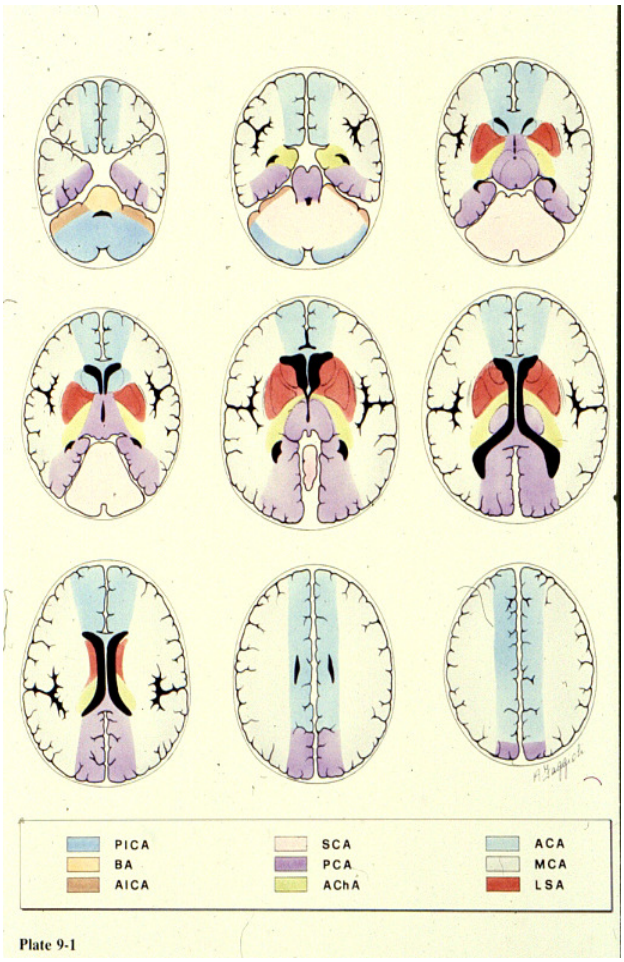

Figure 2.6 – Representation of vascular territories of the cerebral arteries (courtesy of Dr. Savoiardo)

The ACA supplies the medial part of the frontal and the parietal lobe and the anterior portion of the corpus callosum, basal ganglia and internal capsule. (*Figure 2.6*) (21)

The cortical branches of the MCA supply the lateral surface of the hemisphere, except for the medial part of the frontal and the parietal lobe, which is supplied by the ACA, and the inferior part of the temporal lobe, which is supplied by the Posterior Cerebral Artery (PCA). (*Figure 2.6*)

The PCA is divided into P1 and P2 segments by the Posterior Communicating Arteries (PCOM). Penetrating branches to the mesencephalon, subthalamic, basal structures and thalamus arise primarily from the P1 segment and the PCOM. (22) Cortical branches of the PCA supply the inferomedial part of the temporal lobe, occipital lobe visual cortex and splenium of the corpus callosum. (17)

2.5 Cerebral Perfusion

Neuronal activity results in focal changes in hemodynamics, metabolism and blood oxygenation of associated brain areas. (23)

The brain vascular system is both unique and heterogeneous in terms of structure, microvascular organization and function. Cerebral capillary abundance ranges from 260 mm/mm^3 (average of cerebrum white matter) to 2000 mm/mm^3 in the paraventricular and supraoptic nuclei of the hypothalamus. In addition to these quantitative differences, which reflect variations in metabolic rate as well as the existence of specialized endocrine secretory mechanisms, there are also wide variations in capillary structure. (24)

This differences lead to a difference in the regional Cerebral Blood Flow (rCBF) throughout the different areas of the brain. However, rCBF is tightly controlled in order to meet the brain's metabolic demands.

On average the normal cerebral blood flow is approximately 60ml/100g/min, which is roughly 15% of the cardiac output. (25)

2.5.1 Perfusion

In physiology, perfusion is characterized as the volumetric flow rate per volume of tissue. A proper blood perfusion is vital for normal tissue physiology since it is responsible for the transport of oxygen, nutrients and waste products. Also, blood perfusion is the principal part of the thermal regulatory system of the body. (26)

A large perfusion value range has been reported for human tissue (0.001-0.1 ml/ml/s), representing resting muscle to kidneys. (26)

There is a growing interest in the study of blood perfusion as its variations may indicate abnormal physiologic and pathologic conditions.

One important parameter to bear in mind when studying perfusion is the Cerebral Blood Volume (CBV) which is the fraction of the tissue volume occupied by blood vessels. A typical value for the brain is 4%. (27)

Another important parameter to take into account is the velocity of blood in the vessels, which varies from tens of centimeters per second in large arteries to as slow as one millimeter per second in the capillaries. (25)

2.5.2 Perfusion Measuring Techniques

Methods for measuring CBF in humans include Positron Emission Tomography (PET), Single Photon Emission Computed Tomography (SPECT), Xenon-enhanced Computed Tomography (XeCT), Magnetic Resonance Imaging (MRI) with contrast agents such as Gadolinium and Arterial Spin Labeling (ASL) MRI. (28)

PET is a non-invasive diagnostic tool that provides tomographic images of quantitative parameters describing various aspects of brain hemodynamics, including rCBF and rCBV. (29) It requires a radioactive tracer that is introduced into the blood supply. These isotopes are cyclotron products that have a very short half-life. A solution of glucose that has been tagged with a radioactive chemical isotope, usually inhaled $C^{15}O_2$, is introduced into the blood stream and perfusion maps are created from the radioactive emissions. (26)

SPECT was introduced after PET, and generates tomographic images of the three-dimensional distribution of a specific radiopharmaceutical. It is a technique widely used in nuclear medicine for the imaging of many organs, as well as for whole body imaging for the detection of tumors. (30) Brain SPECT is used for perfusion or receptor imaging of the brain. Unlike PET, that uses positron emissions, SPECT uses radioisotopes that emit gamma radiation, like ^{133}Xe and ^{99}Tc. (29)

XeCT has been used for over 20 years in order to evaluate quantitative CBF. (31) Xenon is inhaled and serves as a contrast material. It dissolves rapidly in the blood and enters into the brain. Then its concentration is directly measured by the CT scanner. (29)

Besides these, which are among the most used in the study of brain hemodynamics, there are also other techniques available in the market, such as, dynamic Perfusion Computed Tomography (PTC) (29) (32), Doppler Ultrasound (DU) (29) (33) and MRI Dynamic Susceptibility Contrast (DSC). (29) (34)

3 Magnetic Resonance Imaging

Magnetic Resonance Imaging is an imaging technique used primarily to produce high quality structural medical images of the human body. MRI is based on the principles of Nuclear Magnetic Resonance (NMR) which is a spectroscopic technique used to obtain chemical and physical information about molecules present in a sample. As an image technique it provides an effective, non-invasive and high resolution method of scanning several inner organs with special focus on the human brain (1).

3.1 Physics Principles of MRI

Magnetic Resonance (MR) is based upon the interaction between an applied magnetic field and a nucleus that possesses spin (35). The most common nuclei used in MR investigation are: ^{1}H, ^{13}C, ^{19}F, ^{23}Na and ^{31}P. However, and mainly due to its abundance in living organisms, the most used in clinical applications is ^{1}H. When hydrogen nuclei are not under influence of an external magnetic field (B_0), the spins are randomly oriented and the total magnetization is null because the axis around which the spins precess is completely random and the *x*, *y* and *z* components cancel each other (36).

When these spins are placed under the influence of B_0, they will precess around an axis parallel to the direction of the field and they will align themselves into two energy states: one high-energy (anti-parallel to B_0) and one low energy (parallel to B_0).

The precession frequency (ν) of the nuclei is easily calculated using the Larmor equation (taking into account the gyromagnetic ratio of the nucleus considered, γ):

$$\gamma B_0 = \nu \qquad \text{Equation 3.1}$$

After the application of B_0, a RF pulse at the Larmor frequency and perpendicular to this field is applied, which will dishevel the spins of hydrogen that were aligned in a process called excitation and will tip the net magnetization vector from the longitudinal direction into the transverse plane. This causes the net magnetization to change over time in the transverse plane, generating the MR signal (37).

When the RF pulse is turned off, the MR signal created will decay over time. This phenomenon is called spin relaxation. There are two primary mechanisms that contribute to the loss of the MR signal: longitudinal relaxation and transverse relaxation. For a given substance in a magnetic field of a certain strength, the rates of longitudinal and transverse relaxation are given as time constants (37).

As they lose energy, excited spins in the high-energy state go back to their original low-energy state. This phenomenon is known as longitudinal relaxation (*Figure 3.1*) and the time constant associated with this process is called T_1. The amount of longitudinal magnetization, M_z, present at time t following an excitation point is given by Equation 3.2, where M_0 is the original magnetization. (37)

$$M_z = M_0\left(1 - e^{-t/T_1}\right) \qquad \text{Equation 3.2}$$

After the net magnetization is tipped into the transverse plane by an excitation pulse, it is initially coherent, in the sense that all of the spins in the sample are precessing around the main field vector at about the same phase. That is, they begin their precession within the transverse plane at the same starting point. Over time, the coherence between the spins is gradually lost and they become out of phase. This phenomenon is known as transverse relaxation *Figure 3.1*. The signal lost by this mechanism is called spin-spin decay, described in Equation 3.3, and is characterized by a time constant known as T_2.

$$M_{xy} = M_0 e^{-t/T_2} \qquad \text{Equation 3.3}$$

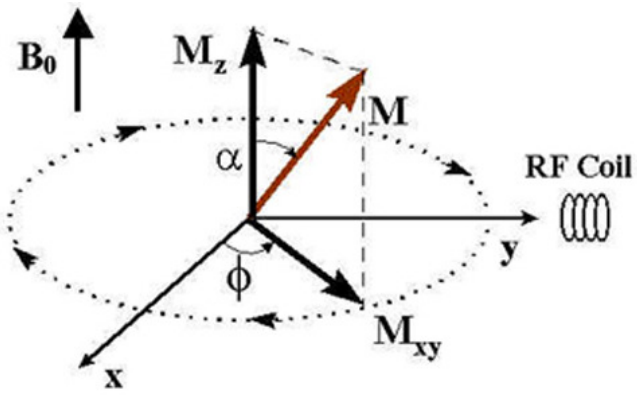

Figure 3.1 – The magnetization M precesses around the z axis with the angle α, and it is divided into the longitudinal component, M_z and the transverse component M_{xy}. A RF coil is placed in the y axis direction to collect the MR signal. (38)

An additional, extrinsic source of differential spin effects is the external magnetic field. Because each spin precesses at a frequency proportional to its local field strength, variations in field from location to location cause spins at different spatial locations to precess at different frequencies, also leading to the loss of coherence. The combined effects of spin-spin interaction and field inhomogeneity lead to signal loss known as T_2* decay, characterized by the time constant T_2*. Note that T_2* decay is always faster than T_2 decay alone, since it includes not only spin-spin interaction but also the additional factor of field inhomogeneity. (37)

When the nuclear magnetic moment is perturbed into the transverse plane the signal obtained by its rephasing will be an oscillating signal that decays away under an exponencial envelope - Free Induction Decay (FID). (39)

3.2 MR pulse sequences

In this sub-chapter a brief introduction to image formation and to pulse sequences is done. Even if it is not this work's objective it is important to bear in mind some of these considerations. For a more extensive reading on this matter it is recommended Bernstein et al (40).

The image formation in MR involves the spatial codification of the signal through various magnetic field gradients. The acquired images may be weighted in diverse parameters depending on the pulse sequence used, and are collected in a spatial frequency space, the *k-space*. At the end of the scan, the data is mathematically processed to produce the final image by performing a 2D inverse Fourier transform.

The *spin-echo* (SE) sequence is one of the most used and is made up of a series of events: 90º pulse – 180º rephasing pulse at TE/2 (Echo Time) – signal reading at TE. This series is repeated at each time interval TR (Repetition Time). With each repetition, a *k-space* line is filled, thanks to a different phase encoding. The 180º rephasing pulse compensates for the constant field heterogeneities to obtain an echo that is weighted in T_2 and not in T_2*. (40)

The *gradient-echo* (GRE) sequence has some differences when compared to the SE sequence, especially regarding the flip angle, which is usually below 90º and the absence of a 180º RF pulse, reducing the time needed to acquire the images, since the longitudinal magnetization component is never inverted by an RF refocusing pulse. Therefore it does not require a long recovery T1 and GRE pulse sequences can use short TR. Adding to the advantage that the less amount of time required represents, there is also another advantage associated with GRE sequence - the fact that it provides images with hypertense blood signal (40).

However, and in order to be used also in functional studies, several sequences have been developed with the objective of reducing even more the acquisition time.

Echo-planar imaging (EPI) uses a different method for data collection. EPI sequences are characterized by a series of gradient reversals in the readout direction. Each reversal produces a gradient echo, with the second half of one readout period being rephased by the first half of the subsequent readout period. Because of the use of gradient echoes, EPI sequences are very sensitive to *T2** effects. The raw data matrix is acquired in a rectilinear, zigzag flashion (*Figure 3.2*) (40).

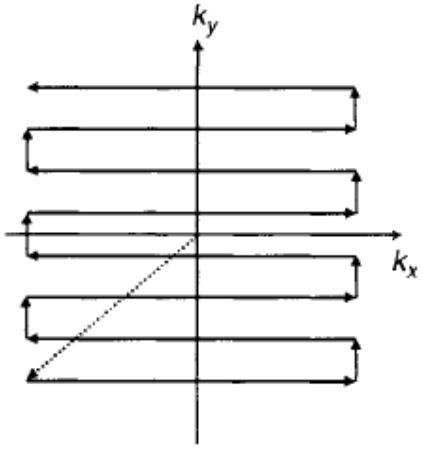

Figure 3.2 – Graphic of EPI k-space coverage order during one TR (40).

Gradient-Echo EPI (GRE-EPI) pulse sequence starts with a selective excitation pulse to produce a FID signal. The flip angle is set to 90º to maximize the Signal to Noise Ratio (SNR). In GRE-EPI each *k-space* line along the phase-encoded direction is acquired at a different TE (40). The scheme of the GRE-EPI pulse sequence may be seen in *Figure 3.3*.

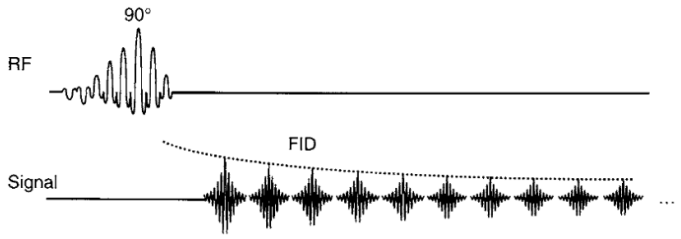

Figure 3.3 – GRE-EPI pulse sequence scheme – After the application of the 90º excitation pulse it may be seen the FID signal that is acquired (adapted from (40))

Spin-Echo EPI (SE-EPI) pulse sequence comprises two selective RF pulses, one excitation pulse with a typical flip angle of 90º and a refocusing pulse with a flip angle of 180º. The two RF pulses generate a SE and during the time window around its peak EPI readout and phase-encoding waveforms are played to produce a series of spatially encoded gradient echoes. Like GRE-EPI, SE-EPI relies on gradient echoes to sample *k-space* lines, except that the gradient echoes are formed under the envelope of a SE instead of a FID (*Figure 3.4*) (40).

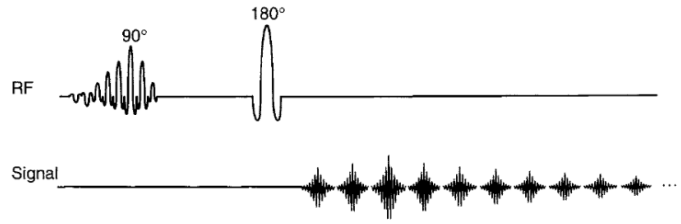

Figure 3.4 – SE-EPI pulse sequence scheme – Unlike GRE-EPI in SE-EPI we may see two pulses applied that produce a series of waveforms (adapted from (40)).

With the use of a refocusing pulse, the prephasing gradient in either the readout or the phase-encoded direction does not have to be played immediately before the readout or the phase-encoding gradient. In many implementations, the prephasing gradients are placed between the excitation and the refocusing pulses.

Images may be weighted in its relaxation times or even in proton density. For a T_1 weighted image in a SE sequence the TR and TE used are short, while in a T_2 weighted image the TR and TE used are long. Some brain images that illustrate this weighting are shown in *Figure 3.5*.

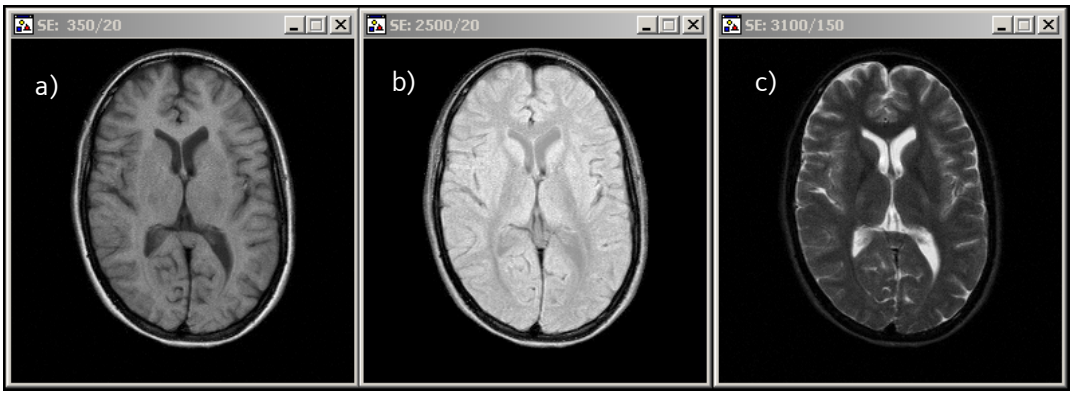

Figure 3.5 – Different contrasts a) T_1 weighted b) Proton-density weighted c)T_2 weighted[1]

3.3 Blood-Oxygenation Level Dependent fMRI

ASL is an innovative technique that addresses some of the main issues concerning the current gold standard for functional studies. Taking that in consideration, it is important to do a brief introduction to BOLD technique, even for comparative purposes.

Paramagnetic deoxyhemoglobin in venous blood is a naturally occurring contrast agent for MRI (41). It has been demonstrated that deoxyhemoglobin alters the proton signal from water molecules surrounding a blood vessel in GE MRI, producing BOLD contrast.

If an area of the brain becomes active through activation due to a certain task, its necessity of ATP will increase, as well as its need for oxygen and glucose. As a result, there is an increase in rCBF mainly in the activated area and consequently there will be an increase in the number of hemoglobin molecules.

When inside the lungs, hemoglobin has a great affinity to oxygen, but by leaving them this affinity changes and the oxygen molecules become more loosely and reversibly bonded to the iron atom that lies in the center of the heme molecule within the hemoglobin complex. (42)

When arriving to the tissues, the oxygen is released from the hemoglobin, leaving the electrons from the iron atom unpaired. This will modify the magnetic field near the deoxygenated hemoglobin.

Hemoglobin is paramagnetic when deoxygenated whereas oxyhemoglobin is diamagnetic so that presence of deoxyhemoglobin in a blood vessel causes susceptibility differences between the vessel and the tissue surrounding it. Such

[1] Images generated with the software *MR Image Expert*

susceptibility differences cause faster dephasing of the MR proton signal, leading to a reduction in the value of T_2*. In a T_2* weighted imaging experiment, the presence of deoxyhemoglobin in the blood vessels causes a darkening of the image in those voxels containing vessels.

It would be expected that with the increase of neural activity, and since oxygen consumption is increased, the level of deoxyhemoglobin in the blood would also increase, and the MR signal would decrease. However, what is actually observed is an increase in signal, which implies a relative decrease in deoxyhemoglobin. This is because upon neural activity, as well as the slight increase in oxygen extraction from the blood, there is a much larger increase in rCBF, bringing with it more oxyhemoglobin (*Figure 3.6*). Thus the bulk effect upon neural activity is a regional decrease in paramagnetic deoxyhemoglobin, and an increase in signal.

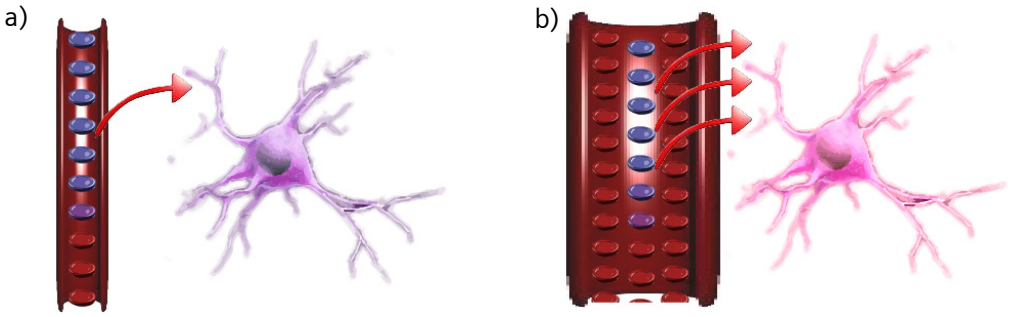

Figure 3.6 – Hemodynamic changes in neuronal activity. a) Rest b) Activation – Red circles represent oxyhemoglobin and its increase is well seen. The blue circles represent deoxyhemoglobin and its relative decrease is also patent in the scheme (adapted from (43)).

In conclusion, BOLD contrast does not reflect a single physiological process, but rather represents the combined effects of rCBF, CBV and $CMRO_2$. So, the BOLD signal observed is a sum of signals produced by separated neural events.

Soon after the stimulus applied, a slight depression is found. This initial dip in the BOLD signal is the result of the increased metabolic activity precisely at the prior to the increase of blood flow, i.e. the local consumption of oxygen increases causing a decrease in the fraction of oxyhemoglobin in relation to the concentration of deoxyhemoglobin (*Figure 3.7*).

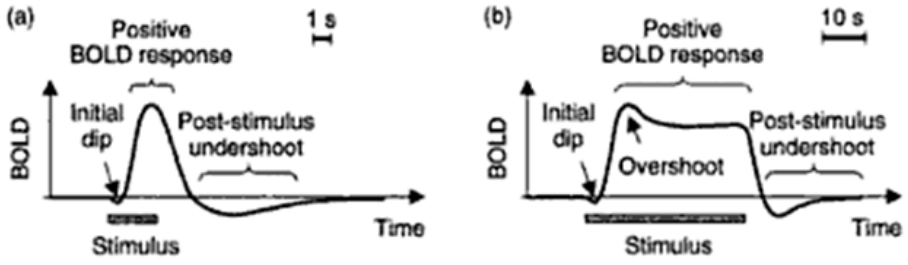

Figure 3.7 – Hemodynamic response function (HRF) - a) response to brief stimulus b) response to long stimulus. (adapted from (44))

Thus, rCBF increases as well as the concentration of oxygen in the blood, giving rise to a positive response in the BOLD signal approximately 5-8 seconds after the stimulus applied. Finally, after the stimulus ceases, it is observed a decrease in the BOLD signal, the post-stimulus undershoot, due to a slower response by the CBV compared to the rCBF (*Figure 3.7*) (44).

3.4 Perfusion fMRI – Arterial Spin Labeling

The non-invasive characteristic of ASL has uncovered a whole new world into the study of human brain function and perfusion physiology. This new technique allows to obtain quantitative information about tissue perfusion by evaluating the rCBF. This is done by assessing the inflow of magnetically tagged arterial water into an imaging slice. Following this assessment, the rCBF is measured from the signal intensity differences of the MR with and without tagging, thereby subtracting out the static magnetization of the imaging slice. (45)

ASL utilizes as tracer the water from the arterial blood, therefore endogenous and diffusible, while other techniques use exogenous, non-diffusible tracers which may not provide Blood-Brain Barrier (BBB) permeability depending on its properties. First, arterial blood water is magnetically labeled just below the region (slice) of interest by applying a 180° degree RF inversion pulse. The result of this pulse is inversion of the net magnetization of the blood water. After a period of transit time, which is a physiological parameter that reflects the time interval for the labeled spins to reach the brain region of interest (46), the labelled water spins arrive to the region of interest and exchange with tissue water. The inflowing inverted spins within the blood water alter total tissue magnetization, reducing it and, consequently, the MR signal and the image intensity. During this time, an image is taken (called the tag image). The experiment is then repeated without labeling the arterial blood to create another image (called the control

image). The control image and the tag image are then subtracted to produce a perfusion image. This image will reflect the amount of arterial blood delivered to each voxel of the slice after a certain transit time.

3.4.1 Arterial Spin Labeling Techniques – PASL and CASL

There are two main types of ASL techniques available in the market: Pulsed ASL (PASL) and Continuous ASL (CASL). Within this last one, there is also a variation which is the pseudo-Continuous ASL (pCASL). However, the current work will only focus on the first one.

The PASL approach labels a thick slab of arterial blood at a single instance in time, and the imaging is performed after a time long enough for that spatially labeled blood to reach the tissue and exchange at the region of interest as seen in *Figure 3.8*. (47)

In 1994, Edelman proposed the first pulsed ASL scheme, known as Echo Planar Imaging and Signal Targeting with Alternating Radiofrequency (EPISTAR). (48)

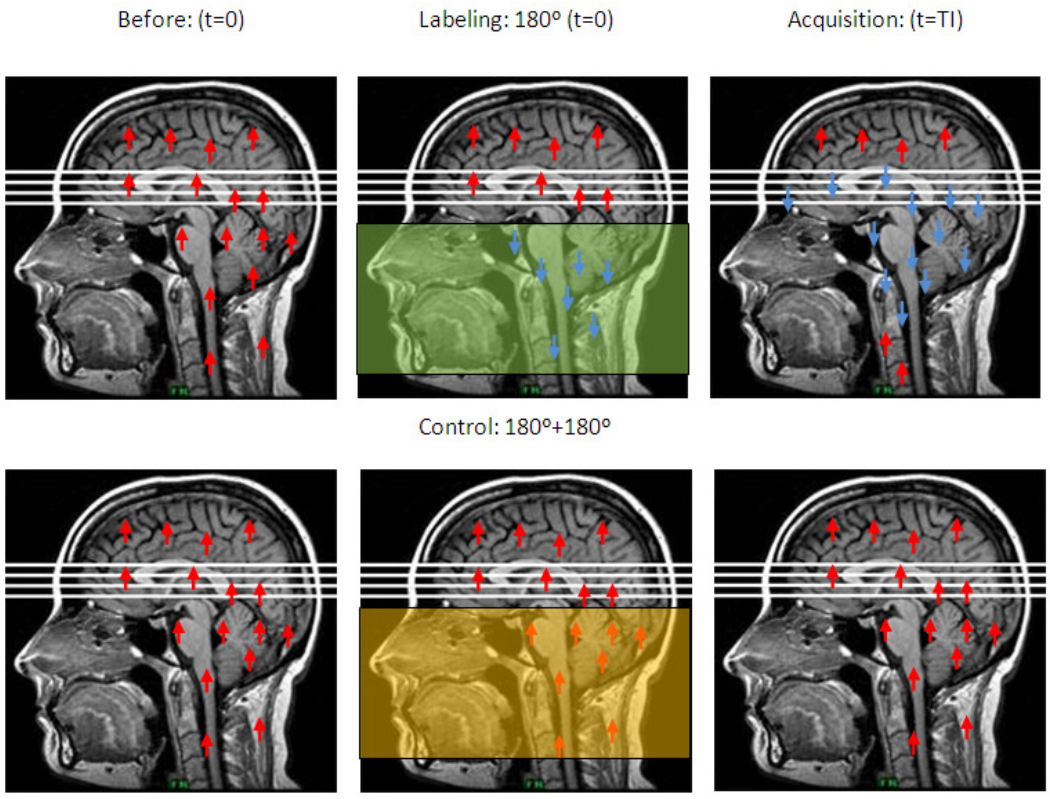

Figure 3.8 – The EPISTAR PASL sequence, which labels everything at once and uses two 180° + 180° = 0° pulses for the control images. As it may ben seen in the top sequence, an inversion pulse (green) is applied and the signal generated by the inverted spins (blue) is acquired at t=TI. On the bottom sequence the inversion pulse is not applied (orange) and the spins (red) are not inverted, generating a control image. (adapted from (47))

Shortly after this sequence was released, an alternative to this asymmetric method of labeling was proposed by Kim et al. (49), who named it Flow Alternating Inversion Recovery (FAIR). In this approach, the label is symmetrically applied using a non-selective inversion pulse, while the control employs a concomitant slice selective gradient pulse (*Figure 3.9*).

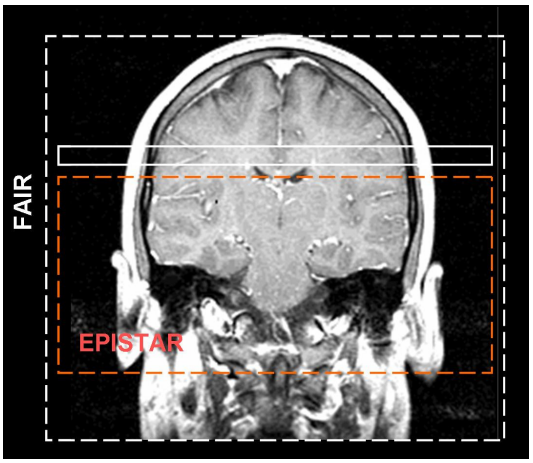

Figure 3.9 – The FAIR PASL sequence compared with EPISTAR sequence. EPISTAR sequence is described in Figure 3.8. For the FAIR sequence it is possible to view the position of the applied inversion label (adapted from (49)).

There is also one third technique, named Proximal Inversion with a Control for Off-Resonance Effects (PICORE) that was developed by Wong et al. (50), and uses a labeling scheme similar to EPISTAR. The only difference is that the inversion slab in the control acquisition was replaced by an RF pulse applied at the same frequency as in the label experiment but in the absence of a magnetic field gradient. (50)

In CASL, arterial blood water is continuously and selectively labeled as it passes through a labeling plane, typically applied at the base of the brain. In this case the spins are labeled using an external coil. Theoretically, CASL has higher Signal-to-Noise Ratio (SNR) than PASL, but it is limited to transmit/receive coils due to high radiofrequency duty cycle. A modification of CASL has therefore been introduced in order to address the fact that external coils are not always available, the pCASL. (51) The method consists of acquiring both control and tag images immediately after a labeling period that matches the arterial transit time. (52) (53)

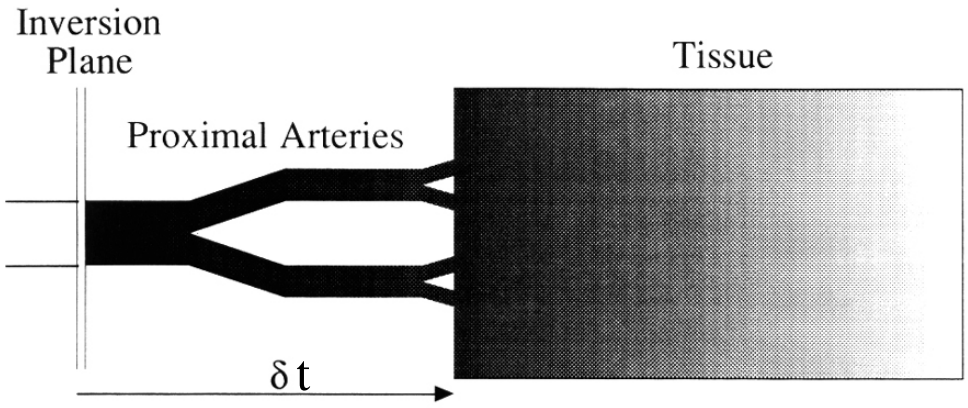

Figure 3.10 – CASL sequence scheme. In CASL there is a continuous inversion pulsed applied in the Inversion Plane. After a period of time δt in which the blood arrives to the acquisition plane the signal is acquired. The signal will weaken as the labeled water in the blood moves through the tissue (54).

Comparing both spin labeling schemes, although CASL provides stronger perfusion contrast, it is more difficult to implement than PASL because of its hardware demands – the external coil, and it deposits a higher level of RF power into the subject.

3.4.2 Perfusion Quantification

A general kinetic model for perfusion quantification was developed by Buxton et al. (55). This model relates the magnetization that is carried into the voxel by arterial blood, magnetization difference $\Delta M(t)$, with the perfusion in that voxel. Then, the amount of magnetization in the tissue at a time t will depend on the history of delivery of magnetization by arterial flow and clearance by venous flow and longitudinal relaxation. $\Delta M(t)$ can be described as a sum over the history of delivery of magnetization to the tissue weighted with the fraction of that magnetization that remains in the voxel. After the inversion pulse, the arterial magnetization difference is $2\alpha M_{ob}$, where M_{ob} is the equilibrium magnetization of arterial blood and the factor α accounts for incomplete inversion during the tagging pulse: α is the fraction of the maximum possible change in the longitudinal magnetization that was achieved. The amount delivered to a particular voxel between t' and $t' + dt'$ is $2\alpha M_{ob} f c(t')$, where f is the CBF (expressed in units of ml of blood per ml of voxel volume per second) and $c(t')$ is the delivery function, which is the normalized arterial concentration of magnetization arriving at the voxel at time t'. The fraction of magnetization that remains at time t is $r(t - t')m(t - t')$ being $r(t)$ the residue function and $m(t)$ the magnetization relaxation function. (55)

Then,

$$\Delta M(t) = 2M_{ob} f \int_0^t c(t')r(t-t')m(t-t')dt'$$

$$= 2M_{ob} f\{c(t) * [r(t)m(t)]\} \qquad \text{Equation 3.4 (55)}$$

where * denotes convolution.

There are some basic assumptions that have been taken into account in order to create this model:

1. The arrival of labeled blood at a particular voxel is assumed to be via uniform plug flow, so that before an initial transit delay Δt, no labeled blood arrives, between $t = \Delta t$ and $t = \Delta t + \tau$ (being τ the time width of the label), the arriving blood is uniformly labeled; and for $t > \Delta t + r$, the arriving blood is again unlabeled.
2. The kinetics of water exchange between tissue and blood are assumed to be described by single compartment kinetics. The essential assumption of single-compartment kinetics is that whatever subcompartments may exist within the tissues are undergoing such rapid exchange of water that their concentration ratios remain constant even though the total tissue concentration is a function of time.
3. After the inversion pulse, the magnetization initially decays with the relaxation time of blood, T_{1b}, but after the labeled water molecules have reached the tissue voxel, the magnetization is assumed to decrease with the relaxation time of the tissue, T_1.

Thus, the standard model can be summarized as:

$$\begin{cases} c(t) = 0 & 0 < t < \Delta t \\ \alpha e^{-\frac{t}{T_{1b}}}\ (pulsed) & \Delta t < t < \tau + \Delta t \\ \alpha e^{-\frac{\Delta t}{T_{1b}}}\ (continuous) & \Delta t < t < \tau + \Delta t \\ 0 & \tau + \Delta t < t \end{cases} \qquad \text{Equation 3.5 (55)}$$

Applying these assumptions to Equation 3.4 leads to the following expression for the PASL difference signal:

$$\Delta M(t) \begin{cases} 0 & 0 < t < \Delta t \\ 2M_{0B} f(t-\Delta t)\alpha e^{-\frac{t}{T_{1b}}} q_p(t) & \Delta t < t < \tau + \Delta t \\ 2M_{0B} f\tau\alpha e^{-\frac{t}{T_{1b}}} q_p(t) & \tau + \Delta t < t \end{cases} \qquad \text{Equation 3.6 (55)}$$

with,

$$q_p(t) = \frac{e^{kt}\left(e^{-k\Delta t} - e^{-kt}\right)}{k(t-\Delta t)} \qquad \Delta t < t < \tau + \Delta t$$

$$= \frac{e^{kt}\left(e^{-k\Delta t} - e^{-k(\tau+\Delta t)}\right)}{k\tau} \quad \tau + \Delta t < t \qquad \text{Equation 3.6 (55)}$$

$$k = \frac{1}{T_{1b}} - \frac{1}{T_1'}$$

$$\frac{1}{T_1'} = \frac{1}{T_1} + \frac{f}{\lambda}$$

Under the normal parameter range, and for $t > dt + \tau$, $q(t)$ is close to the unity.

The parameters Δt and τ are both dependent of vessel geometry and distribution of flow velocities. M_{OB} and T_{1B} are spatially invariant constants that can be estimated. Two alternative modifications (QUIPSS and QUIPSS II) of basic PASL pulse sequence were introduced by Wong et al. (56) in order to eliminate the dependence of the perfusion value from Δt. Moreover, the τ value started to be defined by the user. These modifications are described in more detail in the following subchapter. However, for quantification purposes, the main conclusion drawn from this new introduction is that if the magnetization difference signal is acquired at a time t after $\Delta t + \tau$, then the signal is independent of both Δt and τ and is given by the last branch of the standard kinetic model with $q(t) = 1$, i.e.: If,

$$TI_1 \leq t \qquad \text{Equation 3.7 (55)}$$

$$TI_2 \geq TI_1 + \Delta t$$

Being TI_1 the time of application of the saturation pulse and TI_2 the time when the image is acquired, and:

$$\Delta M(TI_2) = 2M_{0B} f TI_1 e^{-TI_2/TI_{1b}} \qquad \text{Equation 3.8 (55)}$$

That can be rearranged in order to calculate the CBF:

$$CBF = \frac{\lambda \Delta M}{2\alpha M_0 TI_1 e^{-TI_2/T_{1b}}} \qquad \text{Equation 3.9 (55)}$$

Where M_0 is the tissue magnetization, $\lambda = \frac{M_0}{M_{0b}}$, being M_{0b} the equilibrium magnetization of the arterial blood.

In *Figure 3.11* are shown the effects of varying the parameters that are used in Equation 3.9 and how it may affect the PASL signal that is being calculated.

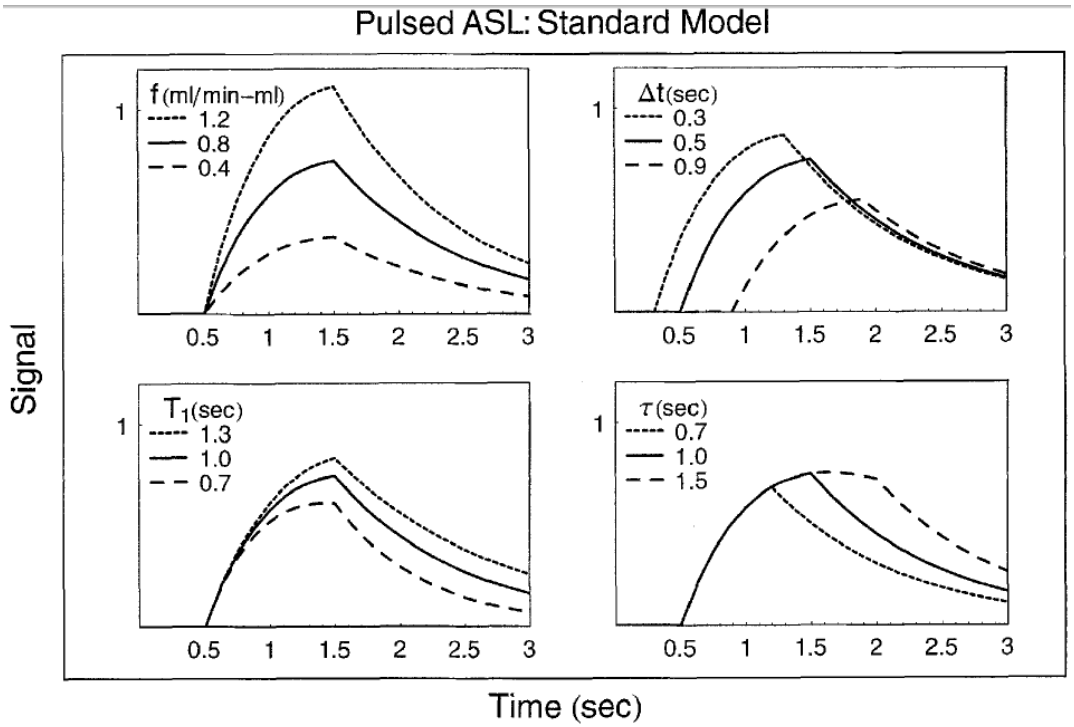

Figure 3.11 - Theoretical curves of pulsed ASL signal versus time calculated from Equation 3.9. (55)

Parameters for solid curve in each plot are f = 0.8 ml/min-ml, Δt = 0.5 s, τ = 1.0 s, and $T1$ = 1.0 s. Each panel illustrates the effect of varying one of these parameters: perfusion f (upper left), transit delay Δt (upper right), tissue relaxation time $T1$ (lower left), and duration of arrival of tagged blood τ (lower right). After the initial transit delay Δt, the ASL curve is proportional to local perfusion at all time points, but the early times are also sensitive to the local value of Δt and the later times are sensitive to the local T_1 (55)

3.4.3 ASL Pulse Sequences

For whatever the sequence used, the ASL difference signal (control-tag image) is approximately proportional to the perfusion. However, several misleading factors, as explained previously, have been reported that complicate the calculation of a quantitative rCBF map.

The ASL sequence pulse used in this work is commercially available by *SIEMENS* – PICORE Q2TIPS.

QUIPSS II is a PASL technique for improving the quantification of perfusion imaging by minimizing two major systematic errors: the variable transit delay from the distal edge of the tagged region to the imaging slices, and the contamination by intravascular signal from tagged blood that flows through the imaging slices. However, residual

errors remain due to incomplete saturation of spins over the slab-shaped tagged region by the QUIPSS II saturation pulse, and spatial mismatch of the distal edge of the saturation and inversion slice profiles. By replacing the original QUIPSS II saturation pulse with a train of thin-slice periodic saturation pulses applied at the distal end of the tagged region, the accuracy of perfusion quantification is improved. (57)

The QUIPSS II with thin-slice TI_1 periodic saturation sequence (Q2TIPS) addresses both of the sources of errors of QUIPSS II. By applying Q2TIPS, the accuracy of perfusion measurements is improved. Figure 3.12 shows the Q2TIPS pulse sequence and positions of the in-plane presaturation slab, the inversion-tagged region, the periodic saturation slice, and the imaging slices.

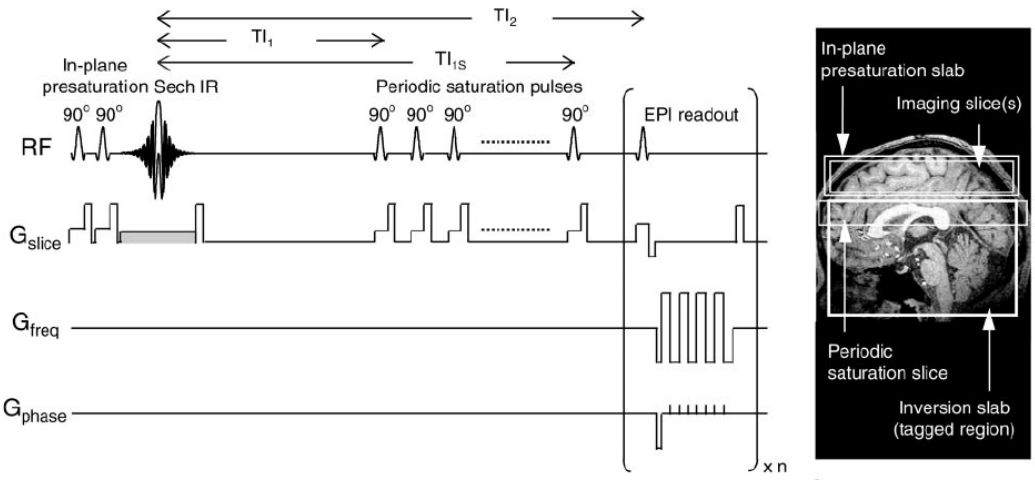

Figure 3.12 – Pulse sequence for Q2TIPS. On the right are shown the locations of the in-plane pre-saturation slab, the imaging slice(s), periodic saturation slice and inversion slab used in the PICORE labeling scheme. Double in-plane 90° presaturation pulses are followed by a hyperbolic secant inversion tagging pulse. The gradient lobe in gray is alternately applied for tag and control states. The first inversion time TI_1 allows the inverted arterial spins to flow to the imaging slab. Periodic saturation pulses applied from TI_1 to TI_{1S} (TI_{1S} is the stop time) consist of a train of 90° excitation pulses each followed by a crusher gradient that eliminates the signal from the large feeding arteries (58). Single or multislice EPI acquisition is applied at TI_2. (57)

In the control measurement, the inversion pulse is applied off-resonance, with a symmetrical frequency relative to the imaging region, such that no inversion occurs in the labeling slab but the same off-resonance effects are present in the imaging slices. The off-resonance effects should therefore be cancelled out on the difference image between control and tag. On the right image are shown the locations of the in-plane presaturation slab, imaging slice(s), periodic saturation slice, and inversion slab used in the PICORE tagging scheme. (57)

4 Methods

The data used for this study has been previously acquired and processed for a different study (59). In the next sections, besides presentation of the data processing steps specific for this work, acquisition and pre-processement methodology will also be summarised for a better understanding of the results.

4.1 Subjects

Functional ASL data in response to a motor task was collected from fifteen adult volunteers (six females, mean age 25.6, range 22-51 years old). Participants were selected not taking into account any type of consideration to ethnicity, race or any other criteria. All subjects were right handed and none of them had a history of major medical, psychiatric or neurological disorders. The experiments were not carried out in the same day neither in the same period of the day, and subject's state was not controlled.

This study was approved by the local ethical committee, and written informed consent was obtained from all volunteers.

4.2 Image Acquisition

Images were acquired on a 3 Tesla equipment – Magnetom Verio MRI System from *SIEMENS* in Hospital da Luz.

The imaging sessions included two different functional ASL protocols, a whole brain EPI and a high-resolution anatomical image.

The whole brain EPI was acquired using the parameters displayed in Table 4.1:

Table 4.1 – Acquisition parameters – EPI readout

EPI readout								
Protocol	TR (ms)	TE (ms)	FA	Num. Vols.	Num. Slices	Slice Thick. (mm)	Matrix Size	FOV (mm^2)
ASL #1	2500	25	90º	91+91	9	8	64 × 64	256 × 256
ASL #2	2500	11	90º	101	9	6	64 × 64	256 × 256

It is important to bear in mind that for ASL Protocol 1 two different images were acquired, one for the resting state and one for the activation state.

The ASL sequence used in this study was PICORE Q2TIPS, commercialized by Siemens. The main acquisition parameters are displayed in Table 4.2:

Table 4.2 – Acquisition parameters – PICORE Q2TIPS

Tagging Sequence: PICORE Q2TIPS						
Protocol	TI_1 (ms)	TI_{1S} (ms)	TI_2 (ms)	Inv. Slab Thick. (cm)	Gap (cm)	Time Acq. (min)
ASL #1	700	1600	1800	1	1.88	7:35
ASL#2	700	1600	1800	1	1.88	4:13

This sequence of Protocol 2 was composed by a block design of five alternate cycles of OFF/ON blocks with 25 sec each. For this scan a total of 101 interleaved tag/control volumes were acquired.

The high-resolution anatomical image was acquired using a 3D T_1 weighted sequence – Magnetization Prepared Rapid Acquisition Gradient Echo (MPRAGE) which provided 160 sagittal slices with 1.0mm of thickness, 256 × 240 mm^2 Field of View (FOV) and a matrix size of 256 × 240, yielding an isotropic spatial resolution of $1mm^3$. Further scan parameters were TR = 2250 ms, TE = 2.26 ms, TI = 900 ms and a flip angle of 90º.

4.3 ASL Image Processing

ASL images were processed in order to obtain quantitative perfusion maps. Firstly, and still in the MRI scanner, images were motion corrected using Prospective Motion Correction (PACE) from Siemens Erlangen (60).

In order to produce Magnetization Difference (*ΔM*) maps, consecutive control and tag images from the motion corrected ASL timeseries were subtracted and the difference images obtained were time averaged using Shell Script Linux routines from a previous work.

4.3.1 Perfusion Quantification Method

Using the Q2TIPS acquisition sequence, perfusion quantification maps can be obtained using Equation 3.9, which is adapted to the specific case of a single-TI ASL sequence:

$$CBF = \frac{\lambda \Delta M}{2\alpha M_0 TI_1 e^{-TI_2/T_{1b}}} \qquad \text{Equation 3.9}$$

Where $\lambda = M_0/M_{0b}$, being M_0 the tissue magnetization and M_{0b} the equilibrium magnetization of arterial blood. A value for Blood-Brain Partition Coefficient $\lambda = 0.9$ was used. α is the fraction of the maximum possible change in the longitudinal magnetization that was achieved and a value of $\alpha = 0.9$ was used to calculate CBF. T_{1b} is the longitudinal relaxation time of the blood and has a value of 1.5s at 3T (61).

The Equation 3.9 presented above was not, however, applied linearly, as corrections of the slice readout timing, TI_2 were taken into account. The slices acquired differ from each other by a factor of time Δt. This information was taken from the DICOM header to correct the slice acquisition timing effect.

This quantification method was applied to the *ΔM* maps, using already implemented Shell Script Linux routines, and perfusion maps were obtained for each subject and functional protocol.

4.3.2 CBF Quantification in Activation and Rest Conditions

In Protocol 1 two images per subject were available to calculate perfusion, one for the activation and one for the rest period. Therefore, each of these images (rest and activation) was used to obtain the corresponding perfusion map. For this calculation two Linux Shell Scripts were written (see Appendix A – Sections A.1 and A.2).

In Protocol 2 only one image per subject containing interleaved periods of activation and rest was available to calculate perfusion. Firstly the rest/activation cycles were split

and all the rest cycles were concatenated in a rest image and all the activation cycles in an activation image. The Linux Shell Script used in this calculation is available in Appendix A – Section A.3.

Four perfusion maps were generated for each subject taking into account the activation (ACT) and rest (REST) periods for each protocol:

Protocol 1

- CBFACT1
- CBFREST1

Protocol 2

- CBFACT2
- CBFREST2

The difference between the CBF of activation and rest was calculated in Equation 4.1:

$$\Delta CBF = CBFACT - CBFREST \quad \text{Equation 4.1}$$

However, the variation is shown in percentage, so the Equation 4.2 was used:

$$\%\Delta CBF = \frac{CBFACT - CBFREST}{CBFREST} \times 100 \quad \text{Equation 4.2}$$

4.4 Perfusion Maps Registration and Brain Territories Segmentation

In order to properly study the brain in detail it was segmented by levels of hierarchy using the information available at *www.talairach.org/labels.txt* and perfusion was calculated for each of these regions displayed below. Each of these regions has an associated label. The document available at *www.talairach.org/labels.txt* was run several times in order to gather all the labels for each region and then all of them were introduced in a Linux Shell routine to be concatenated and the image with the associated region was created (See Appendix A – Section A.4).

Level 1: Hemisphere

- Left Cerebrum
- Right Cerebrum
- Left Cerebellum
- Right Cerebellum
- Left Brainstem
- Right Brainstem
- Inter-Hemispheric

Level 2: Lobe

- Culmen
- Anterior Lobe
- Frontal Lobe
- Frontal-Temporal Space
- Limbic Lobe
- Medulla
- Midbrain
- Occipital Lobe
- Parietal Lobe
- Pons
- Posterior Lobe
- Sub-lobar
- Culmen of Vermis
- Temporal Lobe

Level 3: Gyrus

- Angular Gyrus
- Anterior Cingulate
- Caudate
- Cerebellar Lingual
- Cerebellar Tonsil
- Cingulate Gyrus
- Claustrum
- Cuneus
- Declive

- Declive of Vermis
- Extra-Nuclear
- Fastigium
- Fourth Ventricle
- Fusiform Gyrus
- Inferior Frontal Gyrus
- Inferior Occipital Gyrus
- Inferior Parietal Lobule
- Inferior Semi-Lunar Lobule
- Inferior Temporal Gyrus
- Insula
- Lateral Ventricle
- Lentiform Nucleus
- Lingual Gyrus
- Medial Frontal Gyrus
- Middle Frontal Gyrus
- Middle Occipital Gyrus
- Middle Temporal Gyrus
- Nodule
- Orbital Gyrus
- Paracentral Lobule
- Parahippocampal Gyrus
- Postcentral Gyrus
- Posterior Cingulate
- Precentral Gyrus
- Precuneus
- Pyramis
- Pyramis of Vermis
- Rectal Gyrus
- Subcallosal Gyrus
- Sub-Gyral
- Superior Frontal Gyrus
- Superior Occipital Gyrus
- Superior Parietal Lobule
- Superior Temporal Gyrus
- Supramarginal Gyrus
- Thalamus
- Third Ventricle
- Transverse Temporal Gyrus
- Tuber
- Tuber of Vermis
- Uncus
- Uvula
- Uvula of Vermis

Level 4:

- Cerebro-Spinal Fluid
- Gray Matter
- White Matter

Level 5:

- Amygdala
- Anterior Commissure
- Anterior Nucleus
- Brodmann areas
- Caudate Body
- Caudate Head
- Caudate Tail
- Corpus Callosum
- Dentate
- Hippocampus
- Hypothalamus
- Lateral Dorsal Nucleus
- Lateral Geniculum Body
- Lateral Globus Pallidus
- Lateral Posterior Nucleus
- Mammillary Body
- Medial Dorsal Nucleus
- Medial Geniculum Body
- Medial Globus Pallidus
- Midline Nucleus
- Optic Tract
- Pulvinar
- Putamen
- Red Nucleus
- Substania Nigra
- Subthalamic Nucleus
- Ventral Anterior Nucleus
- Ventral Lateral Nucleus
- Ventral Posterior Lateral Nucleus
- Ventral Posterior Medial Nucleus

Firstly registration of these regions is done in standard Talairach space, where the brain is segmented in several labels, and then registered back into ASL space to calculate the perfusion maps. This registration process is crucial in order to work in the same space where the images are acquired and to obtain a correct evaluation of brain perfusion in ASL space. However, this transition is not made directly, as several steps were taken in order to make a correct registration:

$$Talairach \rightarrow MPRAGE \rightarrow BOLD \rightarrow ASL$$

A Linux Script was designed in order to perform this registration systematically and can be consulted in Appendix A – Section A.5.

Finnally, for each of the regions presented above the four perfusion maps were calculated. The regions calculated were binarized and applied as masks to the perfusion maps already obtained. A Linux Script was written in order to obtain perfusion quantification in all subjects and can be consulted in Appendix A – Section A.6.

5 Results

In this chapter all the results are presented and statistical analysis is performed. Firstly, mean perfusion values are obtained taking into account the considered perfusion maps and then compared between both protocols.

Secondly, all the perfusion results for the regions considered in each level of segmentation done are displayed and statistical comparison between protocols is performed.

Inter-hemispheric comparison is then performed for all the regions considered and values obtained are compared with the ones theoretically expected.

Finally perfusion is measured and studied with more detail in the region that is supposedly activated considering the stimulus used in this work – right hand motor stimulus.

5.1 CBF Quantification – Comparison between Protocols

For perfusion quantification only the rest perfusion maps were considered once only the baseline perfusion is being measured. The values for the fifteen subjects were

calculated after applying a Gray Matter (GM) binary mask to perfusion maps *CBFREST1* and *CBFREST2* and are displayed in Table 5.1.

The perfusion map calculated *CBFREST1* for a male subject is displayed in *Figure 5.1*:

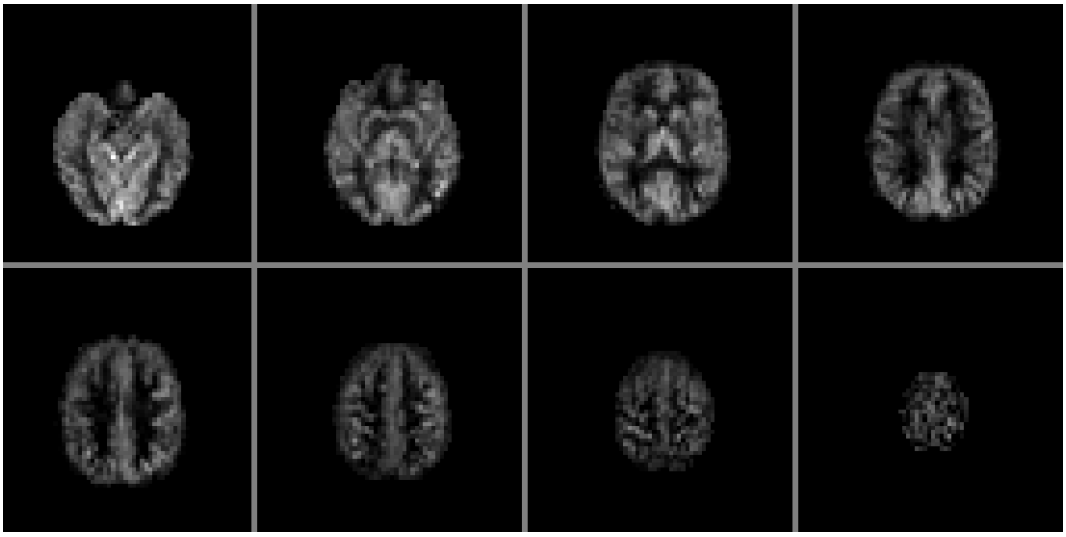

Figure 5.1 – Perfusion map from a male subject. The nine axial slices are displayed from bottom to top. The ninth slice is not displayed as it does not present information.

Table 5.1 – Mean CBF values (ml/100g/min) in GM for each subject for both protocols

CBF mean values ± Standard Error (ml/100g/min)		
	Protocol 1	Protocol 2
Subject 1	63,0 ± 0,6	62,7 ± 0,8
Subject 2	73,3 ± 0,6	70,6 ± 0,8
Subject 3	52,1 ± 0,7	50,4 ± 0,8
Subject 4	67,6 ± 0,9	66,2 ± 0,8
Subject 5	71,2 ± 0,7	56,0 ± 0,9
Subject 6	70,7 ± 0,6	54,0 ± 0,8
Subject 7	65,6 ± 0,6	51,4 ± 0,7
Subject 8	78,0 ± 0,6	79,3 ± 0,8
Subject 9	61,0 ± 0,5	62,5 ± 0,7
Subject 10	65,5 ± 0,5	59,9 ± 0,7
Subject 11	89,3 ± 0,6	77,0 ± 0,7
Subject 12	69,8 ± 0,6	57,0 ± 0,8
Subject 13	60,6 ± 0,5	51,1 ± 0,7
Subject 14	60,7 ± 0,9	46,8 ± 0,7
Subject 15	35,0 ± 0,6	34,8 ± 0,5
Mean	65 ± 4	59 ± 4

As previously stated a normal CBF value is 60 ml/100g/min. As we can see from the results in Table 5.1 the mean values obtained for CBF quantification in this study are 65,564 ml/100g/min for Protocol 1 and 58,633 ml/100g/min for Protocol 2 which are very similar to the one expected. It is important also to compare the values obtained between both protocols and it may be considered that they are similar. Based on the intervals for Protocol 1 we have a range of values of [61; 69] and for Protocol 2 a range of [55; 63]. As it may be seen, these intervals intersect each other.

The results are summarized in *Figure 5.2*:

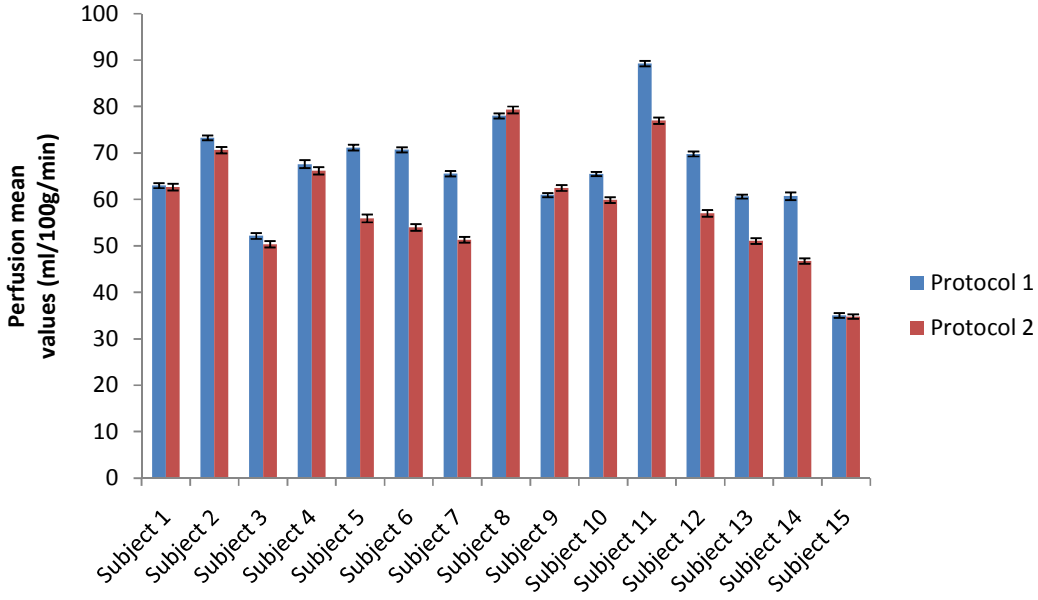

Figure 5.2 – Plot comparing mean perfusion values (ml/100g/min) for both protocols.

A *T Test* under the null hypothesis that the results are different between each other was performed and revealed significant differences in CBF values between both protocols (p=0,0007).

5.2 CBF Quantification – Brain Regions

In this second sub-chapter perfusion quantification for the brain regions described previously is obtained and compared between both protocols.

5.2.1 First level of segmentation - Hemisphere

In the first level of segmentation, brain was divided in the two hemispheres.

An example of a region designed – Left Cerebrum – is shown in *Figure 5.3*. As it was already explained, region segmentation was done in Talairach Standard Space (*Figure*

5.3 a)) and later registred to ASL Space (*Figure 5.3* b)) to be used as a mask in CBF quantification maps already calculated.

All the results for CBF values for this division are shown in Table 5.2 and a plot compiling the mean results obtained for perfusion in activation and rest for the regions considered is shown in *Figure 5.4*.

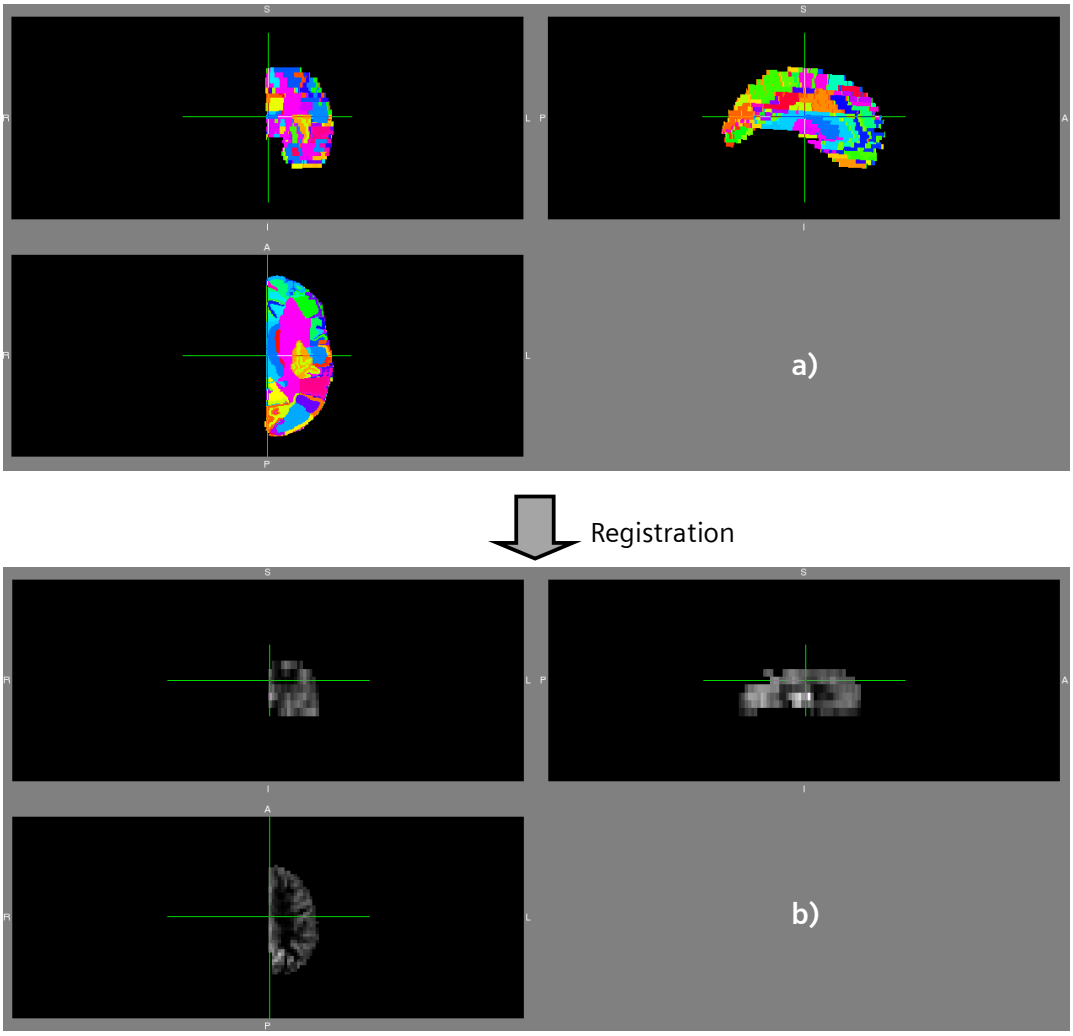

Figure 5.3 – Left Cerebrum in a) Talairach Standard Space b) ASL space – perfusion map

The mean perfusion values for all subjects are displayed in Table 5.2:

Table 5.2 – Mean perfusion values (ml/100g/min) in first level segmentation regions of the brain

CBF mean values ± Standard Error (ml/100g/min)			
		Protocol 1	Protocol 2
Left Cerebrum	Activation	69 ± 4	59 ± 4
	Rest	66 ± 4	56 ± 4
Right Cerebrum	Activation	67 ± 3	55 ± 3
	Rest	62 ± 3	55 ± 3
Left Cerebellum	Activation	138 ± 5	65 ± 7
	Rest	134 ± 5	67 ± 8
Right Cerebellum	Activation	134 ± 6	78 ± 8
	Rest	128 ± 5	79 ± 9

For comparative purposes, the results shown in Table 5.2 are displayed in a plot (*Figure 5.4*):

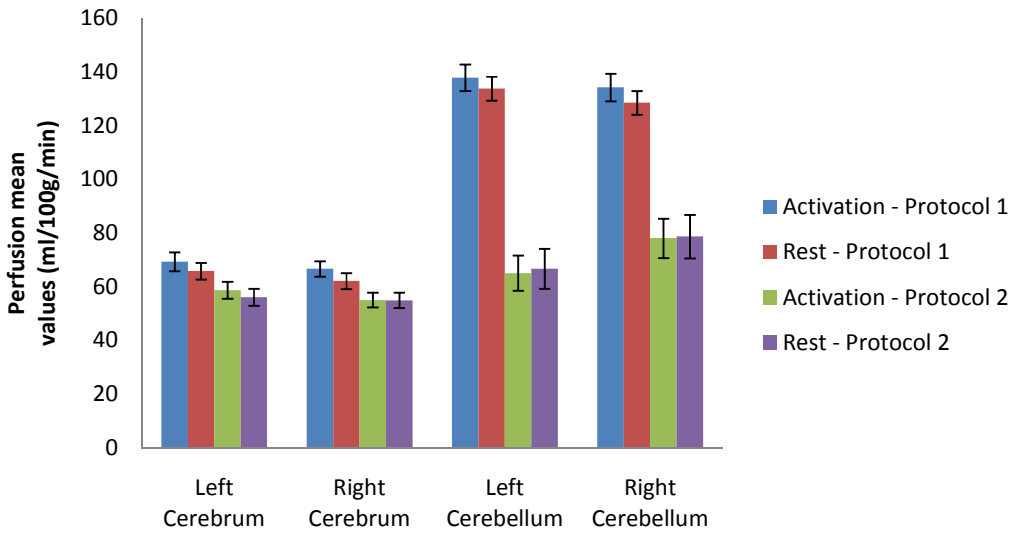

Figure 5.4 - Plot comparing mean perfusion values (ml/100g/min) for both protocols and for the two states in first segmentation level.

Information taken from *Figure 5.4* indicates a tendency for Protocol 1 to return higher values for perfusion than Protocol 2 especially for the Cerebellum. This might be explained by the higher coverage obtained with Protocol 1 which results in a higher number of Cerebellum voxels in these images; as it may be seen in Table 4.1, the slices considered for this Protocol are thicker than for Protocol 2 - Table 4.2.

5.2.2 Second level of segmentation - Lobe

In this second level of segmentation, the brain was divided in its lobes.

An example of a region designed – Left Temporal Lobe – is shown in *Figure 5.5* . As it was already explained, and alike it was done on previous analysis, region segmentation was done in Talairach Standard Space (a)) and later registred to ASL Space (b)) to be used as a mask in CBF quantification maps already calculated.

Perfusion values were obtained for all the regions considered and sub-divided regarding the hemisphere, as it may be seen in the information displayed in Table 5.3.

Two plots compiling the mean results obtained for perfusion in activation and in rest for the regions considered in both left and right hemispheres are shown in *Figure 5.6*.

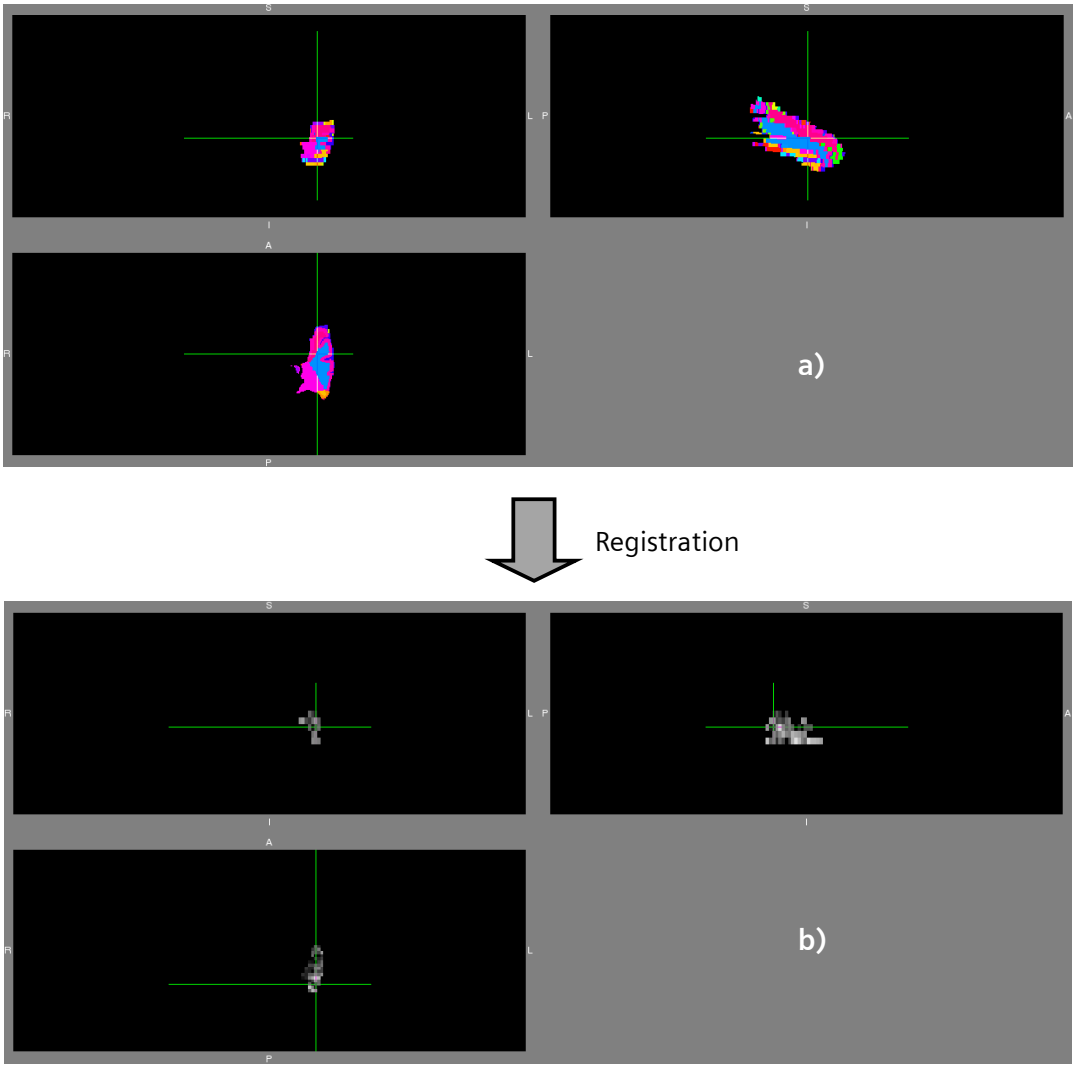

Figure 5.5 – Left Temporal Lobe in a) Talairach Standard Space b) ASL space – perfusion map

Registration was performed to all the regions considered and the perfusion results obtained are summarized in *Figure 5.6* and subsequently displayed in Table 5.3.

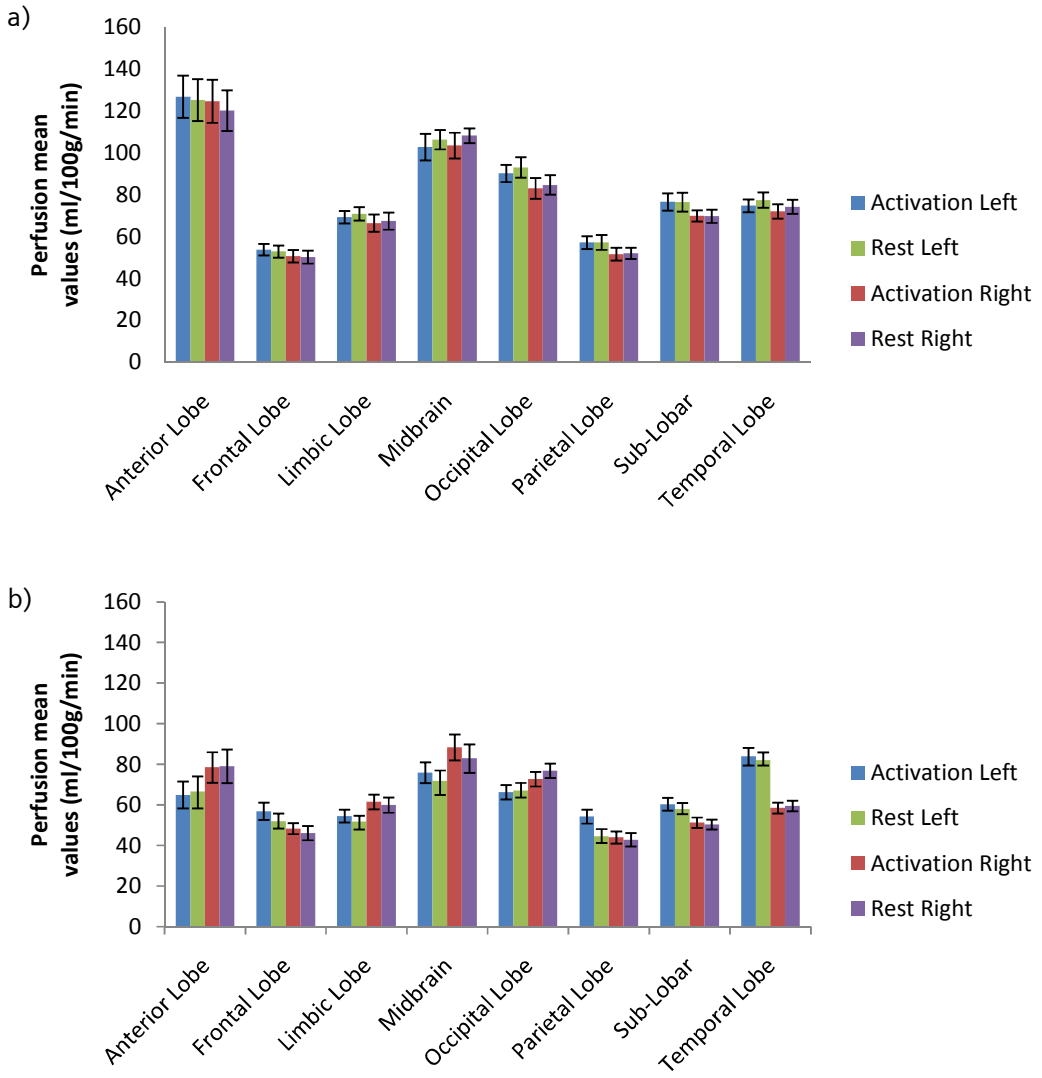

Figure 5.6 - Plots comparing mean perfusion values (ml/100g/min) for both protocols in second segmentation level for a) Protocol 1 b) Protocol 2

As it may be observed in *Figure 5.6* the analysis of the second level segmentation was also done regarding the hemisphere. By doing this it is possible to compare perfusion values in both sides of the brain and comparison is easily done in Table 5.3. In Protocol 1 higher values are obtained with special emphasis in the Anterior Lobe. When evaluating these results it is important to bear in mind the location of the activated hand motor cortex, which is located in the posterior area of the Frontal Lobe. As it may be observed in the results from Left Frontal Lobe in Protocol 2 there is a difference between Activation and Rest states of approximately 10% when the value expected for

PASL acquisitions is situated around 50% (62). This variation is due to the large area considered for this evaluation. As for a comparison with normal values a CBF in Frontal Lobe, which falls mainly in ACA area, around 50 ml/100g/min was expected (63). For Occipital Lobe, lying in PCA area, the theoretical value expected was 53 ml/100g/min (64) and for the Parietal Lobe, it was expected a value around 55 ml/100g/min (65). Finnally for Temporal Lobe, which lies between MCA and PCA areas, the value expected was around 74 ml/100g/min (66). All of these values are very similar to the ones obtained in this study. However, for most of the regions it was impossible to find, for comparison purposes, values in literature.

Table 5.3 – Mean CBF values (ml/100g/min) in second level segmented brain regions

CBF mean values ± Standard Error (ml/100g/min)			
		Protocol 1	Protocol 2
Left Anterior Lobe	Activation	127 ± 10	65 ± 7
	Rest	125 ± 10	67 ± 7
Right Anterior Lobe	Activation	125 ± 10	79 ± 7
	Rest	120 ± 10	79 ± 8
Left Frontal Lobe	Activation	54 ± 3	57 ± 4
	Rest	53 ± 3	52 ± 4
Right Frontal Lobe	Activation	51 ± 3	48 ± 3
	Rest	50 ± 4	46 ± 4
Left Limbic Lobe	Activation	69 ±3	55 ± 3
	Rest	71 ± 4	52 ± 3
Right Limbic Lobe	Activation	66 ± 4	61 ± 4
	Rest	67 ± 4	60 ± 4
Left Midbrain	Activation	103 ± 6	76 ± 5
	Rest	106 ± 5	72 ± 5
Right Midbrain	Activation	103 ± 6	89 ± 6
	Rest	108 ± 4	83 ± 7
Left Occipital Lobe	Activation	90 ± 4	66 ± 4
	Rest	93 ± 5	67 ± 4
Right Occipital Lobe	Activation	83 ± 5	73 ± 4
	Rest	85 ± 5	77 ± 4
Left Parietal Lobe	Activation	57 ± 4	54 ± 4
	Rest	57 ± 4	45 ± 4
Right Parietal Lobe	Activation	52 ± 4	44 ± 3
	Rest	52 ± 3	43 ± 3
Left Sub-Lobar	Activation	77 ± 5	60 ± 3
	Rest	76 ± 5	58 ± 3,
Right Sub-Lobar	Activation	70 ± 3	51 ± 3
	Rest	70 ± 4	50 ± 3
Left Temporal Lobe	Activation	77 ± 5	84 ± 4

	Rest	77 ± 4	82 ± 4
Right Temporal Lobe	Activation	72 ± 4	58 ± 3
	Rest	74 ± 4	60 ± 3

5.2.3 Third level of segmentation – Gyrus

In this third level of segmentation, brain was divided taking into account the brain's Gyri. An example of a region designed – Right Precentral Gyrus – is shown in *Figure 5.7*.

Perfusion values were obtained for all the regions considered and sub-divided regarding the hemisphere, as it may be seen in the information displayed below.

All the results for CBF values are provided attached to this document and may be found in Appendix B - Table B.1.

Two plots compiling the mean results obtained for perfusion within the considered regions in both left and right hemispheres are shown in *Figure 5.8* and Figure 5.9:

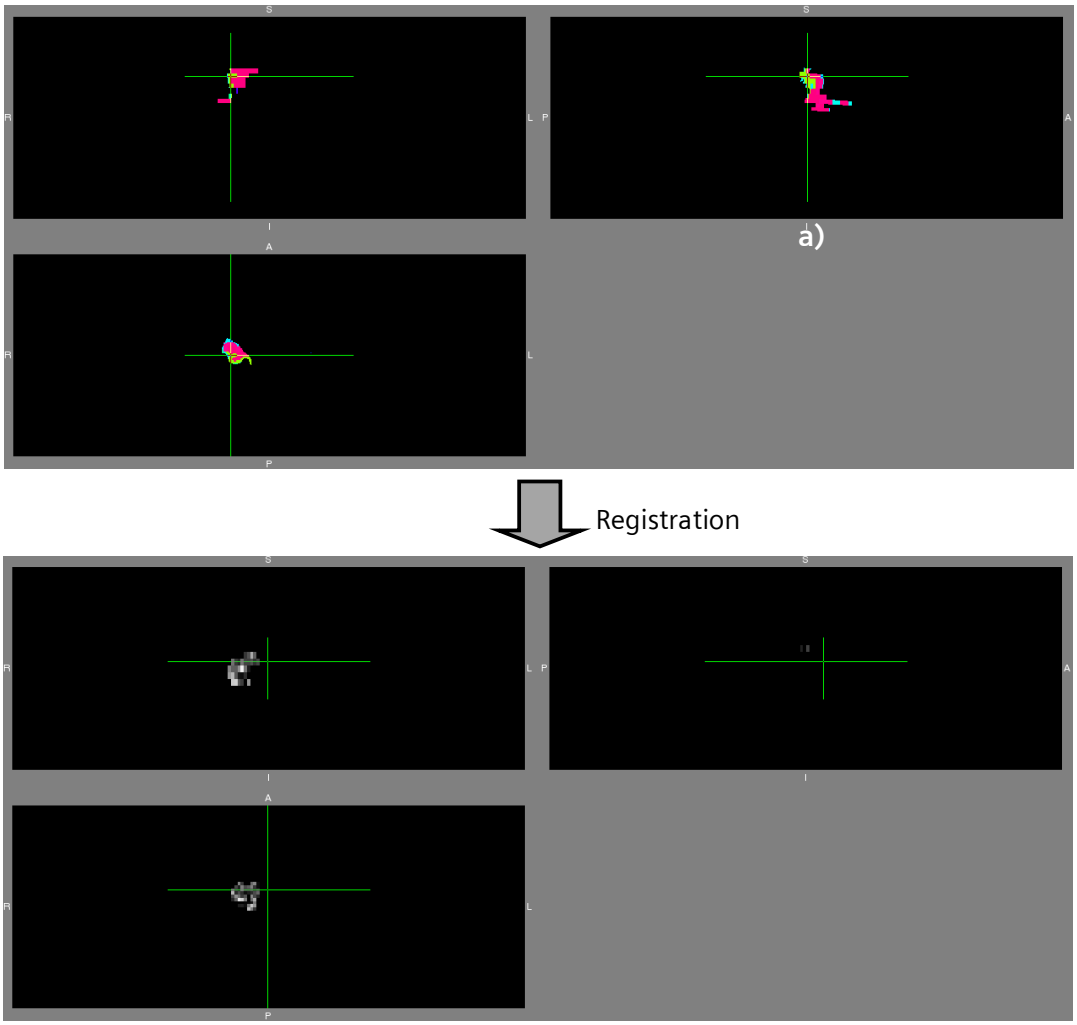

Figure 5.7 - Left Precentral Gyrus in a) Talairach Standard Space b) ASL space – perfusion map

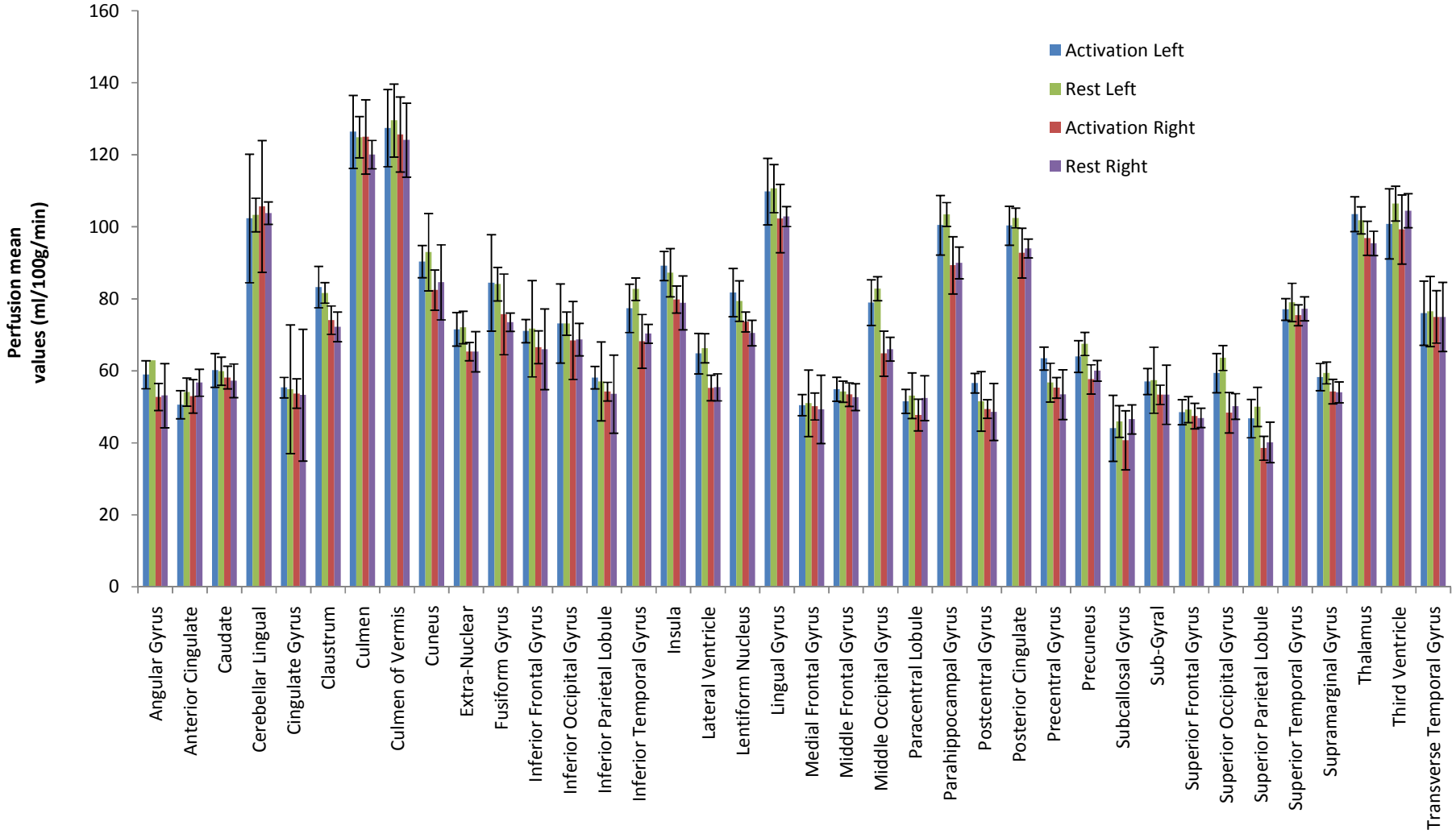

Figure 5.8 – Plot comparing mean perfusion values (ml/100g/min) for Protocol 1 in third segmentation level.

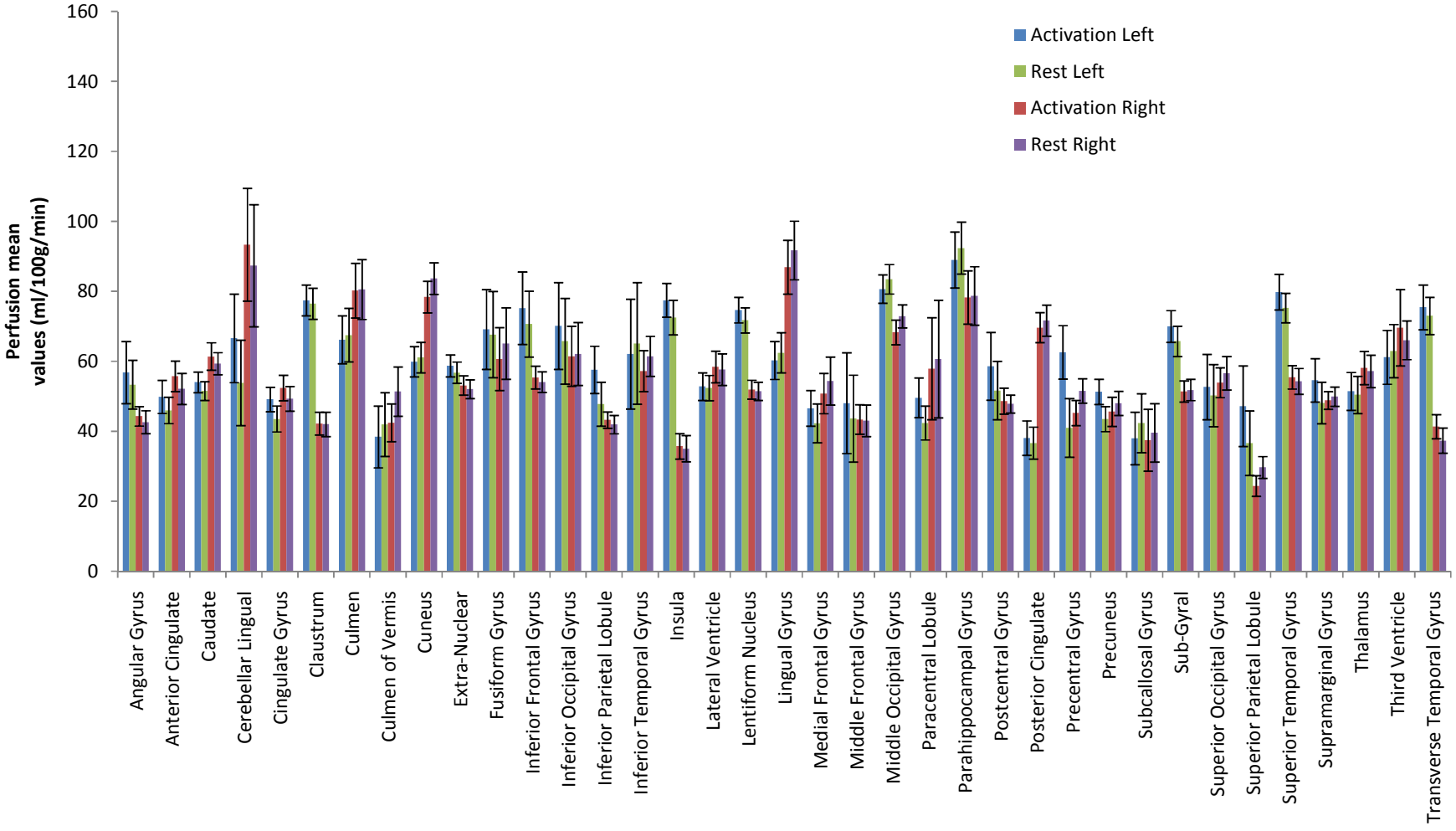

Figure 5.9- Plot comparing mean perfusion values (ml/100g/min) for Protocol 2 in third segmentation level.

In Protocol 1 higher values are obtained specially regarding the Culmen and the Culmen of Vermis. Once again when one is evaluating these results it is important to bear in mind the location of the activated hand motor cortex, which is located in the Precentral Gyrus (67). It is then possible to observe a significant percentage, around 50%, of CBF variation in this area – Left Precentral Gyrus. This variation is according to the theoretical value expected.

As for a comparison with normal values a CBF in Angular Gyrus around 56 ml/100g/min was expected (68). A value for CBF in Anterior Cingulate of around 52 ml/100g/min was expected (69) (70). For Cingulate Gyrus the theoretical value expected was 57 ml/100g/min (68) and for the Cuneus it was expected a value around 55 ml/100g/min (69).

For Inferior Frontal Gyrus, the value expected was around 50 ml/100g/min (68), for Middle Frontal Gyrus a CBF of 46 ml/100g/min and finally for Superior Frontal Gyrus it was expected a CBF around 52 ml/100g/min. (68) (69).

For Superior Temporal Gyrus the value expected was around 65 ml/100g/min and for Parahippocampal Gyrus a value of 46 ml/100g/min. (69)

A normal CBF value for Middle Occipital Gyrus would be 53 ml/100g/min and for Superior Occipital Gyrus 62 ml/100g/min. (68)

Finally for Precuneus we were expecting a value around 41 ml/100g/min, for the Supramarginal Gyrus around 54 ml/100g/min and for Thalamus a value around 66 ml/100g/min (68) (69).

An important region, as already stated, is the Precentral Gyrus and a theoretical value of CBF for this are is 57 ml/100g/min. (68)

All the values summarized above report to baseline perfusion and are displayed, for comparison purposes in Table 5.4:

Table 5.4 – CBF mean values obtained in current study copmpared with the ones from literature:

CBF mean values (ml/100g/min)		
	Literature	**Current Study (approximated mean baseline value – Protocol 2)**
Angular Gyrus	56 (68)	47
Anterior Cingulate	52 (69) (70)	49
Cingulate Gyrus	57 (68)	46
Cuneus	55 (69)	70
Inferior Frontal Gyrus	50 (68)	63
Middle Frontal Gyrus	46 (68)	43
Middle Occipital Gyrus	53 (68)	76
Parahippocampal Gyrus	46 (69)	84
Precentral Gyrus	57 (68)	47
Precuneus	41 (68)	45
Superior Frontal Gyrus	52 (69)	48
Superior Occipital Gyrus	62 (68)	55
Superior Temporal Gyrus	65 (69)	64
Supramarginal Gyrus	54 (69)	49
Thalamus	66 (69)	54

Statistical analysis between Protocols showed significant differences in CBF values (p<0,005). CBF values obtained in Protocol 2 are substantially lower.

5.2.4 Fourth level segmentation – Tissue Type

In this fourth level of segmentation, brain was divided taking into account its tissue types.

An example of a region designed – White Matter – is shown in *Figure 5.10*.

All the results for CBF values are shown in Table 5.5.

A plot compiling the mean results obtained for perfusion in activation and rest for the regions considered in both left and right hemispheres is shown in *Figure 5.11*.

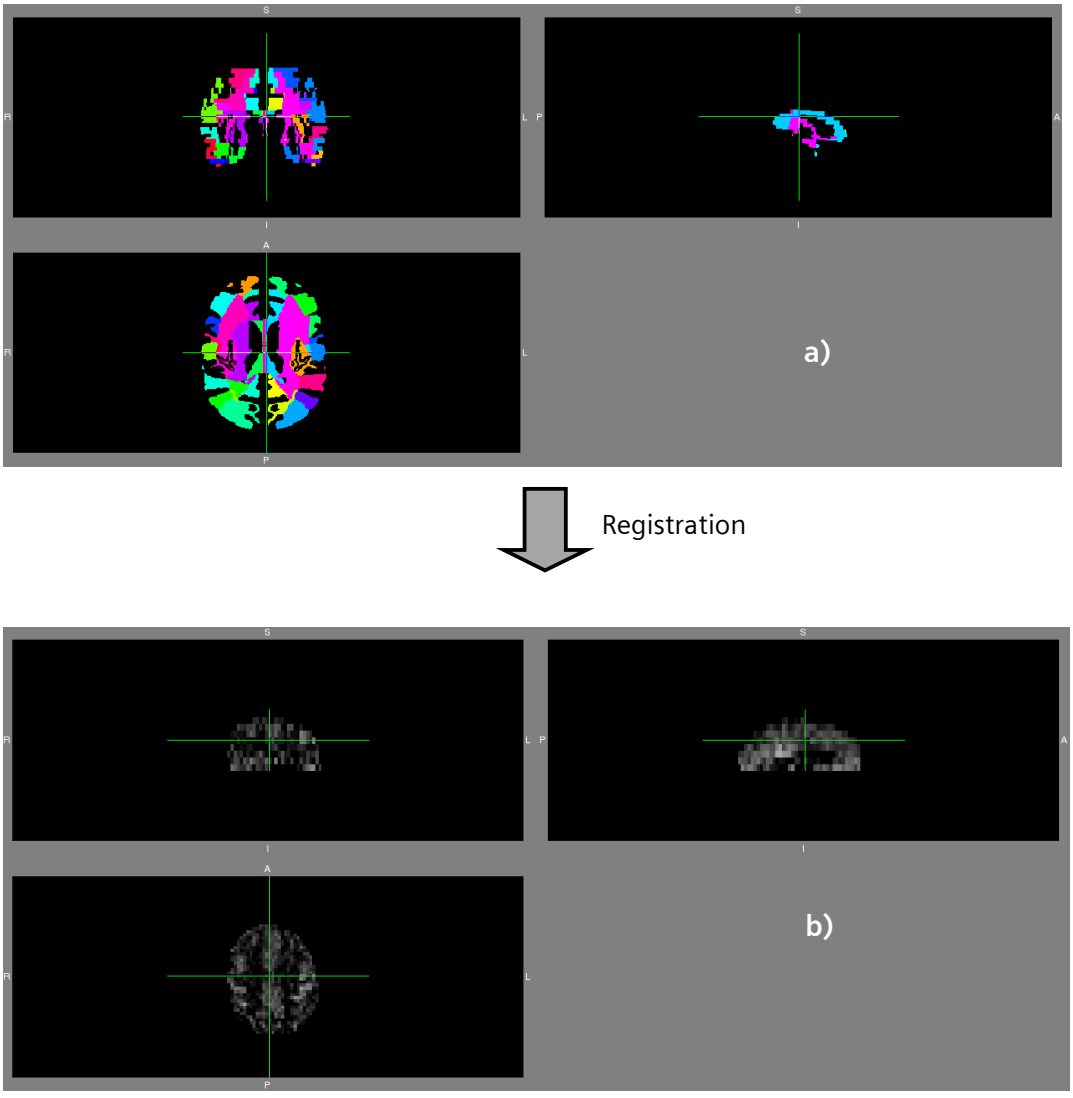

Figure 5.10 – White Matter in a) Talairach Standard Space b) ASL space – perfusion map

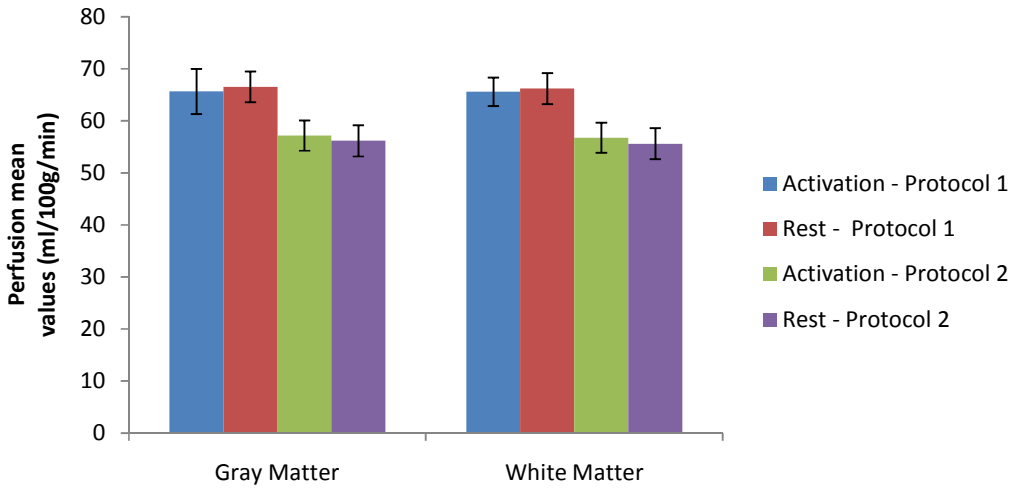

Figure 5.11 - Plot comparing mean perfusion values (ml/100g/min) for both protocols in second segmentation level for Protocol 1 and Protocol 2

Table 5.5 - Mean perfusion values (ml/100g/min) in fourth level segmentation regions of the brain

CBF mean values ± Standard Error (ml/100g/min)			
		Protocol 1	Protocol 2
Gray Matter	Activation	65 ± 3	59 ± 3
	Rest	66 ± 3	59 ± 3
White Matter	Activation	65 ± 3	57 ± 3
	Rest	66 ± 3	56 ± 3

In this sub-chapter the tissue type was taken into account and some discrepancies were found when the values were compared with the ones expected, mainly in White Matter.

A theoretical value of CBF for Gray Matter is around 66 ml/100g/min (71) which is in accordance with the values obtained in this study.

However, the value obtained in White Matter is much higher than what was to be expected – around 37 ml/100g/min (72).

5.2.5 Fifth level segmentation – Cell Type

In this fifth level of segmentation, brain was divided taking into account its cell types.

An example of a region designed – Corpus Callosum – is shown in *Figure 5.12*.

All the results for CBF values may be found attached to this document and are shown in Table B.2

Two plots compiling the mean results obtained for perfusion in activation and rest for the regions considered in both left and right hemispheres are shown in Figure 5.13 and Figure 5.14:

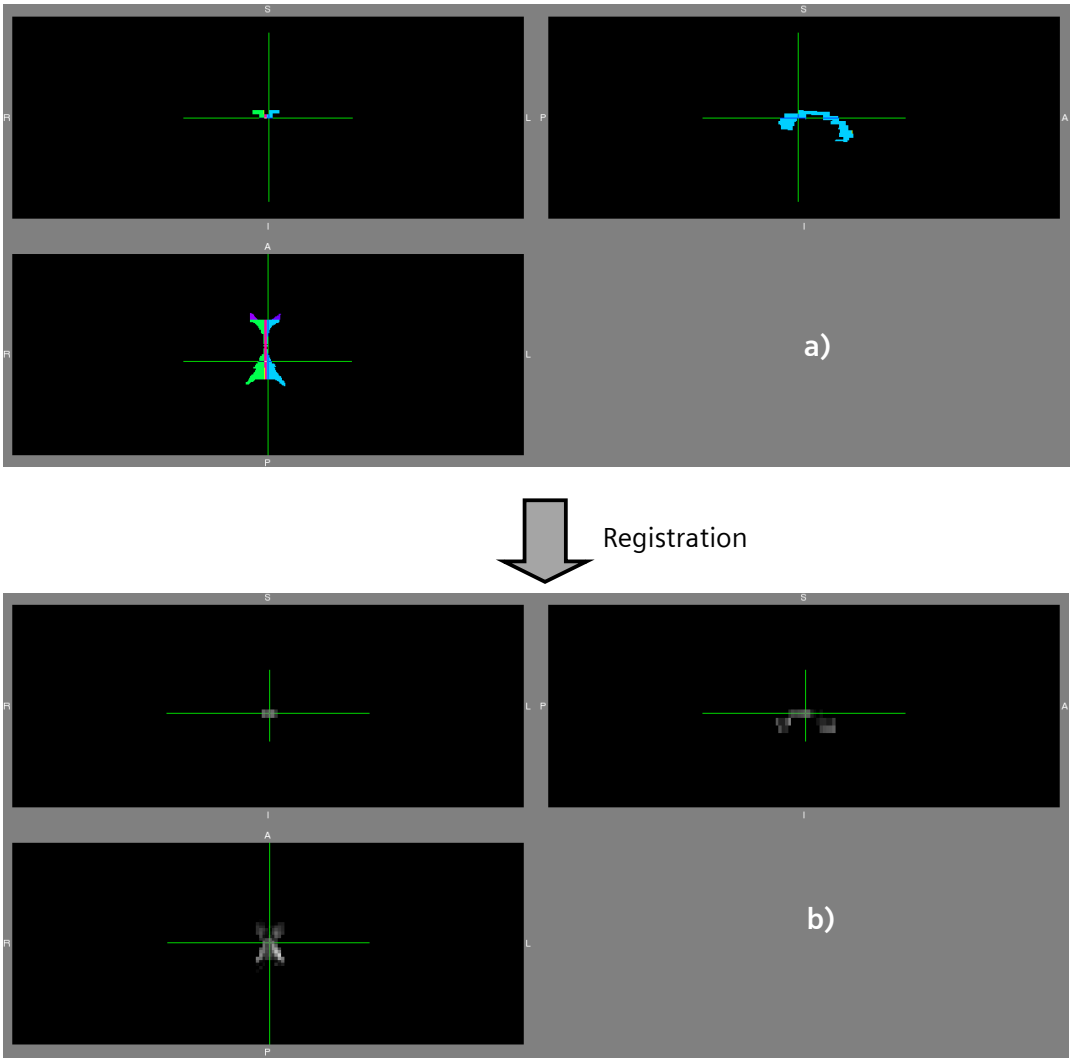

Figure 5.12 – Corpus Callosum in a) Talairach Standard Space b) ASL space – perfusion map

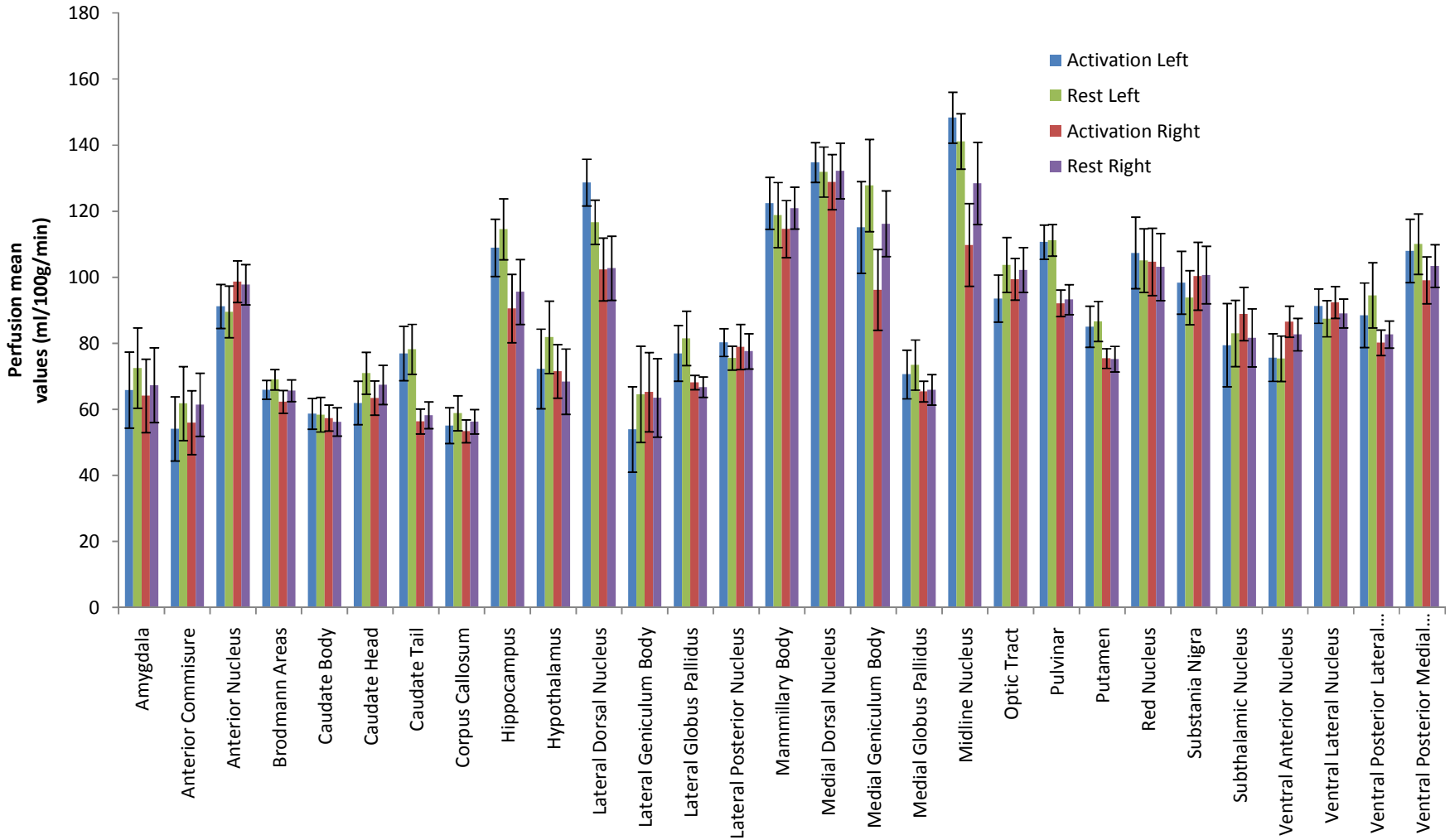

Figure 5.13 - Plot comparing mean perfusion values (ml/100g/min) for Protocol 1 in fifth segmentation level.

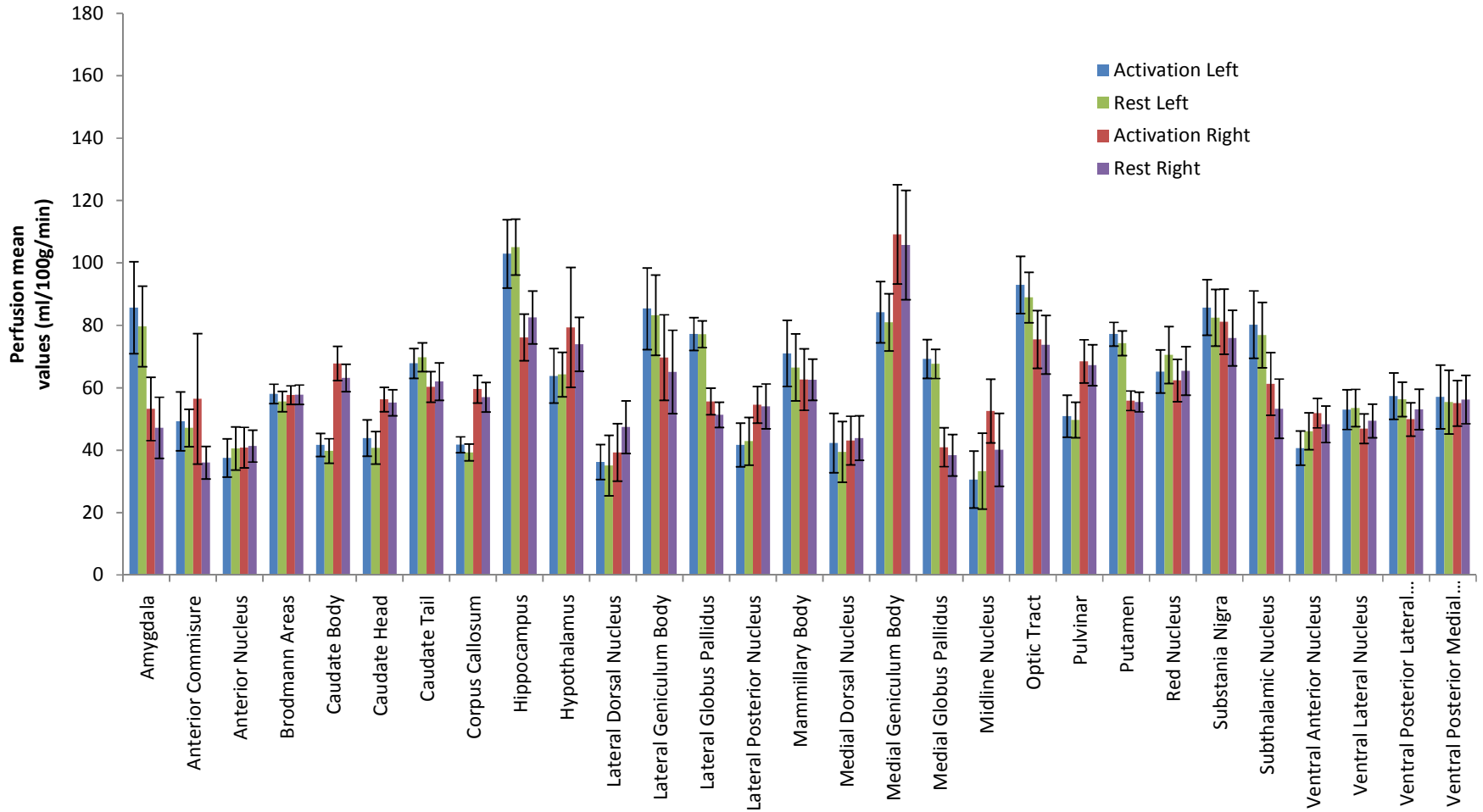

Figure 5.14 - Plot comparing mean perfusion values (ml/100g/min) for Protocol 2 in fifth segmentation level.

Even within other perfusion measuring techniques' studies it has been very hard to find theoretical values for the regions considered in this fifth segmentation level.

However some values were found such as for the Putamen, which theoretically should have a CBF value around 42 ml/100g/min (73) which a concordant value with the one obtained for Protocol 2.

6 Conclusions

6.1 Summary of the thesis and objectives achieved

The present work was aimed to evaluate and quantify perfusion in different regions of the human brain through two different protocols used with the non invasive method of ASL and it could be said that it accomplishes its main objectives.

Comparing both protocols used we also achieved the objective of validating the use of Protocol 2 in clinical trials.

Protocol 1 is not to be used in such exams, as it takes more time than Protocol 2 and has less statistical value. Due to its design, described in Chapter 4, its results do not reflect true CBF changes that should be measured in the alternating activation/rest states but instead it measures CBF values in activation and then in rest, which may lead to misleading results.

The block design of Protocol 2 allows it to be used in functional clinical. It takes less time to conclude, comparing to Protocol 1, which leads to less motion artefacts and less patient discomfort.

Furthermore, we have validated the ASL sequence used and the Protocol 2 by comparing some of the perfusion values obtained with the ones present in literature. It

is important to note the most of the papers cited use other perfusion measuring techniques such as PET, SPECT or XeCT.

This study offers a great detail in perfusion measuring and uses non invasive technology – ASL – so it is quite innovative in this matter.

It is also possible to draw other conclusions from the results obtained. One of them is the fact that, in general, all the perfusion values obtained for Protocol 1 were higher than the ones obtained for Protocol 2. This is explained, as previously stated, by the fact that Protocol 1 has an higher coverage of the brain and consequently more voxels that may contribute to an higher perfusion value.

Moreover there has been also verified a relevant variability between subjects. This might be explained by the higher brain perfusion verified in females over males (74). However, this information was not considered for this study.

Finally evidence was also found for the activation expected in response to the stimulus to which the subjects were submitted – Right Hand Finger Tapping. The primary hand motor cortex is located in the posterior area of the frontal lobe and within this region in the left hemisphere is found a considerable percentage of activation is found. In more detail, the hand motor cortex is located in the Precentral Gyrus and the values calculated in this work reveal an activation/rest difference (%) that is within the range theoretically expected, around 50%.

6.2 Other work undertaken

The opportunity of doing a Master's Thesis in a business context holds several advantages, mainly the fact of interacting with the client and with the business world itself.

During the course of this thesis I participated in a project for *Hospital da Luz* which consisted in programming specific functional paradigms to produce several stimuli to be used in fMRI exams. By having a wide range of differente stimuli, *Hospital da Luz* is now able to perform functional tests to complement clinical exams in order to study brain perfusion and its function.

The software used was *NordikAktiva* from NordicNeuroLab (NNL) and the paradigms programmed were as following:

- Passive Listening – auditory stimulus.
- Rhyming – visual stimulus.

- Semantic Decision – visual stimulus.
- Text Reading vs. Non Linguistic Symbols – visual stimulus.
- Visual Language Comprehension Task – visual stimulus.
- Auditive Language Comprehension Task – visual stimulus.
- Novel vs. Face Familiar Memory encoding/retrieval Task – visual/memory stimulus.
- Visual Object Memory Paradigm – visual/memory stimulus.
- Visual Word Memory Paradigm – visual stimulus.

Attached to the thesis, in Appendix C, is a brief explanation of the programming methodology as well as an example of a functional paradigm – Rhyming.

6.3 Limitations & Future work

As a technique that is only now becoming commercially available there are still several aspects to bear in mind and a huge amount of studies that can be performed in the future.

The major limitation found during this study was the comparison with other similar perfusion studies, especially regarding the regions considered. An ASL perfusion study as detailed as the current one was not found so all the values obtained are compared with the ones calculated through other perfusion techniques.

An extension of the current work might be, using all the scripts provided, to design new regions taking into account the brain vascular territories and to study perfusion to evaluate the artery that supplies each region.

This study would be of great importance in clinical cases of aneurysms and artery occlusions or to study some cases of hypoperfusion in more detailed regions (75).

6.4 Final findings

This thesis has represented a great challenge to me.

Doing a scientific thesis in a business environment has given me the opportunity to develop skills in both worlds, especially considering the huge amount of work that establishing this balance carries.

I have broadened my horizons with all situations I have been through, the difficulties I overcame and the people I contacted with.

At the end of it all it has been a rewarding experience that will stay in my mind forever and that has teached me never to give up.

It has undoubtly marked the beginning of my professional career.

References

1. **Carrigton, A. and McLachlan A.** *Introduction to Magnetic Resonance.* London : Chapman and Hall, 1967.

2. **Kim, S. et al.** Insights into new techniques for high resolution functional MRI. *Current Opinion in Neurobiology.* 2002, Vol. 12, 5, pp. 607-615.

3. **Gould, K.** PET Perfusion Imaging and Nuclear Cardiology. *Journal of Nuclear Medicine.* 1991, Vol. 32, pp. 579-606.

4. **Paul, A. et al.** Gated Myocardial Perfusion SPECT: Basic Principles, Technical Aspects, and Clinical Applications. *Journal of Nuclear Medicine.* 2004, Vol. 32, 4, pp. 179-187.

5. *CT Perfusion.* **Wiesmann, M.** München : s.n., 2006, Vol. 9.

6. **Brown, M. and Semelka, R.** *MRI - Basic Principles and Applications.* New Jersey : Wiley-Liss, 2003.

7. **Golay, X. et al.** Arterial spin labeling: benefits and pitfalls of high magnetic field. *Neuroimaging Clinics of North America.* 2006, Vol. 16, 2, pp. 259-268.

8. **Pina, J.A. Esperança.** *Anatomia Humana da Relação.* Lisbon : LIDEL, 2000.

9. **Neary, Crossman and.** *Neuroanatomy: an illustrated colour text.* s.l. : Elsevier Health Sciences, 2000.

10. **Netter, Frank.** *Atlas of Neuroanatomy and Neurophysiology.* New Jersey : Comtan, 2002.

11. **Laming, P. et al.** *Gial Cells - Their Role in Behaviour.* Cambridge : Cambridge University Press, 1998.

12. **Luria, A.R.** The Functional Organization of the Brain. *Scientific American.* 1970, Vol. 222, 3, pp. 66-78.

13. **Clare, Stuart.** *Functional MRI: Methods and Applications.* Nottingham : University of Nottingham, 1997. PhD Thesis.

14. **Lancaster, J. et al.** Automated Talairach Atlas Labels For Functional Brain Mapping. *Human Brain Mapping.* 2000, Vol. 20, pp. 120-131.

15. **Talairach, J.** *Co-Planar stereotaxic atlas of the human brain.* New York : Thieme, 1988.

16. **Sheldon, JJ.** *Blood Vessels of the scalp and brain* . New Jersey : CIBA Pharmaceutical Company , 1981.

17. *The vascular territories in the cerebellum and brainstem: CT and MR study*. **Savoiardo, M. et al.** 2, s.l. : AJNR, 1987, Vol. 8, pp. 199-209.

18. *The vascular territories of the carotid and vertebrobasilar systems. Diagrams based on CT studies of infarcts.* **Savoiardo, M.** 4, s.l. : IJNS, 1986, Vol. 7, pp. 405-409.

19. **Scott, Marietta.** *Towards a Quantitative Methodology for the Assessment of Cerebral Blood Flow in Magnetic Resonance Imaging.* Faculty of Medical and Human Sciences. Manchester : University of Manchester, 2005. PhD Thesis.

20. *MR Imaging of Posterior Fossa Infarctions: Vascular Territories and Clinical Correlates.* **Cormier, P. et al.** Chicago : RadioGraphics, 1992, Vol. 12, pp. 1079-1096.

21. *Corpus Callosum Infarcts with Atypical Clinical and Radiologic Presentations.* **Kasaw, . et al.** s.l. : AJNR, 2000, Vol. 21, pp. 1876-1880.

22. *Posterior Cerebral Artery Stroke.* **Helseth, E.** Oregon : s.n., 2010.

23. **Chen, J. et al.** Cerebral Blood Flow measurement using fMRI and PET: a cross-validation study. *IJBI.* 2008.

24. **Scremin, O.** Cerebral Vascular System. [book auth.] George Paxinos and Jürgen k. Mai. *The Human Nervous System.* s.l. : Academic Press, 2004.

25. **Buxton, R.** *Introduction to functional magnetic resonance imaging: principles and techniques.* Cambridge : Cambridge University Press, 2002.

26. **Ricketts, P. et al.** Non-invasive blood perfusion measurements using a combined temperature and heat flux surface probe. *IJHMT*. 2008, Vol. 51.

27. **Leenders, K. et al.** Cerebral Blood Flow, Blood Volume and Oxygenation utilization - Normal Values and Effect of Age. *Brain.* 1989, Vol. 113, 1, pp. 27-47.

28. **Liu, T. et al.** Measurement of cerebral perfusion with arterial spin labeling: Part 1. Methods. *JINS.* 2007, Vol. 13, pp. 1-9.

29. **Wintermark, M. et al.** Comparative Overview of Brain Perfusion Imaging Techniques. *Journal of Neuroradiology.* 32, 2005, pp. 294-314.

30. **Warwick, J.** Imaging of Brain Function using SPECT. *Metabolic Brain Disease.* 2004, Vol. 19.

31. **Drayer, BP et al.** Xenon enhanced CT for analysis of cerebral integrity, perfusion and blood flow. *Stroke.* 1978, Vol. 9, pp. 123-130.

32. **Eastwood, J. et al.** Perfusion CT with Iodinated Contrast Material. *AJR.* 2003, Vol. 180, pp. 3-12.

33. **Schöning, M et al.** Estimation of cerebral blood flow through color duplex sonography of the carotid and vertebral arteries in healthy adults. *Storke.* 1994, Vol. 25, 1, pp. 17-22.

34. **Speck, O. et al.** Perfusion MRI of the human brain with dynamic susceptibility contrast: Gradient-echo versus spin-echo techniques. *JMRI.* 2000, Vol. 12, 3, pp. 381-387.

35. **Brown, Mark and Semelka, Richard.** *MRI - Basic Principles and Applications.* New Jersey : Wiley-Liss, 2003.

36. **Silva, Carla.** *Princípios Físicos das Imagens de Ressonância Magnética Nuclear.* Faro : Universidade do algarve, 2007.

37. **Huettel, S.** *Functional Magnetic Resonance.* Sunderland : Sinauer, 2004.

38. Hyperpolarized Noble Gas MRI Laboratory. *Department of Radiology*. [Online] Harvard Medical School, 2006. [Cited: October 25, 2010.] http://www.spl.harvard.edu/archive/HypX/theory1.html.

39. **Jezzard, P. et al.** *Functional MRI: An Introduction to Methods.* Oxford : Oxford University Press, 2001.

40. **Bernstein, M. et al.** *Handbook of MRI Pulse Sequence.* Chicago : Elsevier, 2001.

41. **Ogawa, S.** Brain magnetic resonance imaging with contrast dependent on blood oxygenation. *Biophysics.* 1990, Vol. 87, pp. 9868-9872.

42. **Ogata, R.** Mechanism of Cooperative Oxygen Binding to Hemoglobin. *PNAS.* 1972, Vol. 69, 2.

43. Physiological basis of brain activation and BOLD contrast. *IMAIOS.* [Online] [Cited: June 14, 2010.] http://www.imaios.com/en/e-Courses/e-MRI/Functional-MRI/brain-activation-bold-contrast.

44. **Tofts, P.** *Quantitative MRI of the Brain.* West Sussex : John Wiley and Sons, 2003.

45. **Çavusoglu, M.** Comparison of pulsed arterial labeling encoding schemes and absolute perfusion quantfication. *Magnetic Resonance Imaging.* 2009, 27, pp. 1039-1045.

46. **Wang, J.** Arterial Transit Time Imaging with Flow Encoding Arterial Spin Tagging (FEAST). *Magnetic Resonance in Medicine.* 2003, Vol. 50, pp. 599-607.

47. **Petersen, E.T. et al.** Non-invasive measurement of perfusion: a critical review of arterial spin labelin techniques. *British Journal of Radiology.* 2006, 79, pp. 688-701.

48. **Edelman, R. et al.** EPISTAR MRI: Multislice mapping of cerebral blood flow. *MRM.* 1998, 40, pp. 800-805.

49. **Kim, S.** Quantification of Relative Cerebral Blood Flow Change by Flow-Sensitive Alternating Inversion Recovery (FAIR) Technique: Application to Functional Mapping. *MRM.* 1995, Vol. 34, pp. 293-301.

50. **Wong, E. et al.** Implementation of quantitative perfusion imaging techniques for functional brain mapping using pulsed arterial spin labeling. *NMR in Biomedicine.* 1997, Vol. 10, pp. 237-249.

51. *Comparison of reproducibility between continuous, pulsed, and pseudo-continuous arterial spin labeling.* **Chen, Y. et al.** Stockholm : s.n., 2010.

52. **Hernandez-Garcia, L. et al.** Fast, Pseudo-Continuous Arterial Spin Labeling for Functional Imaging using Two-Coil System. *Magnetic Resonance in Medicine.* 2004, Vol. 51, pp. 577-585.

53. **Dai, W. et al.** Modified Pulsed Continuous Arterial Spin Labeling of a Single Artery. *Magnetic Resonance in Medicine*. 2010.

54. **Alsop, D. et al.** Reduced transit-time sensitivity in noninvasive magnetic resonance imaging of human cerebral blood flow. *JCBFM*. 1996, Vol. 16, pp. 1236-1249.

55. **Buxton, R. et al.** A General Kinetic Model for Quantitative Perfusion Imaging with Arterial Spin Labeling. *MRM*. 1998, 40, pp. 383-396.

56. **Wong, E. et al.** Quantitative Imaging of Perfusion Using a Single Subtraction (QUIPSS and QUIPSS II). *MRM*. 1998, 39, pp. 702-707.

57. **Luh, W. et al.** QUIPSS II with thin-slice TI1 periodic saturation: a method for improving accuracy of quantitative perfusion imaging using pulsed arterial spin labeling. *MRM*. 1999, 41, pp. 1246-1254.

58. **Kemeny, S. et al.** Comparison of continuous overt speech fMRI using BOLD and arterial spin labeling. *Human Brain Mapping*. 2005, Vol. 24, 3, pp. 173-183.

59. **Pimentel, M.** *Functional Brain Perfusion Evaluation with Arterial Spin Labeling at 3 Tesla*. Lisboa : Faculdade de Ciências e Tecnologia - Universidade Nova de Lisboa, 2009.

60. **Erlangen, Siemens AG.** Motion under Control with Prospective Acquisition Correction (PACE). Malvern : s.n.

61. **Lu, H. et al.** Determining the longitudinal relaxation time (T1) of blood at 3.0 Tesla. *Magnetic Resonance in Medicine*. 2004, Vol. 52, 3, pp. 679-682.

62. **Wang, J. et al.** Arterial Spin Labeling Perfusion fMRI With Very Low Task Frequency. *Magnetic Resonance in Medicine*. 2003, Vol. 49, pp. 796-802.

63. **Hatazawa, J. et al.** Regional Cerebral Blood Flow Response in Gray Matter Heterotopia during Finger Tapping: An Activation Study with Positron Emission Tomography. *AJNR*. 1996, Vol. 17, pp. 479-482.

64. **Ishii, K. et al.** Cerebral Blood Flow Changes in the Primary Motor and Premotor Cortices during hyperventilation. *Annals of Nuclear Medicine*. 1998, Vol. 12, 1, pp. 29-33.

65. **Amin, F. et al.** *Partial Volume Correction of PET Images to detect a potential decreased CBF in patients with Parkinson's disease*. Department of Health Science and Technology . Aalborg : Aalborg University, 2009.

66. **Wolf, R.** Detection of Mesial Temporal Lobe Hypoperfusion in Patients with Temporal Lobe Epilepsy by Use of Arterial Spin Labeled Perfusion MR Imaging. *AJNR*. 2001, Vol. 22, pp. 1334-1341.

67. **Lee, H. et al.** Location of the Primary Motor Cortex in Schizencephaly. *AJNR*. 1999, Vol. 20, pp. 163-166.

68. **Hatazawa, J. et al.** Regional cerebral blood flow, blood volume, oxygen extraction fraction, and oxygen utilization rate in normal volunteers measured by the autoradiographic technique and the single breath inhalation method. *Annals of Nuclear Medicine*. 1995, Vol. 9, 1, pp. 15-21.

69. **Ito, H. et al.** Changes in cerebral blood flow and cerebral oxygen metabolism during neural activation measured by positron emission tomography: comparison with blood oxygenation level-dependent contrast measured by functional magnetic resonance imaging. *Journal of Cerebral Blood Flow & Metabolism*. 2005, Vol. 25, pp. 371-377.

70. —. Database of normal human cerebral blood flow measured by SPECT: I. Comparison between I-123-IMP, Tc-99m-HMPAO, and Tc-99m-ECD as referred with O-15 labeled water PET and voxel-based morphometry. *Annals of Nuclear Medicine*. 2006, Vol. 20, 2, pp. 131-138.

71. **Jackson, A. et al.** *Dynamic Constrast-Enhanced Magnetic Resonance Imaging in Oncology*. Berlin : Springer, 2005.

72. **Carroll, T. et al.** Absolute Quantification of Cerebral Blood Flow With Magnetic Resonance, Reproducibility of the Method, and Comparison With H215O Positron Emission Tomography. *Journal of Cerebral Blood Flow & Metabolism*. 2002, Vol. 22, pp. 1149-1156.

73. **Miyazawa, N. et al.** Xenon Contrast-Enhanced CT Imaging of Supratentorial Hypoperfusion in Patients with Brain Stem Infarction. *AJNR*. 1999, Vol. 20, pp. 1858-1862.

74. **Parkes, L.** Normal cerebral perfusion measurements using arterial spin labeling: Reproducibility, stability, and age and gender effects. *MRM*. 2004, Vol. 51, 4, pp. 736-743.

75. **Ohta, H. et al.** Hypoperfusion of right hemisphere on brain SPECT in a patient with exanthem subitum and left hemisparesis. *Annals of Nuclear Medicine*. 2000, Vol. 14, 3, pp. 223-225.

76. **Hendee, W. and E., Ritenour.** *Medical Imaging Physics.* New York : Wiley-Liss, 2002.

77. MRI Sequences - Echo Planar (EPI). *IMAIOS.* [Online] [Cited: June 9, 2010.] http://www.imaios.com/en/e-Courses/e-MRI/MRI-Sequences/echo-planar-imaging.

78. **Wu, W.et al.** Feasibility of velocity selective arterial spin labeling in functional MR. *JCBFM.* 2007, Vol. 27, pp. 831-838.

79. **Magistretti, P. et al.** Cellular mechanisms of brain energy metabolism and their relevance to functional brain imaging. *PTRSL.* 1999, Vol. 354, pp. 1155-1163.

80. **Silva, C. A. et al.** Entropy generation and human aging: Lifespan entropy and effect of diet composition and caloric restriction diets. *Journal of Thermodynamics.* 2009.

81. **Pollock, J.M. et al.** Anoxic injury-associated cerebral hyperperfusion identified with arterial spin-labeled MR imaging. *AJNR.* 2008, Vol. 29, 7.

82. **Tomasian, A. et al.** 3D High-spatial-resolution cerebral MR venography at 3T: a contrast-dose-reduction study. *AJNR.* 2009, Vol. 30, 2.

83. **Schwertfeger, N. et al.** Cerebrovascular reactivity over time course in healthy subjects. *JNS.* 2006, Vol. 249, pp. 135-139.

84. **Chiara, S. et al.** Cerebrovascular reactivity by transcranial Doppler-ultrasonography in insulin-dependent diabetic patients. *CD.* 1993, Vol. 3, pp. 111-115.

85. **Behzadi, Yashar.** *Variability in Functional Magnetic Resonance Imaging: Influence of the Baseline Vascular State and Physiological Fluctuations.* San Diego : University of California, 2006. PhD Thesis.

86. FSL. *FMRIB Software Library.* [Online] Oxford University Centre for Functional MRI of the Brain. [Cited: March 1, 2010.] http://www.fmrib.ox.ac.uk/fsl/.

87. **Wang, J.** Arterial Transit Time Imaging with Flow Encoding Arterial Spin Tagging (FEAST). *Magnetic Resonance in Medicine.* 2003, Vol. 50, pp. 599-607.

88. **Sheldon, J.** *Blood Vessels of the scalp and brain .* New Jersey : CIBA Pharmaceutical Company, 1981.

89. **Buxton, R. et al.** General Kinetic Model for Quantitative Perfusion Imaging with Arterial Spin Labeling. *Magnetic Resonance in Medicine.* 1998, Vol. 40, pp. 383-396.

90. **Lu, H. et al.** Determining the longitudinal relaxation time (T1) of blood at 3.0 Tesla. *Magnetic Resonance in Medicine.* 2004, Vol. 52, 3, pp. 679-682.

91. **Xiao, J. et al.** Quantification of cerebral blood flow by flow-sensitive alternating inversion recovery exempting separate T1 measurement in healthy volunteers. *CMJ*. 2009, Vol. 119, 24, pp. 2096-2100.

Appendix A – Auxiliar Information for Perfusion Quantification

In this section of the thesis are displayed all the auxiliar calculations, Linux Shell Scripts and information needed in order to perform perfusion quantification in all the regions considered.

Section A.1

Linux Shell Script designed to obtain perfusion map CBFACT1:

```
#!/bin/sh
###################################
echo -e "Qual o subject em estudo? \c"
read subject

path=/home1/joaom/DATA-HLuz-MPimentel-Preproc/$subject;

echo "Encontra-se na directoria $path"

mkdir ${path}/DM_M0_images;
```

```
mkdir ${path}/vols;
r1=asl_act;


for filename in  ${r1}; do


      navs=`fslval ${path}/${filename}.nii dim4`;
      nslices=`fslval ${path}/${filename}.nii dim3`;

      ## Separate the averages
      fslsplit ${path}/${filename} ${path}/vols/vol -t;
      rm ${path}/vols/vol0000.nii.gz;


      ## Subtract Control and  Tag images
      COUNTER=1
      while [  $COUNTER -lt $navs ]; do
         echo Volume $COUNTER
         if [ $COUNTER -lt 10 ]; then
                fslmaths ${path}/vols/vol000$COUNTER.nii.gz -mul -1
${path}/vols/vol000$COUNTER.nii.gz -odt float;
              else
                fslmaths ${path}/vols/vol00$COUNTER.nii.gz -mul -1
${path}/vols/vol00$COUNTER.nii.gz -odt float;
              fi
         #let COUNTER=COUNTER+2
              COUNTER=`echo "$COUNTER+2" | bc`;
       done

      ## Create new time series
      fslmerge -t ${path}/asl_temp ${path}/vols/vol00*.nii.gz;

      ## Subtraction and Mean of time series
      fslmaths ${path}/asl_temp -Tmean -mul 2 ${path}/DM_M0_images/${filename}_DM -odt
float;

      ## Determining M0 image
      fslsplit ${path}/Magnet_eq.nii ${path}/Magnet_eq_slices -z;
      fslmaths ${path}/manatomica.nii -bin ${path}/manatomica_mask;
      fslsplit ${path}/manatomica_mask.nii.gz ${path}/manatomica_mask_slices -z;

      ### Applying masks slice by slice
      COUNT=0
      while [ $COUNT -lt $nslices ]; do
              echo Calculating slice $COUNT
              fslmaths ${path}/Magnet_eq_slices000$COUNT.nii.gz -mas
${path}/manatomica_mask_slices000$COUNT.nii.gz  ${path}/M0_image_slices000$COUNT  -
odt float;
              COUNT=`echo "$COUNT+1" | bc`;
      done
```

```
    ### Create new M0 image
    fslmerge -z ${path}/DM_M0_images/M0_image ${path}/M0_image_slices000*.nii.gz;

    ##Calculating CBF_act1 (through the first method MP)
    lambda=0.9;
    alfa=0.9;
    TI1=0.7;
    TI2=1.8;
    T1a=1.5;

    fslsplit ${path}/DM_M0_images/asl_act_DM.nii.gz ${path}/DM_M0_images/mean -z;
    fslsplit ${path}/DM_M0_images/M0_image.nii.gz ${path}/DM_M0_images/meanM0_ -z;

    ### Applying masks slice by slice
    COUNT=0
    while [ $COUNT -lt $nslices ]; do
        echo Applying mask to slice $COUNT
        fslmaths ${path}/DM_M0_images/mean000$COUNT.nii.gz -mas
${path}/manatomica_mask_slices000$COUNT.nii.gz
${path}/DM_M0_images/mean_masked000$COUNT -odt float;
        COUNT=`echo "$COUNT+1" | bc`;
    done

    ### Read file with time corrections
    echo -e "Qual o ficheiro que deseja para a correcao temporal? \c"
    read file

    TI2_initial=$TI2 ;
    t=0 ;
    while [ $t -lt $nslices ] ; do
        s=`echo "$t+1" | bc`;
        time=`grep s_${s} ${path}/$file | awk '{print $2}'`
        TI2=`echo "$TI2_initial +($time/1000)" | bc -l`
        M0=`fslstats ${path}/DM_M0_images/meanM0_000${t}.nii.gz -M`
        echo "$M0" >> ${path}/${filename}_M0values.txt ;
        DM=`fslstats ${path}/DM_M0_images/mean_masked000${t}.nii.gz -M`
        echo "$DM" >> ${path}/${filename}_DMvalues.txt ;
        fslmaths ${path}/DM_M0_images/mean_masked000${t}.nii.gz -mul `echo
"$lambda*e($TI2/$T1a)" | bc -l` -div `echo "2*$M0*$alfa*$TI1" | bc -l` -mul 6000
${path}/DM_M0_images/CBFM0_${t} -odt float ;

        t=`echo "$t+1" | bc`
    done

    fslmerge -z ${path}/CBFACT1 ${path}/DM_M0_images/CBFM0_*.nii.gz ;

    rm ${path}/M0_image_slices000* ;
    rm ${path}/Magnet_eq_slices000* ;
    rm ${path}/DM_M0_images/CBFM0_* ;
    rm ${path}/DM_M0_images/mean000* ;
    rm ${path}/DM_M0_images/meanM0_000* ;
    rm ${path}/DM_M0_images/mean_masked000* ;

done
```

Section A.2

Linux Shell Script designed to obtain perfusion map CBFREST1:

```
#!/bin/sh

###################################
echo -e "Qual o subject em estudo? \c"
read subject

path=/home1/joaom/DATA-HLuz-MPimentel-Preproc/$subject;

echo "Encontra-se na directoria $path"

mkdir ${path}/vols1;

r1=asl_rest;

for filename in  ${r1}; do

      navs=`fslval ${path}/${filename}.nii dim4`;
      nslices=`fslval ${path}/${filename}.nii dim3`

      ## Separate the averages
      fslsplit ${path}/${filename} ${path}/vols1/vol -t;
      rm ${path}/vols1/vol0000.nii.gz;

      ## Subtract Control and  Tag images
      COUNTER=1
      while [  $COUNTER -lt $navs ]; do
         echo Volume $COUNTER
         if [ $COUNTER -lt 10 ]; then
               fslmaths          ${path}/vols1/vol000$COUNTER.nii.gz          -mul          -1
${path}/vols1/vol000$COUNTER.nii.gz -odt float;
            else
               fslmaths          ${path}/vols1/vol00$COUNTER.nii.gz          -mul          -1
${path}/vols1/vol00$COUNTER.nii.gz -odt float;
            fi
         #let COUNTER=COUNTER+2
            COUNTER=`echo "$COUNTER+2" | bc`;
       done

      ## Create new time series
      fslmerge -t ${path}/asl_temp1 ${path}/vols1/vol00*.nii.gz;

      ## Subtraction and Mean of time series
      fslmaths ${path}/asl_temp1 -Tmean -mul 2 ${path}/DM_M0_images/${filename}_DM -odt
float;

     ##Calculating CBF_rest1
      lambda=0.9;
      alfa=0.9;
      TI1=0.7;
      TI2=1.8;
      T1a=1.5;

      fslsplit ${path}/DM_M0_images/asl_rest_DM.nii.gz ${path}/DM_M0_images/mean -z;
      fslsplit ${path}/DM_M0_images/M0_image.nii.gz ${path}/DM_M0_images/meanM0_ -z;
```

```
### Applying masks slice by slice
    COUNT=0
    while [ $COUNT -lt $nslices ]; do
        echo Applying mask to slice $COUNT
        fslmaths ${path}/DM_M0_images/mean000$COUNT.nii.gz -mas
${path}/manatomica_mask_slices000$COUNT.nii.gz
${path}/DM_M0_images/mean_masked000$COUNT -odt float;
        COUNT=`echo "$COUNT+1" | bc`;
    done

    ### Read file with time corrections
    echo -e "Qual o ficheiro que deseja para a correcao temporal? \c"
    read file

    TI2_initial=$TI2 ;

    t=0 ;
    while [ $t -lt $nslices ] ; do
        s=`echo "$t+1" | bc`;
        time=`grep s_${s} ${path}/$file | awk '{print $2}'`
        TI2=`echo "$TI2_initial +($time/1000)" | bc -l`

        M0=`fslstats ${path}/DM_M0_images/meanM0_000${t}.nii.gz -M`
        fslmaths ${path}/DM_M0_images/mean_masked000${t}.nii.gz -mul `echo
"$lambda*e($TI2/$T1a)" | bc -l` -div `echo "2*$M0*$alfa*$TI1" | bc -l` -mul 6000
${path}/DM_M0_images/CBFM0_${t} -odt float ;

        t=`echo "$t+1" | bc`
    done

    fslmerge -z ${path}/CBFREST1 ${path}/DM_M0_images/CBFM0_*.nii.gz ;

    rm ${path}/DM_M0_images/CBFM0_* ;
    rm ${path}/DM_M0_images/mean000* ;
    rm ${path}/DM_M0_images/meanM0_000* ;
    rm ${path}/DM_M0_images/mean_masked000* ;

done
```

Section A.3

Linux Shell Script designed to obtain perfusion map CBFACT2 and CBFREST2:

```
#!/bin/sh

###################################
echo -e "Qual o subject em estudo? \c"
read subject

path=/home1/joaom/DATA-HLuz-MPimentel-Preproc/$subject;
echo "Encontra-se na directoria $path"


mkdir ${path}/vols2;
mkdir ${path}/vols2/volsrest;
mkdir ${path}/vols2/volsact;
```

```
r1=asl_bold;

for filename in  ${r1}; do

    navs=`fslval ${path}/${filename}.nii dim4`;
    nslices=`fslval ${path}/${filename}.nii dim3`

    ## Separate the averages
    fslsplit ${path}/${filename} ${path}/vols2/vol -t;
    rm ${path}/vols2/vol0000.nii.gz;

    ## Separate periods of activation and control
    x=1
    while [ $x -lt $navs ]; do
        if [ $x -le 9 ]; then
           cp ${path}/vols2/vol000$x.nii.gz ${path}/vols2/volsrest;
        elif [ $x = 10 ]; then
           cp ${path}/vols2/vol00$x.nii.gz ${path}/vols2/volsrest;
        elif [ $x -ge 11 ] && [ $x -le 20 ]; then
           cp ${path}/vols2/vol00$x.nii.gz ${path}/vols2/volsact;
        elif [ $x -ge 21 ] && [ $x -le 30 ]; then
           cp ${path}/vols2/vol00$x.nii.gz ${path}/vols2/volsrest;
        elif [ $x -ge 31 ] && [ $x -le 40 ]; then
           cp ${path}/vols2/vol00$x.nii.gz ${path}/vols2/volsact;
        elif [ $x -ge 41 ] && [ $x -le 50 ]; then
           cp ${path}/vols2/vol00$x.nii.gz ${path}/vols2/volsrest;
        elif [ $x -ge 51 ] && [ $x -le 60 ]; then
           cp ${path}/vols2/vol00$x.nii.gz ${path}/vols2/volsact;
        elif [ $x -ge 61 ] && [ $x -le 70 ]; then
           cp ${path}/vols2/vol00$x.nii.gz ${path}/vols2/volsrest;
        elif [ $x -ge 71 ] && [ $x -le 80 ]; then
           cp ${path}/vols2/vol00$x.nii.gz ${path}/vols2/volsact;
        elif [ $x -ge 81 ] && [ $x -le 90 ]; then
           cp ${path}/vols2/vol00$x.nii.gz ${path}/vols2/volsrest;
        elif [ $x -ge 91 ] && [ $x -le 99 ]; then
           cp ${path}/vols2/vol00$x.nii.gz ${path}/vols2/volsact;
        elif [ $x = 100 ]; then
           cp ${path}/vols2/vol0$x.nii.gz ${path}/vols2/volsact;
        fi
        x=`echo "$x+1" | bc`;
    done

    fslmerge -t ${path}/vols2/volsact/act ${path}/vols2/volsact/vol0*.nii.gz ;
    fslmerge -t ${path}/vols2/volsrest/rest ${path}/vols2/volsrest/vol00*.nii.gz ;
    rm ${path}/vols2/volsact/vol0*.nii.gz ;
    rm ${path}/vols2/volsrest/vol00*.nii.gz ;

    fslsplit ${path}/vols2/volsact/act.nii.gz ${path}/vols2/volsact/vol -t ;
    rm ${path}/vols2/volsact/act.nii.gz ;
    fslsplit ${path}/vols2/volsrest/rest.nii.gz ${path}/vols2/volsrest/vol -t ;
    rm ${path}/vols2/volsrest/rest.nii.gz ;
```

```
## Subtract Control and Tag images from both volsact and volsrest
    COUNTER=0
    while [  $COUNTER -lt 50 ]; do
      echo Volume $COUNTER
      if [ $COUNTER -lt 10 ]; then
            fslmaths ${path}/vols2/volsact/vol000$COUNTER.nii.gz -mul -1
${path}/vols2/volsact/vol000$COUNTER.nii.gz -odt float;
          else
            fslmaths ${path}/vols2/volsact/vol00$COUNTER.nii.gz -mul -1
${path}/vols2/volsact/vol00$COUNTER.nii.gz -odt float;
          fi
      #let COUNTER=COUNTER+2
          COUNTER=`echo "$COUNTER+2" | bc`;
    done

    ## Create new time series
    fslmerge -t ${path}/asl_temp2_act ${path}/vols2/volsact/vol00*.nii.gz;

    ## Subtraction and Mean of time series
    fslmaths ${path}/asl_temp2_act -Tmean -mul 2
${path}/DM_M0_images/${filename}_DM_act -odt float;

    COUNTER1=0
    while [  $COUNTER1 -lt 50 ]; do
      echo Volume $COUNTER1
      if [ $COUNTER1 -lt 10 ]; then
            fslmaths ${path}/vols2/volsrest/vol000$COUNTER1.nii.gz -mul -1
${path}/vols2/volsrest/vol000$COUNTER1.nii.gz -odt float;
          else
            fslmaths ${path}/vols2/volsrest/vol00$COUNTER1.nii.gz -mul -1
${path}/vols2/volsrest/vol00$COUNTER1.nii.gz -odt float;
          fi
      #let COUNTER1=COUNTER1+2
          COUNTER1=`echo "$COUNTER1+2" | bc`;
    done

    ## Create new time series
    fslmerge -t ${path}/asl_temp2_rest ${path}/vols2/volsrest/vol00*.nii.gz;

    ## Subtraction and Mean of time series
    fslmaths ${path}/asl_temp2_rest -Tmean -mul 2
${path}/DM_M0_images/${filename}_DM_rest -odt float;

    ## Determining M0 image
    fslsplit ${path}/Magnet_eq_2.nii ${path}/Magnet_eq_2_slices -z;

### Applying masks slice by slice
    COUNT2=0
    while [ $COUNT2 -lt $nslices ]; do
          echo Calculating slice $COUNT2
          fslmaths ${path}/Magnet_eq_2_slices000$COUNT2.nii.gz -mas
${path}/manatomica_mask_slices000$COUNT2.nii.gz
${path}/M0_image1_slices000$COUNT2 -odt float;
          COUNT2=`echo "$COUNT2+1" | bc`;
    done

### Create new M0 image
    fslmerge -z ${path}/DM_M0_images/M0_image1 ${path}/M0_image1_slices000*.nii.gz;
```

```
##Calculating CBFACT2

    lambda=0.9;
    alfa=0.9;
    TI1=0.7;
    TI2=1.8;
    T1a=1.5;

    fslsplit ${path}/DM_M0_images/asl_bold_DM_act.nii.gz ${path}/DM_M0_images/mean -z;
    fslsplit  ${path}/DM_M0_images/M0_image1.nii.gz  ${path}/DM_M0_images/meanM01_ -
z;

    ### Applying masks slice by slice
    COUNT3=0
    while [ $COUNT3 -lt $nslices ]; do
        echo Applying mask to slice $COUNT3
        fslmaths ${path}/DM_M0_images/mean000$COUNT3.nii.gz -mas
${path}/manatomica_mask_slices000$COUNT3.nii.gz
${path}/DM_M0_images/mean_masked000$COUNT3 -odt float;
        COUNT3=`echo "$COUNT3+1" | bc`;
    done

    t=0;
    while [ $t -lt $nslices ] ; do
        M0=`fslstats ${path}/DM_M0_images/meanM01_000${t}.nii.gz -M`
        fslmaths ${path}/DM_M0_images/mean_masked000${t}.nii.gz -mul `echo
"$lambda*e($TI2/$T1a)" | bc -l` -div `echo "2*$M0*$alfa*$TI1" | bc -l` -mul 6000
${path}/DM_M0_images/CBFM0_${t} -odt float ;

      t=`echo "$t+1" | bc`

    done

    fslmerge -z ${path}/CBFACT2 ${path}/DM_M0_images/CBFM0_*.nii.gz ;

    rm ${path}/DM_M0_images/CBFM0_*.nii.gz ;

##Calculating CBFREST2

    lambda=0.9;
    alfa=0.9;
    TI1=0.7;
    TI2=1.8;
    T1a=1.5;

    fslsplit ${path}/DM_M0_images/asl_bold_DM_rest.nii.gz ${path}/DM_M0_images/mean1 -
z;

    ### Applying masks slice by slice
    COUNT4=0
    while [ $COUNT4 -lt $nslices ]; do
        echo Applying mask to slice $COUNT4
        fslmaths ${path}/DM_M0_images/mean1000$COUNT4.nii.gz -mas
${path}/manatomica_mask_slices000$COUNT4.nii.gz
${path}/DM_M0_images/mean_masked1000$COUNT4 -odt float;
        COUNT4=`echo "$COUNT4+1" | bc`;
    done
```

```
s=0;
    while [ $s -lt $nslices ] ; do
        M0=`fslstats ${path}/DM_M0_images/meanM01_000${s}.nii.gz -M`
        fslmaths ${path}/DM_M0_images/mean_masked1000${s}.nii.gz -mul `echo "$lambda*e($TI2/$T1a)" | bc -l` -div `echo "2*$M0*$alfa*$TI1" | bc -l` -mul 6000 ${path}/DM_M0_images/CBFM0_${s} -odt float ;

      s=`echo "$s+1" | bc`

    done

    fslmerge -z ${path}/CBFREST2 ${path}/DM_M0_images/CBFM0_*.nii.gz ;

    rm ${path}/DM_M0_images/CBFM0_*.nii.gz ;
    rm ${path}/M0_image1_slices000*.nii.gz ;
    rm ${path}/Magnet_eq_2_slices000*.nii.gz ;
    rm ${path}/manatomica_mask_slices000*.nii.gz ;
    rm ${path}/asl_tem*.nii.gz
    rm ${path}/DM_M0_images/mean_masked000*.nii.gz ;
    rm ${path}/DM_M0_images/mean_masked1000*.nii.gz ;
    rm ${path}/DM_M0_images/mean000*.nii.gz ;
    rm ${path}/DM_M0_images/mean1000*.nii.gz ;
    rm ${path}/DM_M0_images/meanM01_000*.nii.gz ;
    rm ${path}/vols/vol00*.nii.gz ;
    rm ${path}/vols1/vol00*.nii.gz ;
    rm ${path}/vols2/vol0*.nii.gz ;
    rm ${path}/vols2/volsact/vol00*.nii.gz ;
    rm ${path}/vols2/volsrest/vol00*.nii.gz ;
    rmdir ${path}/vols2/volsact/ ;
    rmdir ${path}/vols2/volsrest/ ;
    rmdir ${path}/vol*/ ;

done
```

Section A.4

Linux Shell Script designed to define regions segmented by level of hierarchy:

```
#!/bin/sh

###################################
path=/home1/joaom/DATA-HLuz-MPimentel-Preproc/

r1=Talairach-labels-1mm;

for filename in ${r1}; do

  ### Escolha da labels para a ROI
  echo -e "Quantas labels quer considerar para a sua regiao? \c"
  read labels
```

```
 COUNT=1
  while [ $COUNT -le $labels ]; do
     echo -e "Indique a label $COUNT: \c"
     read label
     fslmaths ${path}/${r1} -thr ${label} -uthr ${label} ${path}/Talairach_ROI_l${COUNT}.nii.gz
     COUNT=`echo "$COUNT+1" | bc`;
  done

  ###Cálculo da ROI tendo em conta as labels escolhidas
  COUNT=`echo "$COUNT-1" | bc`;

  if [ $COUNT = "1" ]; then

  mv ${path}/Talairach_ROI_l${COUNT}.nii.gz ${path}/Talairach_ROI.nii.gz ;

  else

     COUNT1=1

     fslmaths ${path}/Talairach_ROI_l${COUNT1} -add ${path}/Talairach_ROI_l`echo
"${COUNT1}+1" | bc` ${path}/Talairach_ROI.nii.gz

     COUNT1=3
     while [ $COUNT1 -le $COUNT ]; do
          fslmaths ${path}/Talairach_ROI -add ${path}/Talairach_ROI_l${COUNT1}
${path}/Talairach_ROI.nii.gz
          COUNT1=`echo "$COUNT1+1" | bc`;
     done

  fi

  echo -e "Qual o nome da regiao que acabou de calcular? \c"
  read regiao

  mv ${path}/Talairach_ROI.nii.gz ${path}/Talairach_${regiao}.nii.gz

done

rm ${path}/Talairach_ROI*.nii.gz
```

Section A.5

Linux Shell Script designed to obtain correct registration:

```
#!/bin/sh

############################
# ASL MPRAGE Talairach Registration

echo -e "Qual o subject em estudo? \c"
read subject

path=/home1/joaom/DATA-HLuz-MPimentel-Preproc/$subject;
```

```
echo "Encontra-se na directoria $path"

mkdir ${path}/Reg;

im1='MPRAGE';

## Processing MPRAGE image

   echo "A processar imagem MPRAGE."
   echo ""

   fslswapdim ${path}/${im1} RL PA IS ${path}/Reg/MPRAGE1.nii
   bet ${path}/Reg/MPRAGE1.nii ${path}/Reg/MPRAGE1_bet.nii -c 76 117 158

## Registo MPRAGE to MNI

   flirt -usesqform -in ${path}/Reg/MPRAGE1_bet -ref ${path}/MNI152_T1_1mm_brain.nii.gz -
out ${path}/Reg/MPRAGE_2_MNI -omat ${path}/Reg/MPRAGE_2_MNI.mat
   echo "A registar MPRAGE."
   echo ""

## Registo BOLD to MPRAGE

   flirt -usesqform -in ${path}/bold_MoCo.nii -ref ${path}/Reg/MPRAGE1_bet.nii.gz -out
${path}/Reg/BOLD_2_MPRAGE -omat ${path}/Reg/BOLD_2_MPRAGE.mat
   echo "A registar BOLD."
   echo ""

## Registo ASL to BOLD

   ### Ler ficheiro que se pretende registar:
   echo -e "Qual o ficheiro que deseja para o registo? \c"
   read file

   flirt -usesqform -in ${path}/$file -ref ${path}/bold_MoCo.nii -out
${path}/Reg/ASL_2_BOLD.nii -omat ${path}/Reg/ASL_2_BOLD.mat
   echo ""
   echo "A registar ASL."
   echo ""

## Registo ASL to MNI

   convert_xfm -omat ${path}/Reg/ASL_2_MPRAGE.mat -concat
${path}/Reg/BOLD_2_MPRAGE.mat ${path}/Reg/ASL_2_BOLD.mat
   convert_xfm -omat ${path}/Reg/ASL_2_MNI.mat -concat ${path}/Reg/MPRAGE_2_MNI.mat
${path}/Reg/ASL_2_MPRAGE.mat
   flirt -in ${path}/${file} -ref ${path}/MNI152_T1_1mm_brain.nii.gz -applyxfm -init
${path}/Reg/ASL_2_MNI.mat -out ${path}/Reg/ASL_2_MNI.nii.gz

## Registo MNI to ASL

   convert_xfm -omat ${path}/Reg/MNI_2_ASL.mat -inverse ${path}/Reg/ASL_2_MNI.mat
   flirt -in ${path}/MNI152_T1_1mm_brain.nii.gz -ref ${path}/${file} -applyxfm -init
${path}/Reg/MNI_2_ASL.mat -out ${path}/Reg/MNI_2_ASL.nii.gz
```

Section A.6

Linux Shell Script to obtain perfusion mean values, for a specific region, for all the four perfusion maps already obtained:

```
#!/bin/sh

subject1=AF;
subject2=ANA;
subject3=CS;
subject4=FG;
subject5=FS;
subject6=JD;
subject7=JN;
subject8=JS;
subject9=MA;
subject10=MF;
subject11=MM;
subject12=MP;
subject13=NF;
subject14=RL;
subject15=RT;

echo -e "Qual a regiao que deseja calcular? \c"
read file1
echo ""

for filename in subject*; do

path=/home1/joaom/DATA-HLuz-MPimentel-Preproc/;
path1=/home1/joaom/DATA-HLuz-MPimentel-Preproc/subjects/$filename;

echo "A processar  $filename"
echo ""

 file2=CBFACT1;

  flirt -in ${path}/Talairach_${file1}.nii.gz -ref ${path1}/${file2}.nii.gz -applyxfm -init ${path1}/Reg/MNI_2_ASL.mat -out ${path1}/Talairach_${file1}_to_ASL_vfinal.nii.gz
  fslmaths ${path1}/Talairach_${file1}_to_ASL_vfinal.nii.gz -bin ${path1}/Talairach_${file1}_to_ASL_bin_vfinal.nii.gz -odt int

  ### Cálculo do valor de CBF médio e desvio padrão  na região considerada:
  fslmaths  ${path1}/${file2}.nii.gz  -mas  ${path1}/Talairach_${file1}_to_ASL_bin_vfinal.nii.gz ${path1}/ASL_${file1}_vfinal.nii.gz -odt float
  CBFmean=`fslstats ${path1}/ASL_${file1}_vfinal.nii.gz -M`
  CBFstd=`fslstats ${path1}/ASL_${file1}_vfinal.nii.gz -S`
  echo "$CBFmean" >> ${path}/${file2}_${file1}_CBFmeanvalue_vfinal.txt ;
  echo "$CBFstd" >> ${path}/${file2}_${file1}_CBFstd_vfinal.txt ;
```

```
file2=CBFREST1;

  flirt -in ${path}/Talairach_${file1}.nii.gz -ref ${path1}/${file2}.nii.gz -applyxfm -init
${path1}/Reg/MNI_2_ASL.mat -out ${path1}/Talairach_${file1}_to_ASL_vfinal.nii.gz
  fslmaths ${path1}/Talairach_${file1}_to_ASL_vfinal.nii.gz -bin
${path1}/Talairach_${file1}_to_ASL_bin_vfinal.nii.gz -odt int

  ### Cálculo do valor de CBF médio e desvio padrão  na região considerada:
  fslmaths ${path1}/${file2}.nii.gz -mas ${path1}/Talairach_${file1}_to_ASL_bin_vfinal.nii.gz
${path1}/ASL_${file1}_vfinal.nii.gz -odt float
  CBFmean=`fslstats ${path1}/ASL_${file1}_vfinal.nii.gz -M`
  CBFstd=`fslstats ${path1}/ASL_${file1}_vfinal.nii.gz -S`
  echo "$CBFmean" >> ${path}/${file2}_${file1}_CBFmeanvalue_vfinal.txt ;
  echo "$CBFstd" >> ${path}/${file2}_${file1}_CBFstd_vfinal.txt ;

  file2=CBFACT2;

  flirt -in ${path}/Talairach_${file1}.nii.gz -ref ${path1}/${file2}.nii.gz -applyxfm -init
${path1}/Reg/MNI_2_ASL.mat -out ${path1}/Talairach_${file1}_to_ASL_vfinal.nii.gz
  fslmaths ${path1}/Talairach_${file1}_to_ASL_vfinal.nii.gz -bin
${path1}/Talairach_${file1}_to_ASL_bin_vfinal.nii.gz -odt int

  ### Cálculo do valor de CBF médio e desvio padrão  na região considerada:
  fslmaths ${path1}/${file2}.nii.gz -mas ${path1}/Talairach_${file1}_to_ASL_bin_vfinal.nii.gz
${path1}/ASL_${file1}_vfinal.nii.gz -odt float
  CBFmean=`fslstats ${path1}/ASL_${file1}_vfinal.nii.gz -M`
  CBFstd=`fslstats ${path1}/ASL_${file1}_vfinal.nii.gz -S`
  echo "$CBFmean" >> ${path}/${file2}_${file1}_CBFmeanvalue_vfinal.txt ;
  echo "$CBFstd" >> ${path}/${file2}_${file1}_CBFstd_vfinal.txt ;

  file2=CBFREST2;

  flirt -in ${path}/Talairach_${file1}.nii.gz -ref ${path1}/${file2}.nii.gz -applyxfm -init
${path1}/Reg/MNI_2_ASL.mat -out ${path1}/Talairach_${file1}_to_ASL_vfinal.nii.gz
  fslmaths ${path1}/Talairach_${file1}_to_ASL_vfinal.nii.gz -bin
${path1}/Talairach_${file1}_to_ASL_bin_vfinal.nii.gz -odt int

  ### Cálculo do valor de CBF médio e desvio padrão  na região considerada:
  fslmaths ${path1}/${file2}.nii.gz -mas ${path1}/Talairach_${file1}_to_ASL_bin_vfinal.nii.gz
${path1}/ASL_${file1}_vfinal.nii.gz -odt float
  CBFmean=`fslstats ${path1}/ASL_${file1}_vfinal.nii.gz -M`
  CBFstd=`fslstats ${path1}/ASL_${file1}_vfinal.nii.gz -S`
  echo "$CBFmean" >> ${path}/${file2}_${file1}_CBFmeanvalue_vfinal.txt ;
  echo "$CBFstd" >> ${path}/${file2}_${file1}_CBFstd_vfinal.txt ;

done
```

Appendix B – Mean perfusion values for third and fifth level of segmentation

Table B.1 – Mean perfusion values (ml/100g/min) in third level segmentation regions of the brain

CBF mean values ± Standard Error (ml/100g/min)			
		Protocol 1	Protocol 2
Left Angular Gyrus	Activation	58 ± 4	57 ± 9
	Rest	63 ± 4	53 ± 7
Right Angular Gyrus	Activation	53 ± 4	44 ±3
	Rest	53 ± 4	43 ± 3
Left Anterior Cingulate	Activation	51 ± 4	50 ± 5
	Rest	54 ± 3	46 ± 4
Right Anterior Cingulate	Activation	53 ± 5	55 ± 5
	Rest	57 ± 5	52 ± 4
Left Caudate	Activation	60 ± 5	54 ± 3
	Rest	60 ± 5	51 ± 3

Right Caudate	Activation	58 ± 3	61 ± 4
	Rest	57 ± 3	59 ± 3
Left Cerebellar Lingual	Activation	102 ± 18	66 ± 13
	Rest	103 ± 18	54 ± 12
Right Cerebellar Lingual	Activation	106 ± 18	93 ± 16
	Rest	103 ± 19	87 ± 17
Left Cingulate Gyrus	Activation	55 ± 3	49 ± 3
	Rest	55 ± 3	43 ± 3
Right Cingulate Gyrus	Activation	54 ± 4	52 ± 3
	Rest	53 ± 4	49 ± 3
Left Claustrum	Activation	83 ± 6	77 ± 4
	Rest	82 ± 6	76 ± 4
Right Claustrum	Activation	74 ± 4	42 ± 3
	Rest	72 ± 5	42 ± 3
Left Culmen	Activation	126 ± 10	66 ± 6
	Rest	125 ± 10	67 ± 8
Right Culmen	Activation	125 ± 10	80 ± 8
	Rest	120 ± 10	80 ± 9
Left Culmen of Vermis	Activation	127 ± 10	38 ± 9
	Rest	130 ± 10	42 ± 9
Right Culmen of Vermis	Activation	126 ± 10	42 ± 5
	Rest	124 ± 10	51 ± 7
Left Cuneus	Activation	90 ± 5	60 ± 4
	Rest	93 ± 5	61 ± 4
Right Cuneus	Activation	82 ± 5	78 ± 4
	Rest	85 ± 5	84 ± 4
Left Extra-Nuclear	Activation	72 ± 5	59 ± 3
	Rest	72 ± 5	57 ± 3
Right Extra-Nuclear	Activation	65 ± 3	53 ± 2
	Rest	65 ± 3	52 ± 2
Left Fusiform Gyrus	Activation	84 ± 13	69 ± 11
	Rest	84 ± 13	67 ± 12
Right Fusiform Gyrus	Activation	76 ± 11	60 ± 9
	Rest	74 ± 10	65 ± 10
Left Inferior Frontal Gyrus	Activation	71 ± 3	75 ± 10
	Rest	72 ± 3	70 ± 9
Right Inferior Frontal Gyrus	Activation	67 ± 4	55 ± 3
	Rest	66 ± 4	54 ± 3
Left Inferior Occipital Gyrus	Activation	73 ± 11	70 ± 12
	Rest	73 ± 11	65 ± 12
Right Inferior Occipital Gyrus	Activation	68 ± 11	61 ± 8
	Rest	69 ± 11	62 ± 9
Left Inferior Parietal	Activation	58 ± 3	58 ± 6

Gyrus	Rest	57 ± 3	47 ± 6
Right Inferior Parietal Gyrus	Activation	54 ± 3	43 ± 2
	Rest	53 ± 3	41 ± 2
Left Inferior Temporal Gyrus	Activation	77 ± 7	62 ± 15
	Rest	83 ± 7	65 ± 17
Right Inferior Temporal Gyrus	Activation	68 ± 7	57 ± 6
	Rest	70 ± 7	61 ± 6
Left Insula	Activation	89 ± 4	77 ± 5
	Rest	87 ± 4	72 ± 5
Right Insula	Activation	80 ± 4	35 ± 4
	Rest	79 ± 4	35 ± 4
Left Lateral Ventricle	Activation	65 ± 5	52 ± 4
	Rest	66 ± 5	52 ± 4
Right Lateral Ventricle	Activation	55 ± 3	58 ± 4
	Rest	55 ± 3	57 ± 4
Left Lentiform Nucleus	Activation	82 ± 6	75 ± 4
	Rest	79 ± 6	72 ± 4
Right Lentiform Nucleus	Activation	74 ± 3	52 ± 3
	Rest	71 ± 3	51 ± 3
Left Lingual Gyrus	Activation	110 ± 9	60 ± 5
	Rest	111 ± 9	62 ± 5
Right Lingual Gyrus	Activation	102 ± 9	87 ± 8
	Rest	103 ± 9	92 ± 8
Left Medial Frontal Gyrus	Activation	50 ± 3	46 ± 5
	Rest	51 ± 3	42 ± 5
Right Medial Frontal Gyrus	Activation	50 ± 3	51 ± 5
	Rest	49 ± 4	54 ± 7
Left Middle Frontal Gyrus	Activation	55 ± 3	48 ± 14
	Rest	54 ± 3	43 ± 13
Right Middle Frontal Gyrus	Activation	53 ± 3	43 ± 4
	Rest	52 ± 3	43 ± 4
Left Middle Occipital Gyrus	Activation	79 ± 6	80 ± 4
	Rest	83 ± 7	83 ± 4
Right Middle Occipital Gyrus	Activation	65 ± 6	68 ± 3
	Rest	66 ± 6	72 ± 3
Left Paracentral Lobule	Activation	52 ± 3	49 ± 5
	Rest	53 ± 3	42 ± 4
Right Paracentral Lobule	Activation	48 ± 4	57 ± 14
	Rest	52 ± 5	60 ± 16
Left Parahippocampal Gyrus	Activation	100 ± 8	88 ± 7
	Rest	103 ± 9	92 ± 7
Right Parahippocampal Gyrus	Activation	89 ± 8	78 ± 7
	Rest	90 ± 8	78 ± 8

Left Postcentral Gyrus	Activation	57 ± 3	58 ± 9
	Rest	51 ± 3	51 ± 8
Right Postcentral Gyrus	Activation	49 ± 2	48 ± 4
	Rest	48 ± 2	47 ± 3
Left Posterior Cingulate	Activation	100 ± 5	38 ± 5
	Rest	102 ± 6	36 ± 4
Right Posterior Cingulate	Activation	92 ± 7	69 ± 4
	Rest	94 ± 7	71 ± 4
Left Precentral Gyrus	Activation	63 ± 3	62 ± 8
	Rest	56 ± 3	41 ± 8
Right Precentral Gyrus	Activation	55 ± 3	47 ± 3
	Rest	53 ± 3	51 ± 3
Left Precuneus	Activation	64 ± 4	51 ± 3
	Rest	67 ± 5	43 ± 3
Right Precuneus	Activation	58 ± 4	45 ± 4
	Rest	60 ± 4	48 ± 3
Left Subcallosal Gyrus	Activation	44 ± 9	38 ± 7
	Rest	46 ± 9	42 ± 8
Right Subcallosal Gyrus	Activation	41 ± 8	37 ± 9
	Rest	46 ± 10	39 ± 8
Left Sub-Gyral	Activation	57 ± 3	70 ± 4
	Rest	57 ± 4	65 ± 4
Right Sub-Gyral	Activation	53 ± 3	51 ± 3
	Rest	53 ± 3	51 ± 3
Left Superior Frontal Gyrus	Activation	48 ± 4	N.D.
	Rest	49 ± 4	N.D.
Right Superior Frontal Gyrus	Activation	47 ± 4	N.D.
	Rest	47 ± 4	N.D.
Left Superior Occipital Gyrus	Activation	59 ± 5	52 ± 9
	Rest	64 ± 7	50 ± 9
Right Superior Occipital Gyrus	Activation	48 ± 6	54 ± 4
	Rest	50 ± 6	57 ± 4
Left Superior Parietal Gyrus	Activation	47 ± 5	47 ± 11
	Rest	50 ± 5	37 ± 10
Right Superior Parietal Gyrus	Activation	38 ± 3	24 ± 3
	Rest	40 ± 3	29 ± 3
Left Superior Temporal Gyrus	Activation	77 ± 3	80 ± 5
	Rest	79 ± 3	75 ± 4
Right Superior Temporal Gyrus	Activation	75 ± 3	55 ± 3
	Rest	77 ± 3	54 ± 3
Left Supramarginal Gyrus	Activation	58 ± 4	54 ± 6
	Rest	59 ± 4	48 ± 6
Right Supramarginal	Activation	54 ± 3	49 ± 3

Gyrus	Rest	54 ± 3	50 ± 3
Left Thalamus	Activation	103 ± 5	51 ± 5
	Rest	101 ± 5	50 ± 5
Right Thalamus	Activation	96 ± 5	58 ± 5
	Rest	95 ± 4	57 ± 4
Left Third Ventricle	Activation	100 ± 10	61 ± 8
	Rest	106 ± 9	63 ± 8
Right Third Ventricle	Activation	99 ± 10	70 ± 11
	Rest	104 ± 8	66 ± 5
Left Transverse Temporal Gyrus	Activation	76 ± 9	75 ± 6
	Rest	77 ± 10	73 ± 5
Right Transverse Temporal Gyrus	Activation	75 ± 7	41 ± 3
	Rest	75 ± 8	37 ± 3

N.D. – Non Detected

Table B.2 - Mean perfusion values (ml/100g/min) in third level segmentation regions of the brain

CBF mean values ± Standard Error (ml/100g/min)			
		Protocol 1	Protocol 2
Left Amygdala	Activation	66 ± 12	86 ± 15
	Rest	72 ± 12	80 ± 13
Right Amygdala	Activation	64 ± 11	53 ± 10
	Rest	67 ± 11	47 ± 10
Left Anterior Commissure	Activation	54 ± 10	49 ± 9
	Rest	62 ± 11	47 ± 6
Right Anterior Commissure	Activation	56 ± 10	56 ± 21
	Rest	61 ± 10	36 ± 5
Left Anterior Nucleus	Activation	91 ± 7	38 ± 6
	Rest	89 ± 8	41 ± 7
Right Anterior Nucleus	Activation	99 ± 6	41 ± 7
	Rest	97 ± 6	41 ± 5
Left Brodmann Areas	Activation	66 ± 3	58 ± 3
	Rest	69 ± 3	56 ± 3
Right Brodmann Areas	Activation	62 ± 3	58 ± 3
	Rest	66 ± 3	58 ± 3
Left Caudate Body	Activation	59 ± 5	41 ± 4
	Rest	58 ± 5	40 ± 4
Right Caudate Body	Activation	57 ± 4	68 ± 5
	Rest	56 ± 4	63 ± 4
Left Caudate Head	Activation	62 ± 7	44 ± 6
	Rest	71 ± 6	41 ± 5
Right Caudate Head	Activation	63 ± 5	56 ± 4

	Rest	67 ± 6	55 ± 4
Left Caudate Tail	Activation	77 ± 8	68 ± 5
	Rest	78 ± 8	70 ± 5
Right Caudate Tail	Activation	56 ± 4	60 ± 5
	Rest	58 ± 4	62 ± 6
Left Corpus Callosum	Activation	55 ± 5	42 ± 3
	Rest	59 ± 5	39 ± 3
Right Corpus Callosum	Activation	53 ± 3	60 ± 4
	Rest	56 ± 4	57 ± 5
Left Hippocampus	Activation	109 ± 9	103 ± 11
	Rest	114 ± 9	105 ± 9
Right Hippocampus	Activation	90 ± 10	76 ± 7
	Rest	95 ± 10	83 ± 8
Left Hypothalamus	Activation	72 ± 12	64 ± 9
	Rest	81 ± 11	64 ± 7
Right Hypothalamus	Activation	71 ± 8	79 ± 19
	Rest	68 ± 10	74 ± 9
Left Lateral Dorsal Nucleus	Activation	128 ± 7	36 ± 6
	Rest	116 ± 7	35 ± 10
Right Lateral Dorsal Nucleus	Activation	102 ± 10	39 ± 9
	Rest	102 ± 10	47 ± 8
Left Lateral Geniculum Body	Activation	53 ± 13	85 ± 13
	Rest	64 ± 15	83 ± 13
Right Lateral Geniculum Body	Activation	65 ± 12	70 ± 14
	Rest	63 ± 12	61 ± 13
Left Lateral Globus Pallidus	Activation	77 ± 8	77 ± 5
	Rest	81 ± 8	77 ± 4
Right Lateral Globus Pallidus	Activation	68 ± 2	56 ± 4
	Rest	66 ± 3	51 ± 4
Left Lateral Posterior Nucleus	Activation	80 ± 4	42 ± 7
	Rest	75 ± 4	43 ± 8
Right Lateral Posterior Nucleus	Activation	79 ± 7	55 ± 6
	Rest	77 ± 5	54 ± 7
Left Mammillary Body	Activation	122 ± 8	71 ± 11
	Rest	119 ± 10	67 ± 11
Right Mammillary Body	Activation	114 ± 9	63 ± 10
	Rest	121 ± 6	63 ± 7
Left Medial Dorsal Nucleus	Activation	135 ± 6	42 ± 10
	Rest	132 ± 8	39 ± 10
Right Medial Dorsal Nucleus	Activation	129 ± 8	43 ± 8
	Rest	132 ± 8	44 ± 7
Left Medial Geniculum Body	Activation	115 ± 14	84 ± 10
	Rest	127 ± 14	81 ± 9

Right Medial Geniculum Body	Activation	96 ± 12	109 ± 16
	Rest	116 ± 10	106 ± 18
Left Medial Globus Pallidus	Activation	71 ± 7	69 ± 6
	Rest	73 ± 8	68 ± 5
Right Medial Globus Pallidus	Activation	65 ± 3	41 ± 6
	Rest	66 ± 5	38 ± 7
Left Midline Nucleus	Activation	148 ± 8	31 ± 9
	Rest	141 ± 8	33 ± 12
Right Midline Nucleus	Activation	110 ± 13	53 ± 10
	Rest	128 ± 12	40 ± 12
Left Optic Tract	Activation	94 ± 7	93 ± 9
	Rest	104 ± 8	89 ± 8
Right Optic Tract	Activation	99 ± 6	76 ± 9
	Rest	102 ± 7	74 ± 9
Left Pulvinar	Activation	111 ± 5	51 ± 6
	Rest	111 ± 5	50 ± 6
Right Pulvinar	Activation	92 ± 4	68 ± 7
	Rest	93 ± 5	67 ± 7
Left Putamen	Activation	85 ± 6	77 ± 4
	Rest	87 ± 6	74 ± 4
Right Putamen	Activation	75 ± 3	56 ± 3
	Rest	75 ± 3	55 ± 3
Left Red Nucleus	Activation	107 ± 11	65 ± 7
	Rest	105 ± 10	71 ± 9
Right Red Nucleus	Activation	105 ± 10	62 ± 7
	Rest	103 ± 10	65 ± 8
Left Substania Nigra	Activation	98 ± 10	86 ± 9
	Rest	93 ± 8	82 ± 9
Right Substania Nigra	Activation	100 ± 10	81 ± 10
	Rest	101 ± 9	76 ± 9
Left Subthalamic Nucleus	Activation	79 ± 13	80 ± 11
	Rest	83 ± 10	77 ± 10
Right Subthalamic Nucleus	Activation	88 ± 8	61 ± 10
	Rest	82 ± 9	53 ± 10
Left Ventral Anterior Nucleus	Activation	76 ± 7	41 ± 5
	Rest	75 ± 7	46 ± 6
Right Ventral Anterior Nucleus	Activation	86 ± 5	52 ± 5
	Rest	83 ± 5	48 ± 6
Left Ventral Lateral Nucleus	Activation	91 ± 5	53 ± 6
	Rest	87 ± 5	54 ± 6
Right Ventral Lateral Nucleus	Activation	92 ± 5	47 ± 5
	Rest	89 ± 4	49 ± 5
Left Ventral Posterior	Activation	89 ± 10	57 ± 7

Lateral Nucleus	Rest	95 ± 10	56 ± 6
Right Ventral Posterior Lateral Nucleus	Activation	80 ± 4	50 ± 5
	Rest	83 ± 4	53 ± 6
Left Ventral Posterior Medial Nucleus	Activation	108 ± 10	57 ± 10
	Rest	110 ± 9	55 ± 10
Right Ventral Posterior Medial Nucleus	Activation	99 ± 7	55 ± 7
	Rest	103 ± 6	56 ± 7

Appendix C – Implementation of Functional Paradigms

The functional paradigms were programmed using eXtensible Markup Language (XML) and were composed of four different parts that require each other to function correctly:

- Slides
- Trials
- Description
- Main Program

The Slides block is the lowest level. It is used to read the files that are used to stimulate the patient's brain.

After reading it, the Trials organize the Slides that have been uploaded to the program in order to produce a coherent stimulus.

Finally, the Main Program organizes the Trials and gives to the hardware other type of information, such as TR, TI and Volumes that will be needed.

A brief Description may also be programmed in order to give some information to the Technician and some instructions to the Patient.

The program for the Rhyming paradigm is shown next:

Slides:

```
<?xml version="1.0" encoding="windows-1252"?>
<IncludeSlides>
	<Slide>
		<name>Active1</name>
		<Picture>./Activation/Rhy.001.jpg</Picture>
	</Slide>
	<Slide>
		<name>Active2</name>
		<Picture>./Activation/Rhy.002.jpg</Picture>
	</Slide>
	<Slide>
		<name>Active3</name>
		<Picture>./Activation/Rhy.003.jpg</Picture>
	</Slide>
	<Slide>
		<name>Active4</name>
		<Picture>./Activation/Rhy.004.jpg</Picture>
	</Slide>
	<Slide>
		<name>Active5</name>
		<Picture>./Activation/Rhy.005.jpg</Picture>
	</Slide>
	<Slide>
		<name>Active6</name>
		<Picture>./Activation/Rhy.006.jpg</Picture>
	</Slide>
	<Slide>
		<name>Active7</name>
		<Picture>./Activation/Rhy.007.jpg</Picture>
	</Slide>
	<Slide>
		<name>Active8</name>
		<Picture>./Activation/Rhy.008.jpg</Picture>
	</Slide>
	<Slide>
		<name>Active9</name>
		<Picture>./Activation/Rhy.009.jpg</Picture>
	</Slide>
	<Slide>
		<name>Active10</name>
		<Picture>./Activation/Rhy.010.jpg</Picture>
	</Slide>
	<Slide>
		<name>Active11</name>
		<Picture>./Activation/Rhy.011.jpg</Picture>
	</Slide>
	<Slide>
		<name>Active12</name>
		<Picture>./Activation/Rhy.012.jpg</Picture>
	</Slide>
```

```
<Slide>
        <name>Active13</name>
        <Picture>./Activation/Rhy.013.jpg</Picture>
</Slide>
<Slide>
        <name>Active14</name>
        <Picture>./Activation/Rhy.014.jpg</Picture>
</Slide>
<Slide>
        <name>Active15</name>
        <Picture>./Activation/Rhy.015.jpg</Picture>
</Slide>
<Slide>
        <name>Active16</name>
        <Picture>./Activation/Rhy.016.jpg</Picture>
</Slide>
<Slide>
        <name>Active17</name>
        <Picture>./Activation/Rhy.017.jpg</Picture>
</Slide>
<Slide>
        <name>Active18</name>
        <Picture>./Activation/Rhy.018.jpg</Picture>
</Slide>
<Slide>
        <name>Active19</name>
        <Picture>./Activation/Rhy.019.jpg</Picture>
</Slide>
<Slide>
        <name>Active20</name>
        <Picture>./Activation/Rhy.020.jpg</Picture>
</Slide>
<Slide>
        <name>Active21</name>
        <Picture>./Activation/Rhy.021.jpg</Picture>
</Slide>
<Slide>
        <name>Active22</name>
        <Picture>./Activation/Rhy.022.jpg</Picture>
</Slide>
<Slide>
        <name>Control1</name>
        <Picture>./Control/Cont1.bmp</Picture>
</Slide>
<Slide>
        <name>Control2</name>
        <Picture>./Control/Cont2.bmp</Picture>
</Slide>
<Slide>
        <name>Control3</name>
        <Picture>./Control/Cont3.bmp</Picture>
</Slide>
<Slide>
        <name>Control4</name>
        <Picture>./Control/Cont4.bmp</Picture>
</Slide>
<Slide>
        <name>Control5</name>
```

```
            <Picture>./Control/Cont5.bmp</Picture>
        </Slide>
        <Slide>
            <name>Control6</name>
            <Picture>./Control/Cont6.bmp</Picture>
        </Slide>
</IncludeSlides>
```

Trials:

```
<?xml version="1.0" encoding="windows-1252"?>
<IncludeTrials>
        <Trial>
            <name>Instructions</name>
            <show>
                <item>Instructions</item>
            </show>
        </Trial>
        <Trial>
            <name>Start</name>
            <show>
                <item>Start</item>
                <overlap>true</overlap>
            </show>
            <register>
                <key>s</key>
            </register>
            <clear />
        </Trial>
        <Trial>
            <name>Off</name>
            <clear />
            <wait>$OffBlockLength</wait>
        </Trial>
        <Trial>
            <name>active1</name>
            <show>
                <item>Active1</item>
                <duration>$OnShowDuration</duration>
            </show>
        </Trial>
        <Trial>
            <name>active2</name>
            <show>
                <item>Active2</item>
                <duration>$OnShowDuration</duration>
            </show>
        </Trial>
        <Trial>
            <name>active3</name>
            <show>
                <item>Active3</item>
                <duration>$OnShowDuration</duration>
            </show>
        </Trial>
        <Trial>
            <name>active4</name>
            <show>
```

```
                <item>Active4</item>
                <duration>$OnShowDuration</duration>
        </show>
</Trial>
<Trial>
        <name>active5</name>
        <show>
                <item>Active5</item>
                <duration>$OnShowDuration</duration>
        </show>
</Trial>
<Trial>
        <name>active6</name>
        <show>
                <item>Active6</item>
                <duration>$OnShowDuration</duration>
        </show>
</Trial>
<Trial>
        <name>active7</name>
        <show>
                <item>Active7</item>
                <duration>$OnShowDuration</duration>
        </show>
</Trial>
<Trial>
        <name>active8</name>
        <show>
                <item>Active8</item>
                <duration>$OnShowDuration</duration>
        </show>
</Trial>
<Trial>
        <name>active9</name>
        <show>
                <item>Active9</item>
                <duration>$OnShowDuration</duration>
        </show>
</Trial>
<Trial>
        <name>active10</name>
        <show>
                <item>Active10</item>
                <duration>$OnShowDuration</duration>
        </show>
</Trial>
<Trial>
        <name>active11</name>
        <show>
                <item>Active11</item>
                <duration>$OnShowDuration</duration>
        </show>
</Trial>
<Trial>
        <name>active12</name>
        <show>
                <item>Active12</item>
                <duration>$OnShowDuration</duration>
```

```
        </show>
</Trial>
<Trial>
        <name>active13</name>
        <show>
                <item>Active13</item>
                <duration>$OnShowDuration</duration>
        </show>
</Trial>
<Trial>
        <name>active14</name>
        <show>
                <item>Active14</item>
                <duration>$OnShowDuration</duration>
        </show>
</Trial>
<Trial>
        <name>active15</name>
        <show>
                <item>Active15</item>
                <duration>$OnShowDuration</duration>
        </show>
</Trial>
<Trial>
        <name>active16</name>
        <show>
                        <item>Active16</item>
                <duration>$OnShowDuration</duration>
        </show>
</Trial>
<Trial>
        <name>active17</name>
        <show>
                <item>Active17</item>
                <duration>$OnShowDuration</duration>
        </show>
</Trial>
<Trial>
        <name>active18</name>
        <show>
                <item>Active18</item>
                <duration>$OnShowDuration</duration>
        </show>
</Trial>
<Trial>
        <name>active19</name>
        <show>
                <item>Active19</item>
                <duration>$OnShowDuration</duration>
        </show>
</Trial>
<Trial>
        <name>active20</name>
        <show>
                <item>Active20</item>
                <duration>$OnShowDuration</duration>
        </show>
</Trial>
```

```
<Trial>
	<name>active21</name>
	<show>
		<item>Active21</item>
		<duration>$OnShowDuration</duration>
	</show>
</Trial>
<Trial>
	<name>active22</name>
	<show>
		<item>Active22</item>
		<duration>$OnShowDuration</duration>
	</show>
</Trial>
<Trial>
	<name>control1</name>
	<show>
		<item>Control1</item>
		<duration>$OnShowDuration</duration>
	</show>
</Trial>
<Trial>
	<name>control2</name>
	<show>
		<item>Control2</item>
		<duration>$OnShowDuration</duration>
	</show>
</Trial>
<Trial>
	<name>control3</name>
	<show>
		<item>Control3</item>
		<duration>$OnShowDuration</duration>
	</show>
</Trial>
<Trial>
	<name>control4</name>
	<show>
		<item>Control4</item>
		<duration>$OnShowDuration</duration>
	</show>
</Trial>
<Trial>
	<name>control5</name>
	<show>
		<item>Control5</item>
		<duration>$OnShowDuration</duration>
	</show>
</Trial>
<Trial>
	<name>control6</name>
	<show>
		<item>Control6</item>
		<duration>$OnShowDuration</duration>
	</show>
</Trial>
</IncludeTrials>
```

Main Program:

```
<ParameterDescriptionFile>
	<!-- Variables -->
	<Variables>
		<VolPrBlock>10</VolPrBlock>
		<OffBlockLength>30000</OffBlockLength>
		<OnShowDuration>5000</OnShowDuration>
		<InstructionTime>5000</InstructionTime>
	</Variables>
	<!-- Main Settings -->
	<Settings>
		<Name>Rhyming</Name>
		<Instruction>
		</Instruction>
		<Include Language="Portuguese">./Rhyming_description_pt.xml</Include>
		<Include Language="English">./Rhyming_description_eng.xml</Include>
		<Include Language="German">./Rhyming_description_ger.xml</Include>
		<Slices>32</Slices>
		<TimeToRepeat>3000/2</TimeToRepeat>
		<InterPulseInterval>2000</InterPulseInterval>
		<Volumes>90</Volumes>
	</Settings>
	<Defaults>
		<BackGroundColor>Black</BackGroundColor>
		<ForeGroundColor>Grey</ForeGroundColor>
		<DefaultPosition>MidPos</DefaultPosition>
		<DefaultPicture></DefaultPicture>
		<FontSize>36</FontSize>
		<Language>Portuguese</Language>
	</Defaults>
	<!-- Positions -->
	<Position>
		<name>MidPos</name>
		<horizontal>center</horizontal>
		<vertical>center</vertical>
	</Position>
	<!-- Languages -->
	<Languages>
		<Language>English</Language>
		<Language>Portuguese</Language>
		<Language>German</Language>
	</Languages>
	<!--Processing-->
	<!-- Slides -->
	<Include>.\Rhyming_slides.xml</Include>
	<Include Language="Portuguese">.\Rhyming_slides_pt.xml</Include>
	<Include Language="English">.\Rhyming_slides_eng.xml</Include>
	<Include Language="German">.\Rhyming_slides_ger.xml</Include>
	<!-- Trials -->
	<Include>.\Rhyming_trials.xml</Include>
	<!-- Blocks  -->
	<Block>
		<name>Rhyming1</name>
		<trials>active1</trials>
		<trials>active2</trials>
		<trials>active3</trials>
		<trials>active4</trials>
```

```
        <trials>active5</trials>
        <trials>active6</trials>
        <condition>1</condition>
        <order>1</order>
</Block>
<Block>
        <name>Rhyming2</name>
        <trials>active7</trials>
        <trials>active8</trials>
        <trials>active9</trials>
        <trials>active10</trials>
        <trials>active11</trials>
        <trials>active12</trials>
        <condition>1</condition>
        <order>1</order>
</Block>
<Block>
        <name>Rhyming3</name>
        <trials>active13</trials>
        <trials>active14</trials>
        <trials>active15</trials>
        <trials>active16</trials>
        <trials>active17</trials>
        <trials>active18</trials>
        <condition>1</condition>
        <order>1</order>
</Block>
<Block>
        <name>Rhyming4</name>
        <trials>active19</trials>
        <trials>active20</trials>
        <trials>active21</trials>
        <trials>active22</trials>
        <trials>active23</trials>
        <trials>active24</trials>
        <condition>1</condition>
        <order>1</order>
</Block>
<Block>
        <name>Control</name>
        <trials>control1</trials>
        <trials>control2</trials>
        <trials>control3</trials>
        <trials>control4</trials>
        <trials>control5</trials>
        <trials>control6</trials>
        <condition>1</condition>
        <order>1</order>
</Block>
<!-- Session -->
<Session>
        <name>Rhyming</name>
        <runtrial>Start</runtrial>
        <!--<runtrial>Off</runtrial>-->
        <runblock>Control</runblock>
        <runblock>Rhyming1</runblock>
        <runblock>Control</runblock>
        <runblock>Rhyming2</runblock>
```

```
                <runblock>Control</runblock>
                <runblock>Rhyming3</runblock>
                <runblock>Control</runblock>
                <runblock>Rhyming4</runblock>
                <runtrial>Off</runtrial>
        </Session>
</ParameterDescriptionFile>
```